RICE UNIVERSITY

A Tunable Hydrogel System and Pulsatile Flow Bioreactor for the Development of Tissue Engineered Vascular Grafts

by

Melissa Knight McHale

A THESIS SUBMITTED
IN PARTIAL FULFILLMENT OF THE
REQUIREMENTS FOR THE DEGREE

Doctor of Philosophy

APPROVED, THESIS COMMITTEE:

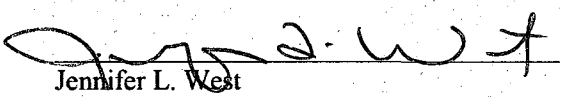

Jennifer L. West
Isabel C. Cameron Professor, Chair
Bioengineering

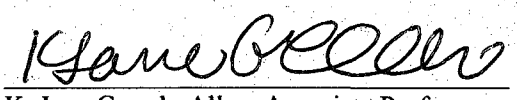

K. Jane Grande-Allen, Associate Professor
Bioengineering

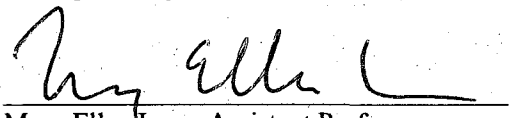

Mary Ellen Lane, Assistant Professor
Biochemistry and Cell Biology

HOUSTON, TEXAS
MAY 2009

ABSTRACT

A Tunable Hydrogel System and Pulsatile Flow Bioreactor for the Development of Tissue Engineered Vascular Grafts

by

Melissa K. McHale

The prevalence of coronary artery disease combined with a paucity of suitable vessel substitutes act as driving forces for cardiovascular tissue engineering research. In this thesis poly(ethylene glycol) diacrylate (PEGDA) hydrogels were investigated as a biomaterial for tissue engineered vascular grafts (TEVG). The global objectives for the work were two-fold. First, a thorough characterization of the hydrogels was warranted to determine material properties and cell interaction characteristics. The second objective was to develop a pulsatile flow culture system for TEVG that was capable of achieving physiologically relevant fluid flow parameters.

Bulk properties of PEGDA hydrogels formed from a range of polymer molecular weights and solution concentrations were characterized. Resultant materials demonstrate tunable stiffness and strength, and network properties that are appropriate for supporting viability of encapsulated cells. Human coronary artery smooth muscle cells seeded on top of these PEGDA hydrogels exhibit changes in attachment, proliferation, and morphology that can be directly correlated to the rigidity of the substrate material. In general, stiffer materials encourage greater attachment, a higher rate of proliferation, and the development of a mature, spread morphology. Finally, these responses were shown to be independently modulated by changing either the hydrogel material properties or the peptide directed bio-adhesiveness of the substrate.

The tissue bioreactor presented in this work is capable of imparting physiological fluid flow (120 mL/min), shear (5-10 dynes/cm^2), pressure waveforms (120/80 mmHg), and pulse rates (60 or 120 bpm). Cell-laden hydrogel constructs cultured for up to 8 wk in this system responded to mechanical stimulation with increases in cell and extracellular matrix (ECM) content and positive modulations to material properties. Though the magnitude of ECM accumulation is quite low, changes in hydrogel stiffness and the presence of degrading enzymes indicate that the encapsulated vascular cells are working towards a more biologically appropriate surrounding. Since all parameters for appropriate TEVG culture are not yet understood, this device will serve as an important tool in the development of a small diameter vessel substitute.

ACKNOWLEDGMENTS

My sincere gratitude is extended to the members of my thesis committee. Dr. Jennifer West, Dr. Jane Grande-Allen, and Dr. Mary Ellen Lane serve as fine examples of excellence in science and education. I thank you for your advice and mentorship as I worked to complete this thesis. My research has been supported by members of the West Lab past and present, especially Mariah Hahn who worked with me in setting up the bioreactor, and April Smith, Logan Hsu, and Alicia Allen who helped keep all the experiments pumping along. I'm grateful to James Moon and Jordan Miller for their infinite technical discussions, and Marcella Estrella for assistance with everything from pumps to parties. Thanks to everyone who helped when I asked, especially in this last semester when I needed it most.

I am fortunate to have wonderful friends like, Kim, who taught me everything I needed to know to get started in research and Dana, who traveled this journey with me all the way from ABE. We're finally done.

I could not have reached this point without the loving support of my family. Thanks, Mom.

Most importantly, thank you to my wonderful husband Martin for his encouragement and patience; and for bringing Lily to the lab for picnics when I couldn't make it home. I am forever indebted.

This thesis was financially supported by a Whitaker Foundation Graduate Fellowship and by grants from the NIH.

TABLE OF CONTENTS

LIST OF TABLES

LIST OF FIGURES

LIST OF EQUATIONS

1. Introduction

1.1 Significance of Cardiovascular Disease

In nearly every year of the past century, cardiovascular disease (CVD) claimed more U.S. lives than any other single cause. The only exception was in 1918 when 28% of the population was infected by an unusually virulent influenza strain. In fact in recent years, CVD deaths have totaled more than the next four leading causes combined (cancer, chronic lower respiratory diseases, accidents, and diabetes mellitus). The latest report from the American Heart Association predicts that in 2008 CVD afflictions will be associated with $448.5 billion in medical costs. Coronary heart disease, which affects the vessels feeding the heart itself, comprises more than half of all CVD cases. In 2005 alone, 469,000 coronary artery bypass procedures were performed in 261,000 patients.[1] This statistic illustrates not only the prevalence of this subset of CVD, but also indicates that the majority of bypass patients require two or more grafts. Multiple or repeat procedures are complicated because although autologous tissues such as the saphenous vein and internal mammary artery are preferred bypass materials, 10% - 40% of patients do not have suitable harvest tissue available.[2] The reasons for excluding autologous transplants are various and include: size mismatch (diameter or length), pervasive venous/arterial disease, and exhaustion due to previous bypass surgery.[2] At present, there is not a sufficient non-autologous replacement material for the small coronary artery, despite the availability of synthetic materials as grafts for larger vessels. Synthetic graft failure in coronary applications motivates the investigation of tissue engineered alternatives.

1.2 Overview of Blood Vessel Biology

1.2.1 Normal Structure and Function

Blood vessels infiltrate most tissues of the body providing a means for the distribution of nutrients and oxygen as well as the removal waste products, and acting as a conduit for the cells, proteins and signaling factors of the immune system. Of the three primary types of vessels, arteries are the largest and most structurally robust. They function to carry oxygenated blood away from the heart and as a result experience the largest mechanical forces of the vascular system. To remain viable in this environment, arteries have developed a tri-layered structure as illustrated in Figure 1-1 .

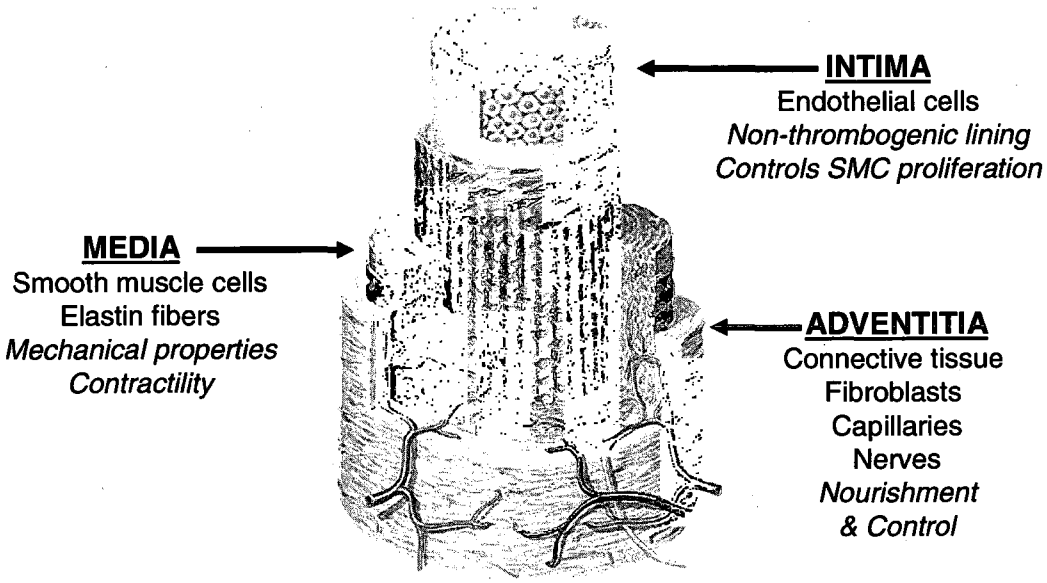

Figure 1-1. Structure of the Arterial Wall.[3] The inner intimal layer consists of a layer of endothelial cells which confers blood compatibility. Smooth muscle cells (SMCs) and highly organized extracellular matrix proteins in the medial layer are primarily responsible for mechanical functionality. The outermost layer, adventitia, consists of connective tissue, microvasculature, and nerves which regulate and nourish the tissue.

The innermost layer, called the intima, consists of an endothelial cell (EC) monolayer that provides a non-thrombogenic conduit for blood flow. Cells of the intima are secured to a basement membrane, which is adjacent to a thin layer of elastic fibers that provide flexibility and maintain the shape of this inner layer. The artery's primary mechanical functionality is conferred by the medial layer, which is populated by smooth muscle cells (SMCs) surrounded by a highly organized extra-cellular matrix. Collagen (mainly types I and III) contribute the majority of the tensile strength of vessel, while elastin fibers provide elasticity. Proteoglycans, like versican and decorin, and hyaluronan dictate the compressive properties and the ECM as a whole results in the vascular viscoelastic behavior.[4] Finally, the adventitia surrounds the artery and contains fibroblasts in a connective tissue permeated by microvasculature and a neuronal network to facilitate autonomic control of the blood vessel.

In normal blood vessels, the endothelium provides a non-thrombogenic surface, providing resistance to the adhesion of platelets and inhibiting the coagulation cascade. The mechanism for this thromboresistance is an EC-mediated homeostasis involving anticoagulant, fibrinolytic, and antiplatelet factors that are either constitutively released or generated in response to offensive stimuli.[5] Platelet activation and adhesion are prohibited by secreted prostacyclin and nitric oxide, and by ecto-ADPase expressed on the EC surface. Anticoagulant molecules are primarily surface bound and include thrombomodulin, herparin-like molecules, von Willebrand factor and protein S. The break down of fibrin is mediated by urokinase-type plasminogen activator and tissue-plasminogen activator (tPA), the latter of which is in turn controlled by plasminogen activator inhibitor-1 to maintain the homeostasis.[5]

1.2.2 Onset and Progression of Vascular Disease

The accumulation of fatty deposits on the vascular wall begins in childhood but does not progress rapidly until damage occurs to the endothelial layer. This injury can be the result of several factors including elevated levels of cholesterol and triglyceride in the blood, high blood pressure, tobacco smoke, and diabetes.[6] Injury to the endothelium is accompanied by a loss of protective factors and increase in adhesive molecules, coagulation activators, and mitogenic factors, which rapidly lead to thrombosis, smooth muscle cell migration and proliferation, and atherosclerosis.[5] In atherosclerosis, lipids, cholesterol, platelets, calcium, and other cellular waste products build up in the vessel wall to form a plaque. When accompanied by the accumulation of a clot and over-proliferating vascular cells, this diseased tissue begins to encroach on the vessel lumen and can block blood flow. It is this final occlusion of the vascular conduit that prompts surgical intervention and in many cases insertion of a vascular bypass graft.

1.3 Current Approaches to Vascular Bypass Grafts

1.3.1 Synthetic Materials and Their Limitations

Synthetic materials such as polyethylene terepthalate (Dacron) and expanded polytetrafluoroethylene (ePTFE or Gore-Tex) work well for peripheral vascular disease and the treatment of vessels with diameters greater than 6 mm.[7, 8] However, these materials are limited to areas of high flow and low resistance[9, 10] due to poor elasticity, low compliance[11] and surface thrombogenicity.[12] A mismatch of material properties (*e.g.* elasticity and compliance) between native tissues and graft materials creates local strain discrepancies and altered flow regimes that contribute to intimal hyperplasia at the site of anastomosis as the result of over-stimulated SMCs.[11] This thickening of the

inner layer of the blood vessel is a common cause of restenosis (*i.e.* re-narrowing of the arterial lumen). In addition, rigid grafts are incapable of storing adequate amounts of elastic energy during systole, and as a result have been shown to propagate less than 60% of this pulsatile energy in diastole.[13] The introduction of polyurethanes as synthetic graft materials has greatly reduced the problems associated with mismatched material properties since its compliance is much closer to that of native vessels.[7] Unfortunately, none of these materials has proven effective in small diameter applications.

In applications of small diameter blood vessels, synthetic devices fail mainly due to thrombosis, which is initiated by the adsorption of plasma protein (e.g. fibronectin) to the material surface. Many of these proteins contain cell binding domains that allow platelet adhesion or thrombin activation on the surface, with the latter stimulating platelet activation, coagulation, and fibrinolysis.[5] The synthetic materials currently available do not possess the thromboresistant qualities of an endothelium, and unfortunately endothelialization of implanted graft materials by cells from the adjacent native vessel is not sufficient (Figure 1-2). Initially SMCs migrate from the adjacent artery and begin to proliferate on the graft surface. This new cell layer is covered by a proliferating layer of endothelial cells.[14] Generally this repair is unsuccessful as over-stimulated SMCs cause intimal hyperplasia at the anastomosis site, resulting in mechanical failure of the device or restenosis of the vessel. Additionally, the slow migration of cells into the implanted biomaterial is quickly surpassed by an almost instantaneous protein adsorption, which as mentioned previously, is a trigger for thrombosis.

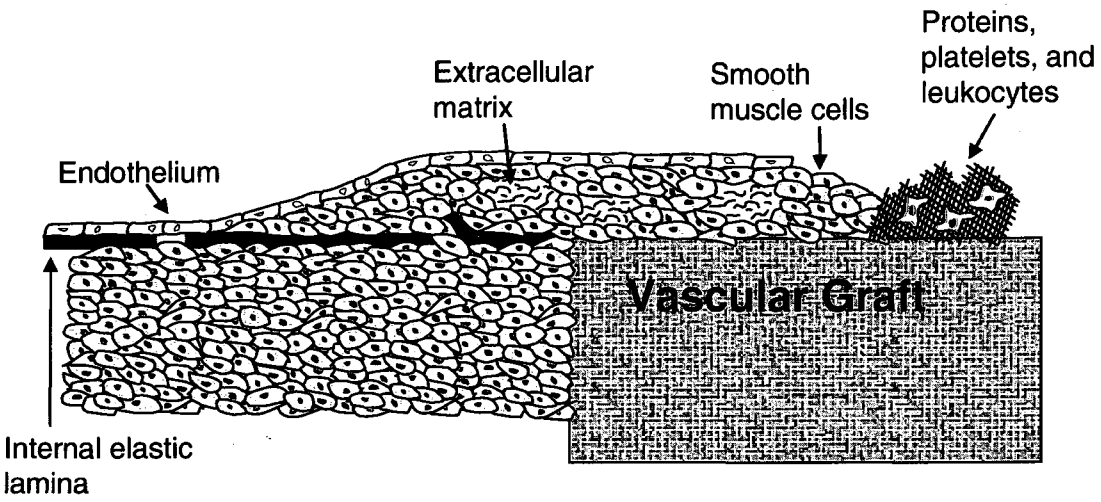

Figure 1-2. Schematic Representation of Vascular Graft Healing Initiated by Smooth Muscle Cell Migration. Cell translocate from the adjacent artery and into the graft material. [14]

1.3.2 Tissue Engineering Approaches

An ideal tissue engineered vascular graft (TEVG) will be biocompatible, contain a confluent endothelium and differentiated quiescent SMCs, and provide sufficient mechanical properties (strength and compliance) at the time of implant to withstand *in vivo* forces and permit suture retention.[15] Tissue engineering approaches to vascular graft development are varied, but in general involve the use of a scaffold in combination with cells and/or other biological factors in an effort to recapitulate native vessel structure and function. Figure 1-3 illustrates the concept of matrix remodeling over time which results in a more native-like tissue.[16] Most often, these constructs are cultured *in vitro* for extended periods of time before implantation in the animal, and frequently some form of bioreactor is used to provide mechanical stimulation during culture.[15, 17, 18]

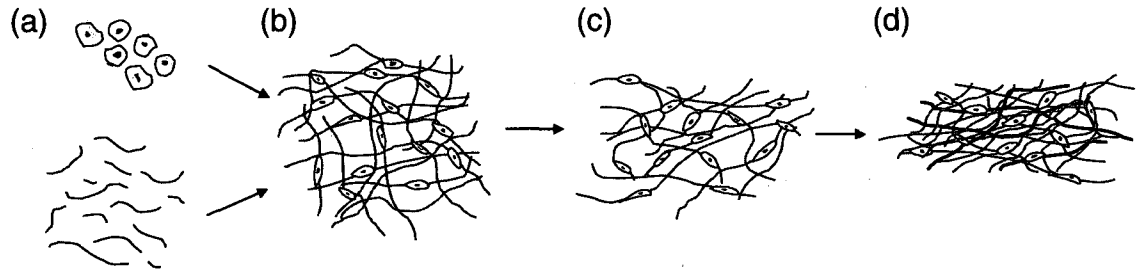

Figure 1-3. Schematic Diagram of Tissue-equivalent Preparation and Maturation. (a) Tissue cells, (e.g. smooth muscle cells or fibroblasts) are mixed with solubilized biomonomers. (b) Addition of a gelation initiator entraps cells within a hydrogel network. (c) Over days, cells contract the network, aligning it in response to mechanical constraints. (d) Over weeks, cells remodel the network, resorbing the original biopolymer and depositing cross-linked collagen fibrils and elastic fibers.[16]

1.3.2.1 Biologically Derived Scaffolds

Collagen is perhaps the most extensively studied scaffold material. In some cases this protein is homogenously purified and then re-solubilized and formed into a gel,[16, 19] and in other instances collagen scaffolds are derived from the ECM of existing tissues (*e.g.* small intestinal submucosa) which have been processed to remove cells and other extraneous components.[20] In either instance, collagen gels are relatively easy to populate with cells, but undergo significant compaction in culture. This compaction, in combination with poor mechanical properties, necessitates the use of a luminal support structure (*e.g.* Dacron) to produce tissue morphologically similar to blood vessels. Tranquillo *et al.* used this contraction to their advantage and placed constructs on a glass mandrel to maintain internal diameter while allowing matrix rearrangement during longitudinal shortening to substantially increase the graft strength.[17] As the major constituent of vascular EMC, collagen has the potential to provide ideal conditions for cellular interactions and matrix remodeling. However, because of poor handling

characteristics and the potential for disease transmission from xenograft sources, collagen matrices are currently not a viable option for vascular graft materials.

In two fairly unique cases, researchers have produced tissue engineered vascular grafts (TEVGs) through non-traditional means. L'Heureux *et al.* cultured SMCs and dermal fibroblasts in monolayer 7 wk and then rolled the thick layers of cells and associated ECM into tubes around a PTFE support.[21] The tubes were cultured in a bioreactor system for an additional 9 wk with ECs seeded in the final 7 d. These constructs had burst strengths of 2000 mmHg, similar to native arteries, but only a 50% patency rate after 1 wk *in vivo*. Perhaps the most significant drawback to this method is the extensive culture time (3 months) required to produce the materials, which precludes its use as a clinical device. In the second case, a silastic tube was inserted into the peritoneal cavities of rabbits and rats and in 2 wk, avascular tissue tubes had formed.[22] When the grafts were implanted in the aorta they showed evidence of active remodeling and 68% remained patent for 4 months. Interestingly, these materials contained significant amounts of elastin, which is known to be important in vascular tissues but notoriously difficult to produce in TEVGs.[22] It is not obvious *a priori* that grafts cultured in humans would develop similarly, but the potential for an autologous cell population is very attractive.

1.3.2.2 Synthetic Scaffolds

Perhaps a logical first step in trying to tissue engineer a small diameter blood vessel is to modify the materials already in use as vascular implants in order to make them less thrombogenic. In attempt to do this, several researchers have seeded endothelial cells on commercially available substrates such as Dacron[23, 24] and ePTFE[25] and allowed

the cells to grow to a confluent monolayer before implantation. ECs on the ePTFE substrate provided 68% patency in peripheral implants.[25] However, these strategies generally employ adsorbed matrix coatings to mediate cellular attachment to the synthetic surface and these coatings are known to spontaneously detach under flow conditions. Denudement results in a loss of protective endothelial cells and exposure of underlying thromboinductive polymer.

Other synthetic polymers investigated for TEVG applications include poly(lactide-*co*-caprolactone) (PLCL),[26] polyglycolic acid (PGA)[18] and polylactic acid (PLA),[27] all of which will spontaneously degrade in culture due to hydrolysis, as well as co-polymers of these materials designed to help mitigate this degradation.[28-31] In contrast, poly(ethylene glycol) or PEG (discussed in detail in a following section) is not susceptible to hydrolysis and due to the potential for covalent modification with proteolytically sensitive moieties, can be designed to allow greater control of the degradation response.[32]

PGA scaffolds were the first used to demonstrate significant potential for the development of vascular grafts *in vitro*.[15] Porous PGA was seeded with SMCs and cultured under pulsatile conditions to create a tissue histologically similar to native vessels. In addition, the new tissue was minimally responsive to contractile agents indicating the potential for *in vivo* functionality. A drawback to this material is the poor mechanical properties of the preliminary mesh, which must be supported during culture to avoid adverse affects of contraction and collapse.[15] Other disadvantages to synthetic polymers in general include a lack of cell interaction capabilities, difficulty in processing, and in some cases, acidic degradation productions which can lead to tissue necrosis.

1.3.2.3 Biochemical Enhancements of TEVGs

In addition to cells and scaffolds, certain types of biochemical factors have garnered notice for their abilities to enhance vascular graft development. Collagen[33, 34] and fibrin[35-37] are popular protein coatings known to enhance cell adhesion to substrates and previously used to attach both ECs and SMCs to synthetic graft materials. This method is complicated, however, by the fact that blood platelet cells will also readily adhere to these ubiquitous matrix proteins and, as such, these specific modifications may actually increase the failure of implanted TEVGs due to thrombosis.[35] To refine this technique and obtain selective cell adhesion, systematic studies of the amino acid sequences of various ECM proteins have produced the minimal peptide unit required for recognition by cell surface receptors.[38-42]

It is now widely known that the integrin binding sequence Arg-Gly-Asp (RGD) derived from fibronectin will bind multiple cells types[43] (including platelets), but that other short peptide sequences like YIGSR or IKVAV from the basement membrane protein laminin will selectively bind ECs and elicit no reactivity from circulating blood cells.[38, 40, 44-48] Jun *et al.* and Massia *et al.* have reported the modification of polymeric materials with YIGSR peptides to generate a significant increase in endothelial cell adhesion, spreading, and migration compared with the unmodified material.[40, 44, 45] In the first study, incorporation of a PEG linker yielded surfaces that were virtually resistant to platelet adhesion.[45] As another example, the peptide VAPG was shown to selectively bind SMCs but not ECs, fibroblasts, or platelets when covalently attached to a PEG hydrogel.[39] SMC adhesion was followed by extensive cell spreading, with both responding to the ligand in a dose dependent manner. These results have important

implications in the creation vascular graft materials which provide selection cell incorporation by are also thromboresistant.

By similar methods (*i.e.* systematic amino acid analysis of ECM proteins), peptide sequences susceptible to cell secreted proteases, such as the matrix metalloproteinases or MMPs, have been identified and incorporated into tissue engineered substrates.[32] These peptides (and thus the engineered matrix they are conjugated to) can be degraded by cells via expression and activation of specifically targeted enzymes such as plasmin, collagenases, and elastases. As a result degradation can be systematically incorporated into otherwise inert materials, like PEG, by evaluating the reaction kinetics and precisely controlling the scaffold formulation.

Other biochemical mediators, including various cytokines, are commonly added as media supplements when culturing vascular graft cells. These include ascorbic acid (vitamin C), transforming growth factor beta (TGF-β) and insulin, which have all been shown to stimulate collagen synthesis by vascular SMCs.[16] In addition, collagen crosslinking agents such as lysyl oxidase[49] or ribose[50] can be added as a media supplement to improve the mechanical properties of TEVGs through ECM stabilization and organization. In some instances, the enzymatic activity of lysyl oxidase has been provided constitutively by transfected SMCs.[51] Platelet derived growth factor (PDGF) is a SMC mitogen and is sufficient transform them from a contractile phenotype, but has no influence on ECs in the quiescent state.[52] Though vascular endothelial growth factor (VEGF) is probably best known for its roles in fetal development and angiogenesis, it is also a potent EC mitogen. This protein further impacts the vascular system by inducing the production of vasoprotective molecules such as nitric oxide and

prostacyclin, which prevent platelet aggregation and leukocyte adhesion in addition to maintaining SMCs in a quiescent state.[52] Consideration must be afforded to all of these factors and more, when designing the optimal strategy for developing a TEVG.

1.4 Biomimetic Poly(ethylene glycol) Hydrogels

PEG has several properties which make it desirable for use as a vessel replacement material. It is known to be relatively inert due to an intrinsic resistance to protein adsorption and cell adhesion[53], which reduces the risk of thrombosis and neointimal hyperplasia common in other synthetic materials. Furthermore, this polymer can be chemically functionalized to have very specific cell interaction moieties including adhesion ligands and segments capable of undergoing cell mediated degradation.[32] Proteins or growth factors, such as those mentioned in the previous section, can be covalently immobilized in a PEG scaffold while maintaining appropriate function.[54] This is a significant advantage because it means that the biochemical factor does not have to be continuously replenished in culture media and instead has prolonged activity, due in part to decreased cellular internalization.

Acrylated PEG mixed with a photoinitiator (2,2-dimethoxy-2-phenyl-acetophenone) is easily polymerized into a hydrated gel upon exposure to long wavelength UV light (10 mW/cm^2, 365 nm) in a process which is amenable to cell encapsulation[55]. A schematic representation of a biomemitic PEG-based hydrogel is shown in Figure 1-4. The low viscosity of PEG precursor solutions means that they are readily formed into various geometries, including tubular structures representative of blood vessels.

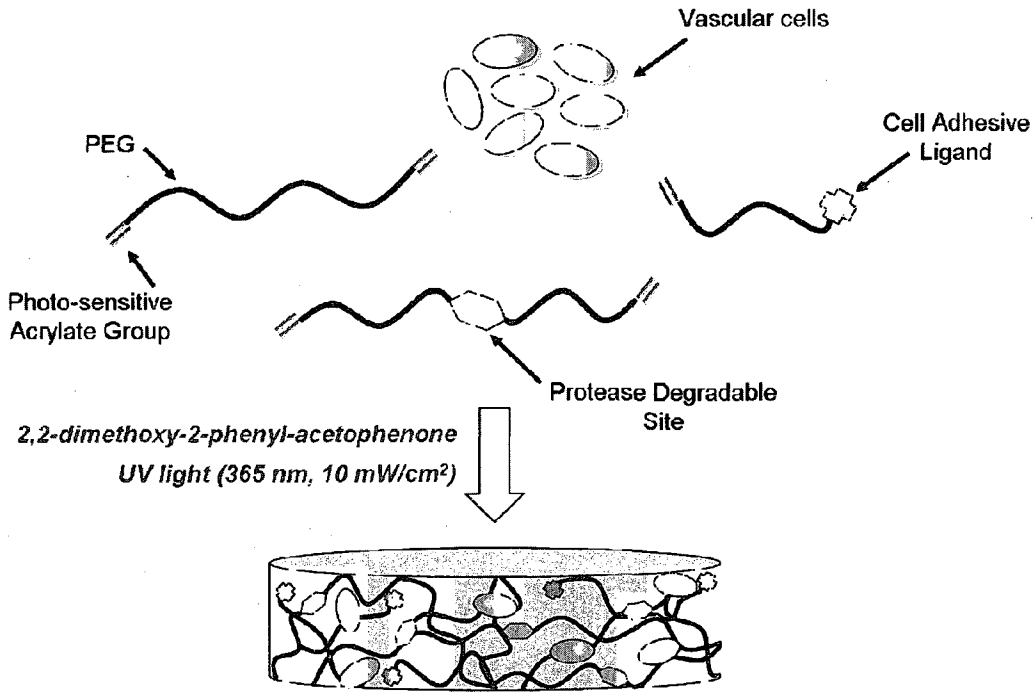

Figure 1-4. Photopolymerization of a Biomimetic PEGDA Hydrogel. Acrylated polymer and functionalized polymer conjugates are made into a hydrated solid upon exposure to long wavelength UV light in the presence of a photoinitiator. This process is compatible with cell encapsulation and the low viscosity of the prepolymer solution makes it amenable to molding into various geometries.

Previous studies have shown the structure of this network to be dependent on the composition of PEG formulation in terms of polymer molecular weight and concentration.[56, 57] Properties of the hydrogel network, including water content and number average molecular weight between crosslinks (M_c), ultimately determine the network mesh size (ζ) and thereby influence the diffusive properties of the material. Since the mechanical properties of hydrogels are dependent on the same factors[58], the relationship between mechanical properties and mesh size has been explored to more fully characterize these materials (current work).

PEG hydrogel properties are predicted to have graded affects on cellular function since recent work indicates that cells actively sense and respond to their substrates,

especially modulations in elastic modulus or rigidity.[59] Because this hydrogel exhibits tunable material properties, there is great potential for its use in fundamental analysis of cell-material interactions, as well as the opportunity to tailor vascular graft substrates for mechanical conditioning.

1.5 Role of Mechanical Stimulation in Developing Vascular Substitutes

1.5.1 The Biological Mechanisms for Cellular Response to Mechanical Environment

Blood vessels reside in a dynamic environment which is continually modulated by fluid forces such as shear, pressure, and strain. In humans the magnitudes of these forces vary from vessel to vessel, but in general arterial shear is 15-25 dyn/cm^2 and venous is 4-5 dyn/cm^2.[60] The strain in the blood vessel wall ranges from 5 – 10%[61, 62] depending on vessel type and patient age/health, and the conventional value for adult blood pressure averages 100 mmHg and varies 20 units above and below this value. On a cellular level, this mechanical stimulation results in the initiation of various signaling pathways directing everything from cytoskeletal rearrangement and migration to programmed cell death.[63] Examples of proposed stretch-induced pathways are shown in Figure 1-5. The transmission of mechanical forces through the ECM and into cells occurs by a number of different mechanisms. Integrins, ion channels, G-coupled proteins, and growth factor receptors[52] all act as sensors for even small changes in force and initiate the transduction of this signal to the nucleus through secondary signaling cascades including PKC, Src, cAMP, FAK and MAPK.[52] The biological affects of these forces on vascular cells have been studied in both two- and three-dimensional experiments, and have significant implications for TEVG development as discussed below.

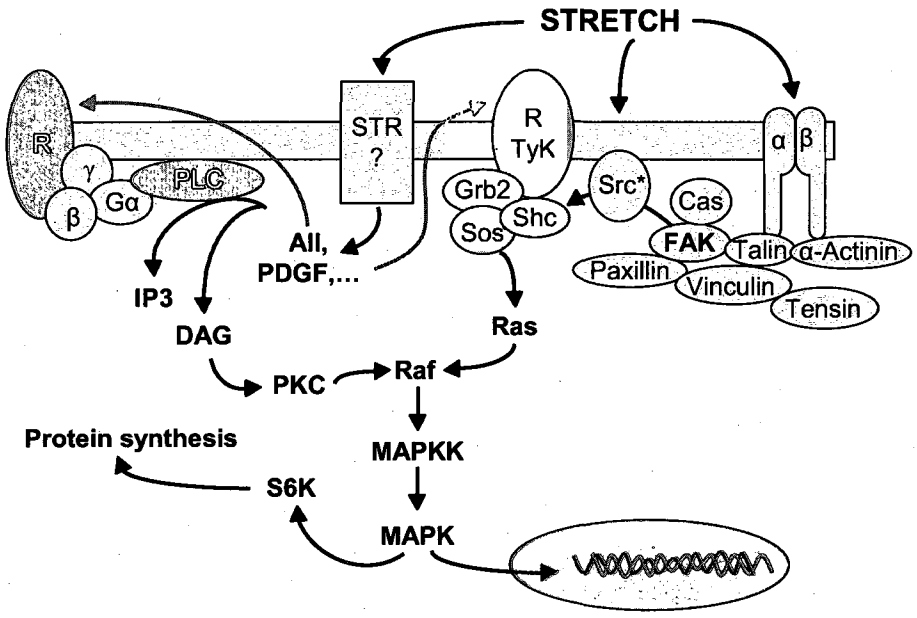

Figure 1-5. Pathways of Mechanical Stretch Transduction in Vascular Cells. Mechanical forces may act on α/ß heterodimer integrins and could activate nonreceptor membrane tyrosine kinases including c-Src*. Activated c-Src* may stimulate FAK autophosphorylation, allowing association of the Shc-Grb2-Sos complex and downstream activation of MAP kinase. MAP kinase may simulate growth or protein synthesis via activation of S6 kinase (S6K). Alternatively, stretch acts on unknown stretch receptors (STR) that stimulate the renin-angiotensin system, leading to the production of Ang II (AII), which in turn acts on G-protein coupled receptors. Autocrine production of growth factors including PDGF may activate tyrosine kinase receptors (R TyK). [63]

1.5.1.1 Response of Cells to Strain and Shear in 2D Culture

Vascular cells cultured in monolayer on distensible substrates have been subjected to cyclic strain and shown to produce significantly more ECM than static controls.[64-66] In ECs strain also promotes migration and tube formation reminiscent of angiogenesis.[67] A study by O'Callaghan and Williams demonstrated increased activity of MMP2 by SMC in cyclic strain which could potentially provide a means of restructuring a TEVG during culture.[65]

Fluid shear forces have also been implicated in a number of biological responses by SMCs including migration and orientation[68], production of NO[69] and even modulation of intracellular pH.[70] In addition, orbital shear stress increased SMC proliferation and induced the normally contractile cells to acquire a synthetic phenotype. The authors surmised that these effects were mediated at least in part by the extracellular signal-regulated protein kinase 1/2 (ERK1/2) pathway based on shear-induced phosphorylation of ERK1/2.[71] This study mimics mechanically induced intimal hyperplasia that would result when SMCs are suddenly exposed to fluid shear forces after injury to the endothelium. Importantly, the authors note clinical relevance by suggesting that this aberrant phenotype is mediated by a pathway amenable to pharmacologic intervention.[71] What they fail to acknowledge, however, is that this result also has significant implications in the design of TEVGs.

One of the goals of vascular tissue engineering is to create a morphologically appropriate medial layer that will include diffuse cellularity and dense, highly organized ECM. To facilitate this, it has been suggested that cells of the synthetic phenotype should be utilized.[52] However, this strategy fails to encourage the contractile function of the vessel cells, which will become important upon implantation *in vivo*. At present it is not obvious if the synthetic phenotype will spontaneously reverse, so alternatively, it may be better to investigate whether certain growth factor cocktails would induce SMC proliferation and ECM production without a loss of the contractile functionality. Drawing definitive conclusions is difficult; especially since it is still unclear how 2D studies like this one relate to 3D culture, and because seemingly contradictory experiments with explanted arteries indicate that endothelial denudement (*i.e.* exposing

SMCs to shear forces) results in appreciable tissue deterioration and wall cell death not otherwise observed for intact controls.[72]

A large number of studies have also investigated the affect of shear on endothelial cells. McIntire and colleagues have spent over two decades elucidating this relationship, more recently with the use of a custom parallel plate flow chamber.[73] Their work has demonstrated that shear forces result in changes in EC morphology and orientation[74, 75], and metabolism[76, 77]. The endothelium initiates a protective response to altered shear regimes as evidenced by increases in antiaggregatory (NO[78], prostacyclin[79, 80]), and profibrinolytic (tissue plasminogen activator[80]) factors and a decrease in the mRNA levels for a SMC mitogen.[60] Microarray studies analyzing cDNA from stimulated cells have provided an abundance of potential gene targets for endothelium therapy applications[81] and tools for extending basic understanding of EC response mechanical stimuli.[82]

Though the exact relationship between the responses of cells on these 2D substrates and those encapsulated in a 3D scaffold is not presently clear, it is evident that vascular cells are sensitive and highly responsive to their mechanical environment. As illustration, recent DNA microarray analysis of co-cultured ECs and SMCs subjected to physiological shear (12 dyn/cm^2) for up to 24 h found differential expression of an astounding 1151 genes.[83] These data allude to the magnitude and complexity of cellular responses to applied mechanical stimuli and reiterate the importance of considering all aspects of the native vessel environment when attempting to recapitulate synthesis of new vascular tissue.

1.5.1.2 Effect of Applying Mechanical Stimulation during TEVG Culture

Blood vessels are exposed to mechanical force during much of vasculogenesis and throughout the tissue's life, so it therefore seems logical that *de novo* synthesis of TEVGs may also benefit from similar stimulation.[15] This hypothesis has been supported by the positive effects of *in vitro* cyclic strain and physiological shear on SMC differentiation and ECM production and organization described previously, and as a result a number of biomimetic bioreactors have been developed.[2, 49] The primary goal of these systems is to improve graft mechanical properties by stimulating the accumulation of a functional ECM.[49]

In a number of cases, cyclic distension has been employed for culture of medial layer equivalents.[15, 17, 19] Typically, cell seeded constructs are cultured over silicone tubing or a similar support device (Figure 1-6), which is inflated to produce cyclic distension of between 5% and 20% and a periodic rate mimetic of either adult or fetal pulsing conditions (60 or 165 beats per min, respectively).[15, 17, 19, 49] The use of a luminal support device makes co-culture of an endothelial layer impossible and may limit nutrient exchange within the graft. Unfortunately, the support is necessary for many of these materials (*e.g.* collagen) because of poor mechanical properties and drastic scaffold compaction after synthesis.[17]

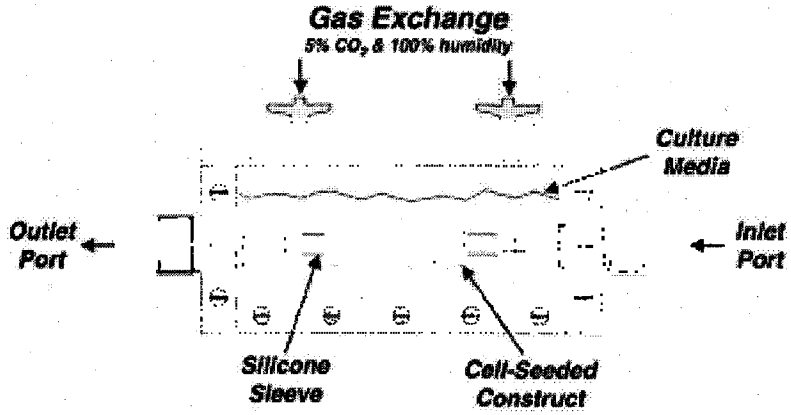

Figure 1-6. Sample Bioreactor Unit. An experimental bioreactor is used to impart cyclic strain onto cell-seeded constructs. The tubular constructs are cultured over thin-walled silicone sleeves that are inflated with pressurized culture medium under pneumatic control to produce a 10% change in the outer diameter of the silicone. Grafts are not in contact with flowing medium. Gas exchange takes place through 0.2 mm syringe filters placed on the top of the bioreactor.[19]

The results from these systems are promising. Niklason, *et al.* cultured PGA scaffolds seeded with SMCs for 8 wk under pulsatile stress and concluded that the resulting tissue was similar to native in terms of collagen content and burst strength.[15] In other work with PGA, Kim *et al.* applied strain at a frequency of 1 Hz and amplitude of 7% and increased both cell density and extracellular matrix production.[18] Elastin production in particular was increased 49% over static controls. Furthermore, cells at the surface and within the mechanically stimulated constructs showed an extremely high occurrence of alignment perpendicular to strain axis after 10 wk in culture. While the mechanical properties of tissue engineered vessels in these experiments did not approach those of native arteries, the dramatic effect on ECM production supports the use of this type of stimulation during culture of TEVGs.[18]

Seliktar and colleagues measured circumferential tensile properties of collagen constructs seeded with SMCs and cultured under dynamic conditions (10% strain, 1

Hz).[19] Again the mechanical stimulation resulted in cell alignment and improved material properties. Interestingly, it also resulted in considerable alignment of collagen fibers within the gel, which were not seen in static controls.[19] Later worked determined that this ECM organization was mediated by an increase in active MMP2 within the constructs[84], which has implications not only for this type of graft maturation, but also for aiding directed degradation of specifically designed substrate materials discussed previously. Furthermore, the authors hypothesize that even greater enhancement of *in vitro* vascular graft development will likely result from optimization of the dynamic culture conditions including both the amplitude and frequency of strain.[19]

Perfusion bioreactors have the added advantage of serving as means for seeding ECs onto the luminal surface of TEVGs.[85-87] Cell attachment is accomplished either by circulating cells at low flow rates or using fluid pressure to force cells into the interstices of the scaffold. The latter method is termed cell sodding.[88] Both methods were investigated for an ePTFE graft functionalized with RGD and the authors report that while sodding improved initial attachment to the graft, there is a significant loss of cells due to handling during simulated implantation manipulation.[86] Perhaps the constructs would have benefited from continued mechanical stimulation following cell attachment to allow ECs to proliferate and fully cover the surface and establish more permanent interactions. In the Niklason study mentioned previously, after 8 wk of pulsatile conditioning, grafts were removed from the luminal support tubing and seeded with ECs under constant flow.[15] Flow was continued for an additional 2 d, after which, the grafts were implanted and subsequently remained patent for 4 wk *in vivo*.[15]

While there seems to be overwhelming evidence in support of mechanical stimulation during TEVG development, the precise nature of this conditioning has yet to be determined.[58] Additional insight may be obtained from work with blood vessels that are explanted and maintained in culture. Gooch and co-workers have devoted significant energies to developing an *ex vivo* perfusion system that preserves tissue viability and key morphological characteristics for up to 28 days.[72, 89] Data from these studies suggest that vessels may be more susceptible to deterioration as the results of increased flow rather than pressure, and also indicate that the endothelium has important protective roles that may necessitate earlier EC seeding for dynamically conditioned TEVGs.[72] Finally, work with both neonatal and adolescent arteries suggest that ideal *ex vivo* flow conditions may be appreciably different from the *in vivo* environment.[72, 89] The exact reason for this discrepancy is unclear, but likely results from a failure to completely recapitulate all of the *in vivo* mechanical constraints. As an example, blood vessels are known to be maintained under longitudinal tension in the body, but this restraint is rarely applied for *ex vivo* culture. These results provide a model for analyzing the mechanical environment of such tissue and a platform from which to generate optimized matrix formulations and culture conditions for tissue engineered materials. In combination with previously discussed TEVG work, these studies provide substantial motivation for continued analysis of construct scaffold and culture conditions as a means of developing a more functional small diameter vascular graft.

2. Biomimetic Poly(ethylene glycol) Hydrogels

2.1 Introduction

Polymers, metals, and ceramics have been widely used as materials in biology and medicine for many years. However, despite the applications of these biomaterials to thousands of medical devices, many lack the ability to properly interface with the biological environment and few have been engineered for optimal performance.[90] Hydrogels are a rapidly expanding class of materials that can be specifically designed to fill this void. These aqueous materials are formed from hydrophilic polymers that are chemically or physically crosslinked to prevent dissolution. High water content and biocompatibility make hydrogels attractive options for cell immobilization and for applications in tissue engineering, drug delivery, and bionanotechnology.[90, 91]

When in service as cell scaffolds or as materials for tissue engineering applications, hydrogels must meet several broad requirements: biocompatibility, non-toxicity, and appropriate mechanical properties. Ideal hydrogel properties must be determined based on the specific tissue application and with consideration for the cell type(s) targeted. In general, high water content is desirable to maintain cell viability and the mechanical properties of the material should be able to withstand any *in vitro* conditioning regimes and *in vivo* forces upon implantation. In addition, the material must possess transport properties that allow diffusion of nutrients and waste products in and out of the pericellular space.[92]

Poly(ethylene glycol) (PEG) is a popular biomaterial choice for tissue engineering based primarily on the polymer's good compatibility with both chemicals and biological environments, low toxicity, and high water solubility.[93] Because of its low toxicity,

PEG has been used in cosmetics and as a stealth coating for the delivery of pharmaceuticals which may be otherwise unstable in the body or have poor solubility.[94] PEG acts as a non-fouling material meaning that it resists protein adsorption and as such becomes essentially invisible in biological environments – avoiding interactions with cells and the immune system.[53] Photopolymerized PEG forms a solid hydrogel material upon exposure to UV light and has been biochemically modified for use as a substrate for a variety of cell types.[32, 57, 95-99]

The overall goals for work in this chapter were to synthesize and characterize the hydrogel materials to be used in future cell applications. This included fabrication of PEG-diacrylate (PEGDA) hydrogels from a range of monomer molecular weights (MW) and in different formulations in order to thoroughly understand the bulk properties of available materials. Biomimetic hydrogel components were synthesized by reacting peptides with PEG-monoacrylate. The peptides used in these studies were designed to promote cell adhesion and allow controlled degradation of the hydrogel matrix. The final objective was to evaluate the incorporation of peptides into these materials, confirming the independent control of biochemical and biomechanical properties in this hydrogel system.

2.2 Methods and Materials

All materials are from Sigma-Aldrich (St. Louis, MO) unless noted otherwise.

2.2.1 Synthesis of PEGDA and PEGDA Derivatives

PEGDA was prepared by combining 0.1 mmol/mL dry PEG (MW 3400 Da, 6000 Da, 10000 Da, or 20000 Da), 0.4 mmol/mL acryloyl chloride (Lancaster Synthesis, Windham, NH), and 0.2 mmoL/ml triethylamine in anhydrous dichloromethane (DCM)

and reacting under argon overnight (Figure 2-1). The solution was then mixed with 2 M K_2CO_3 (Fisher Scientific, Pittsburgh, PA) and allowed to separate into aqueous and organic phases. The organic phase was isolated and subsequently dried with anhydrous $MgSO_4$ (Fisher), and PEGDA was precipitated in diethyl ether (Fisher), filtered, and dried *in vacuo*. Successful acrylation was determined using proton NMR analysis (Avance 400, Bruker, Billerica, MA).

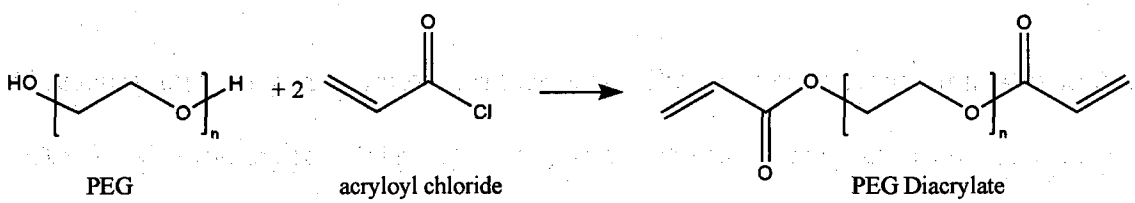

Figure 2-1. PEGDA Reaction Scheme. PEGDA is synthesized by reacting poly(ethylene glycol) with acryloyl chloride under anhydrous conditions.

The peptide RGDS (American Peptide, Sunnyvale, CA) was conjugated to PEG monoacrylate (3400 Da) by reaction with acryloyl-PEG-*N*-hydroxysuccinimide (acryloyl-PEG-NHS, Nektar, Birmingham, AL) at a 1:1 molar ratio for 2 hr in 50 mM sodium bicarbonate buffer, pH 8.5. The collagenase sensitive peptide sequence GGLGPAGGK was synthesized using Fmoc solid phase peptide synthesis and subsequently cleaved from the polystyrene resin by reaction with 95% trifluoroacetic acid, 2.5% deionized (DI) water, and 2.5% triisopropylsilane. The cleaved peptide was precipitated in ether, filtered, dried, and dialyzed against DI H_2O. The peptide was then reacted at a 1:2 molar ratio with acryloyl-PEG-NHS in 50 mM sodium bicarbonate buffer for 2 hr. PEG modification reactions are shown in Figure 2-2. The acrylated products (PEG-RGDS and PEG-LGPA-PEG) were purified by dialysis, lyophilized, and stored at -20°C until use. A

gel permeation chromatography system equipped with UV/vis (260nm) and evaporative light scattering detectors (Polymer Laboratories, Amherst, MA) was used to analyze the resulting PEG-peptide copolymers and confirm successful conjugation.

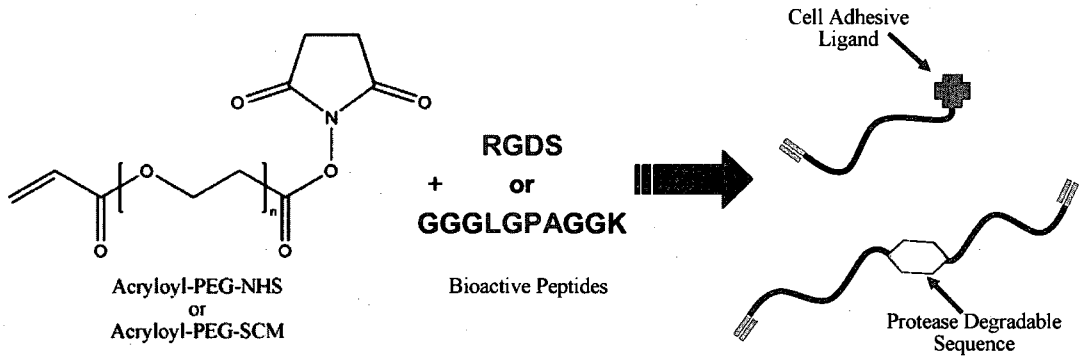

Figure 2-2. Schematic Representation of the Reaction to Create Bioactive PEG Moieties.

During the progress of this work, a change in the commercial practices of Nektar Co. led to the investigation of other sources of functionalized PEG. A product similar to acryloyl-PEG-NHS is acryloyl-PEG-succinimide (acryloyl-PEG-SCM, MW 3400, Laysan Bio, Birmingham, AL) which has the same functionalization but a minor modification to the linker between the PEG chain and the *N*-hydroxysuccinimide reactive group. This modification decreases the ester half-life to 0.75 minutes in aqueous solutions necessitating a protocol change for conjugation reactions. Various organic solvents were investigated before choosing dimethyl sulfoxide (DMSO) based primarily on good solubility of both acryloyl-PEG-SCM and the peptides of interest.

To create cell adhesive molecules, the commercially available RGDS was conjugated to acryloyl-PEG-SCM at a 1.1:1 molar ratio for 24 hr in DMSO using N,N-

diisopropylethylamine (DIPEA) as a base. In addition an RGD peptide sensitive to spectrophotometric detection (GGGWGGRGDS) was synthesized using Fmoc solid phase peptide synthesis as described previously and then conjugated in the same manner as the commercial product. The collagenase sensitive peptide, GGGPQGIWGQGK, was also synthesized and reacted at a molar ratio of 1:2.1 with Acryloyl-PEG-SCM in DMSO with DIPEA as a base. As before, the acrylate derivatized products (PEG-RGDS, PEG-WRGDS, and PEG-PQ-PEG) were purified by dialysis, lyophilized, and stored at -20°C until use.

2.2.2 Photopolymerization of PEGDA Hydrogels

Polymer solutions containing the desired concentrations of PEGDA and PEGDA-peptide conjugates in 10 mM HEPES buffered saline (pH 7.4, HBS) were mixed with a 300 mg/mL solution of the UV photoinitiator 2,2-dimethoxy-2-phenyl-acetophenone dissolved N-vinylpyrrolidone (NVP) at a ratio of 10 μl per mL polymer. The solutions were transferred to transparent molds and exposed to UV light (365 nm, 10 mW/cm^2, UVP, Upland, CA) for 2 min to form hydrogels.

2.2.3 Hydrogel Network Structure Characterization

An understanding of the physical makeup of polymeric hydrogels is important in determining their potential application as biomaterials. The bulk structure of these covalently crosslinked networks influences material properties such as strength and stiffness and also dictates key parameters in biological applications such as water content and permeability. The three most important parameters for characterizing the network structure of hydrogels are the molecular weight between neighboring crosslinks (M_c), the polymer volume fraction in the swollen state ($V_{2,s}$), and the mesh size (ζ).[90] As a

substitute to $V_{2,s}$, one may also report the water content of the material of interest, as in the analysis below. The parameters are obtained through application of the Flory-Rehner theory which assumes that a nonionic hydrogel submerged in a fluid at equilibrium is acted upon by only two forces: the thermodynamic force of mixing between the polymer chains and the fluid, and the elastic retractive force of the polymer chains.[100] Other important hydrogel transport parameters are the mass and volume swelling ratios, q and Q, with these and all previously mentioned metrics, related to one another fundamentally through the material crosslink density, ρ_x.[92]

To analyze network structure and swelling characteristics, PEGDA hydrogels of four different molecular weights (3,400 Da, 6,000 Da, 10,000 Da, and 20,000 Da) and three concentrations (0.05 g/mL, 0.1 g/mL and 0.2 g/mL) were prepared in rectangular glass molds. Additional formulations containing 0.01 g/mL PEG-LGPA-PEG and a mixture of 0.07 g/mL 6,000 Da PEGDA and 0.03 g/mL PEG-LGPA-PEG were evaluated in anticipation of their use in the bioreactor studies with cells. For each formulation, 11 mm diameter disks were photographed, weighed, and then placed in HBS (pH 7.4) for 48 hr to achieve swelling equilibrium. After this time, equilibrium swelling masses were recorded and more digital images acquired. The disks were then dried in a vacuum oven for 48 hr at which point the dry mass of each sample was obtained. Digital images were analyzed to calculate change in surface area with swelling, and the water content, M_c, and ζ were calculated using the following equations:[56]

Equation 2-1. Hydrogel Water Content

$$Water\ Content\ (\%) = \frac{Swell\ Weight - Dry\ Weight}{Swell\ Weight} * 100$$

Equation 2-2. Molecular Weight Between Crosslinks, M_c

$$M_c = \left(V_e + \frac{2}{M_{n(0)}} \right)^{-1}$$

where $M_{n(0)}$ is the number average molecular weight of the starting polymer, and V_e is the number of effective chains per unit volume as defined by

Equation 2-3. Number of Effective Polymer Chains per Volume, V_e

$$V_e = -\frac{\frac{\nu}{V_1}\left[\ln(1-V_{2,s}) + V_{2,s} + \mu V_{2,s}^2\right]}{V_{2,r}\left[\left(\frac{V_{2,s}}{V_{2,r}}\right)^{1/3} - \frac{1}{2}\left(\frac{V_{2,s}}{V_{2,r}}\right)\right]}$$

in which ν is the specific volume of bulk PEG in the amorphous state (0.893 cm^3/g), V_1 is the molar volume of water (18 cm^3/mol), and $V_{2,r}$ and $V_{2,s}$ are the polymer fraction of the hydrogel in the relaxed and swollen state, respectively. A value of 0.426 was used for the Flory-Huggins polymer-solvent interaction parameter (μ), since it was previously found to be constant over a range of $V_{2,s}$ values from 0.04 to 0.2 for PEG in water and PBS.[56]

The hydrogel mesh size in angstroms is calculated as follows

Equation 2-4. Mesh Size, ζ

$$\zeta = \left(r_0^{-2}\right)^{1/2} V_{2,s}^{-1/3}$$

with the average end-to-end distance of the solvent free state of the polymer calculated as

Equation 2-5. End to end Polymer Distance

$$\left(r_0^{-2}\right)^{1/2} = l\left(2\frac{C_n M_c}{M_r}\right)^{1/2}$$

where l is the bond length (1.50 Å), M_r is the molecular weight of the PEG repeat unit (44 g/mol) and C_n is the characteristic ratio for PEG (4). [101]

The mass swelling ratio, q, and the volume swelling ratio, Q, were calculated as follows

Equation 2-6. Mass Swelling Ratio, q

$$q = \frac{M_s}{M_d}$$

Equation 2-7. Volume Swelling Ratio, Q

$$Q = 1 + \frac{\rho_p}{\rho_s}(q - 1)$$

with M_s and M_d equal to the swollen and dry masses of the hydrogel, respectively, and ρ_p and ρ_s the densities of PEG and the solvent. Crosslink densities, ρ_x, for each formulation were computed as

Equation 2-8. Crosslink Density, ρ_x

$$\rho_x = \frac{1}{\nu M_c}$$

2.2.4 Evaluation of Hydrogel Mechanical Properties

Mechanical testing was performed on PEGDA hydrogels of the same formulations used in the network structure analysis above. Dog bone-shaped samples conforming to ASTM D638 standards were cut from pre-swelled hydrogels that had been cast in rectangular molds. Sample dimensions were obtained using digital calipers, and material properties were measured on an Instron Model 3340 materials testing device equipped with a 10 N load cell (Norwood, MA). System control and data analysis were accomplished using Instron Series IX/s software. Uniaxial strain was applied at a rate of 6 mm/min, and the stress-strain data collected was used to calculate the ultimate tensile strength (UTS) and

average elastic modulus. Modulus was defined as the slope of the linear region of the stress-strain curve at a reference stress of 30 kPa.

2.2.5 Analysis of Bioactive Peptide Incorporation into PEGDA Hydrogels

Bioactive moieties, such as the RGDS adhesive ligand, are covalently attached to the PEGDA hydrogel during photopolymerization. The total incorporation of these molecules depends primarily on two properties of the PEG monoacrylate – percent acrylation and conjugation efficiency. It is also reasonable to expect that PEGDA hydrogels that possess significantly different network structures will also incorporate monoacrylated-moities at different rates due to the number and presentation of acrylates in the base hydrogel. To characterize this phenomenon, a spectrophometric method was employed.

The amino acid tryptophan, W, was conjugated to acryloyl-PEG-SCM in a reaction similar to the one described for the peptide RGDS above (2.2.1). L-tryptophan (Sigma) was reacted at a ratio of 50:1 with acryloyl-PEG-SCM in DMSO with a small amount of water to increase amino acid solubility. DIPEA (2 mol per mol PEG) was added and the reaction placed on a rocker at room temperature overnight. The reaction was then diluted 1:1 with water and dialyzed against 1,000 MWCO regenerated cellulose to remove unreacted W. Following dialysis the product was frozen, lyophilized, and stored at -20°C until use.

A 20 mM solution of PEG-W in diH_2O was read on a Cary 50 BIO UV Vis spectrophotometer (Varian Analytical Instruments, Walnut Creek, CA) to obtain the absorbance at 280 nm (ABS_{280}). The molar extinction coefficient of W (5690 M^{-1}) was then used to determine the actual concentration of the solution and thereby the

conjugation efficiency of the reaction. The PEG-W solution was added to volumes of 3,400, 6,000, 10,000, and 20,000 PEGDA to achieve final concentrations of 0, 1, and 2 mM PEG-W. DMAP was added (10 μL/ mL PEGDA) and the solutions allowed to polymerize for 2 min in rectangular molds. Once formed, the hydrogels were soaked in HBS with 0.2 mg/mL sodium azide, and the soak solution changed daily for seven days.

After seven days in HBS, the thickness of each hydrogel was measured using digital calipers. The ABS_{280} of each sample was obtained by placing the hydrogels between two glass slides and inserting it in the spectrophotometer. For each formulation, the 0 mM PEG-W specimen was used as a blank, and the thickness of the gel served as the path length. The ABS_{280} of the rinse solution from each hydrogel sample was also recorded.

2.3 Results and Discussion

2.3.1 Synthesis of PEGDA and PEG Derivatives

PEGDA synthesis resulted in polymer products of 3,400, 6,000, 10,000 and 20,000 Da with acrylation percentages at 80% or greater based on NMR. The yield of conjugated product from the reaction of peptides with acryloyl-PEG-NHS and acryloyl-PEG-SCM is >85% by GPC analysis. For reasons not completely obvious, conjugation to acryloyl-PEG-SCM results in a reduction of its acrylate signal from nearly 90% to less than 50%, which effects incorporation of these products into hydrogels (see 2.3.4 below).

2.3.2 Characterization of Hydrogel Network Structure

The results of the hydrogel network structure characterization are in Table 2-1. As expected, the materials all have high water content (85-98%) and the level of hydration increases with decreasing polymer concentration. Properties of the 70% mixed formulation of 6,000 Da PEGDA and PEG-LGPA-PEG are similar to those for the 6,000

Da gels, while 100% degradable PEGDA lies somewhere between the 10,000 and 20,000 Da formulations. The 0.05 g/mL 20,000 Da formulation has a $V_{2,s}$ value of 0.02, which is just outside the allowable 0.04 for the Flory-Huggins polymer-solvent interaction parameter and as such the calculations dependent on this coefficient may not be completely accurate. However these data are included in Table 2-1 because they do not appear to deviate from other results.

In general, mesh size increases with both increasing molecular weight and decreasing solution concentration, with molecular weight be the most influential factor of the two. The network spacing determined by these results varies from 25 Å to 164 Å and is sufficient for allowing the diffusion of a range biologically relevant molecules from glucose (~3.5 Å)[102] to IgG (~55 Å) [103]. The molecular size between crosslinks, M_c, describes the actual distance between polymerization points and takes into account the chain interactions that occur in these types of materials. In all cases M_c is less than the theoretical maximum distance M_n, indicating that the polymer chains are at less than full extension and/or are entangled.

The mass and volume swelling ratios, q and Q, are related to one another through the specific volume of the polymer, so as expected have paralleled correlations. Both are included in Table 2-1 for completeness and ease of comparison with external studies, though typically only one or the other is necessary. The much larger swelling ratios for 20,000 Da PEGDA formulations are indicators of the significant polymer rearrangements that occur in these hydrogels in comparison to lower MW materials. Also telling is the scale of the crosslink density, ρ_x, which is an order of magnitude higher in 3400 Da

hydrogels compared to those comprised of 20,000 Da PEGDA. These results show good agreement with previous studies involving similarly sized PEG polymers.[104]

Table 2-1. Network Properties of PEGDA Hydrogels

Molecular Weight, M_n (Da)	Concentration (g/mL)	Water Content (%)	Mesh Size (Å)	M_c (Da)	q	Q	ρ_x (mol/L)
3,400	0.05	94 ± 0.2	39 ± 2	592 ± 46	15 ± 0.6	17 ± 0.7	1.9 ± 0.1
	0.1	89 ± 0.6	27 ± 2	411 ± 47	9 ± 0.4	10 ± 0.6	2.7 ± 0.3
	0.2	85 ± 1	25 ± 2	441 ± 56	6 ± 0.4	7 ± 0.5	2.6 ± 0.3
6,000	0.05	94 ± 0.4	44 ± 4	754 ± 107	16 ± 1	18 ± 1.1	1.5 ± 0.2
	0.1	90 ± 0.3	33 ± 1	584 ± 34	10 ± 0.2	11 ± 0.3	1.9 ± 0.1
	0.2	87 ± 0.3	32 ± 1	673 ± 31	7 ± 0.2	8 ± 0.2	1.7 ± 0.1
10,000	0.05	94 ± 0.6	53 ± 8	1030 ± 239	17 ± 1.8	19 ± 2	1.1 ± 0.3
	0.1	92 ± 0.2	47 ± 1	1038 ± 48	12 ± 0.3	14 ± 0.3	1.1 ± 0.1
	0.2	90 ± 0.2	49 ± 4	1257 ± 17	9 ± 0.9	10 ± 1	1.0 ± 0.2
20,000	0.05	98 ± 0.2	*164 ± 14**	*5309 ± 525**	44 ± 1.8	49 ± 5	*0.2 ± 0**
	0.1	97 ± 0.5	141 ± 11	5011 ± 468	30 ± 3.2	34 ± 4	0.2 ± 0
	0.2	95 ± 0.5	112 ± 9	4289 ± 448	19 ± 1.7	21 ± 2	0.3 ± 0
70% Degradable	0.1	90 ± 0.2	37 ± 0.9	694 ± 25	10 ± 0.2	12 ± 0.2	1.6 ± 0.1
100% Degradable	0.1	95 ± 0.1	72 ± 0.7	1813 ± 21	18 ± 0.2	20 ± 0.2	0.6 ± 0

Notes: Degradable formulations are mixtures of PEG-LGPA-PEG and 6000 Da PEGDA and also include 2.8 μmol/mL PEG-RGDS.
**Because the $V_{2,s}$ values of the 20k Da 0.05 g/mL data set are 0.02 they are just outside the allowable 0.04 for the solvent interaction parameter and as such these data points may not be accurate. All data are mean ± standard deviation.*

By digital image analysis, the change in hydrogel surface area from initial polymerization to the equilibrium swelling point was calculated. As shown in Figure 2-3, the most highly concentration formulations exhibit the greatest change in shape. The weight change over the same time period is displayed in Figure 2-4, and is not to be confused with the mass swelling ratio, q, which is based on the change from dry polymer. The percent change in weight for each formulation is greater than the change in surface area, but it is the dimensional change associated with hydrogel swelling that generally presents the most experimental relevance. For example, morphological transformations in progress to equilibrium must be accounted for when synthesizing materials to fit certain physical restraints in testing or conditioning devices. In addition, changes in the total surface area of a substrate result in rearrangement of factors immobilized in the hydrogel matrix (*e.g.* cell adhesion ligands).

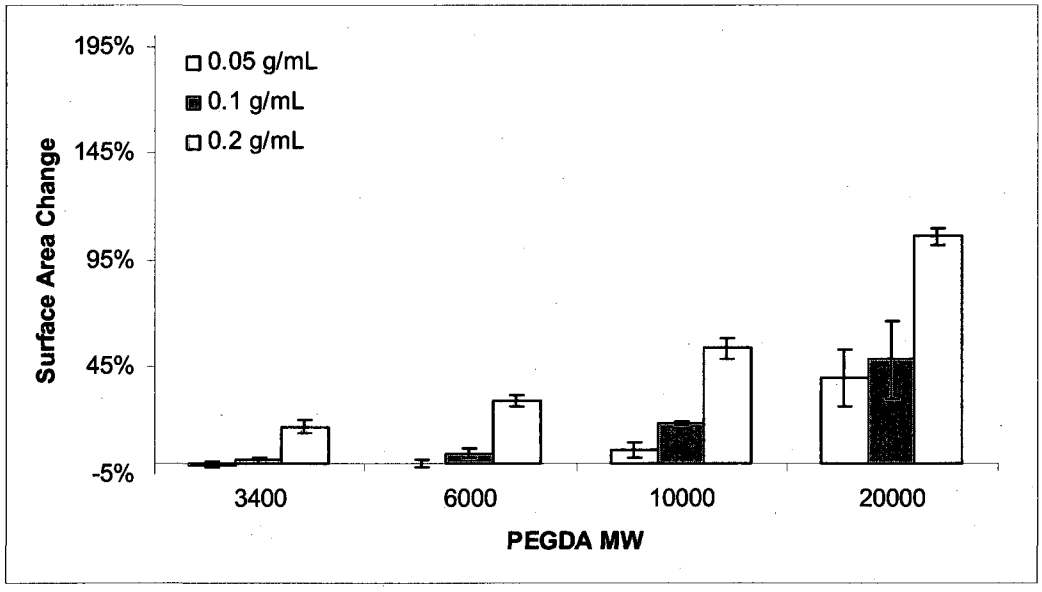

Figure 2-3. Surface Area Change in Hydrogels from Synthesis to Equilibrium Swelling. High MW and solution concentrations result in the greatest change from the initial state, while low MW PEGDA/low concentration combinations actually cause a slight contraction of the matrix.

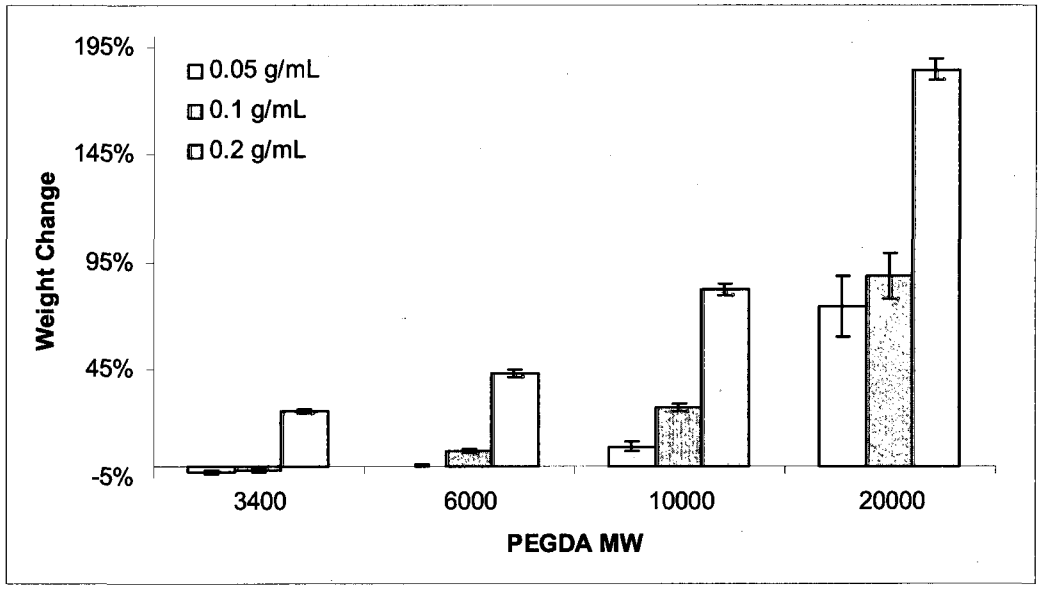

Figure 2-4. Weight Change in PEGDA Hydrogels from Synthesis to Equilibrium Swelling. High MW and solution concentrations result in the greatest change from the initial state, while low MW PEGDA/low concentration combinations actually cause a slight contraction of the matrix.

2.3.3 Evaluation of Hydrogel Mechanical Properties

The PEGDA hydrogel material properties were obtained via tensile tests conducted on the Instron. Evaluation of the 0.05 g/mL 20,000 Da gels was not accomplished due to the poor handling characteristics of these samples. As shown in Figure 2-5 below, as polymer molecular weight increases and/or solution concentration is decreased, the elastic modulus of the material decreases. This trend correlates well with the mesh size data discussed above, and indicates that hydrogels that possess a more open network structure are also less stiff. Though the relationship between polymer molecular weight and ultimate tensile strength is not clear, there is an increase in material strength with increasing solution concentration (Figure 2-6).

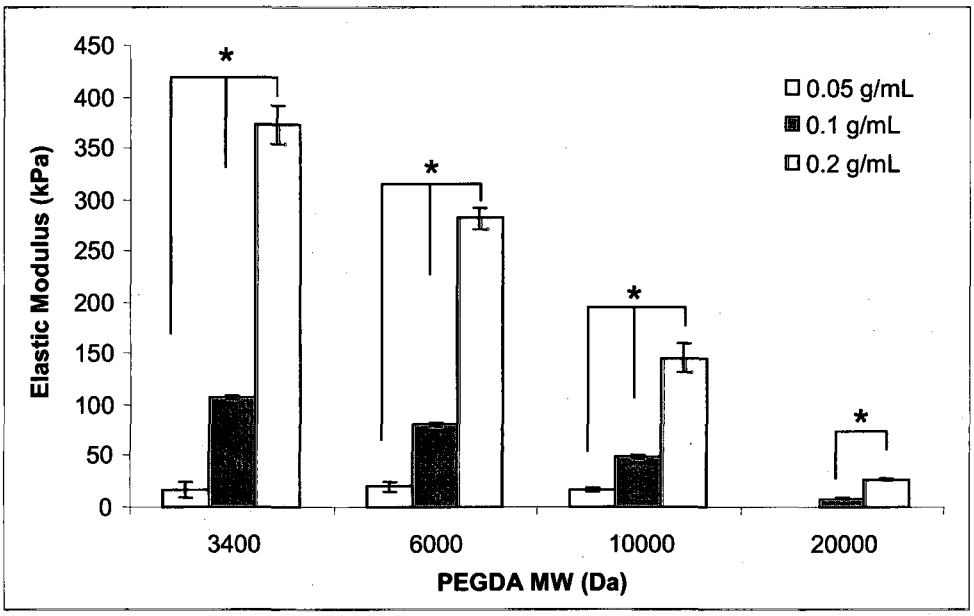

Figure 2-5. Elastic Modulus of PEGDA Hydrogels. A clear relationship between hydrogel formulation and stiffness was demonstrated by varying polymer molecular weight and solution concentration. *p< 0.05, other significant differences exist but are not designated here for clarity of the data.

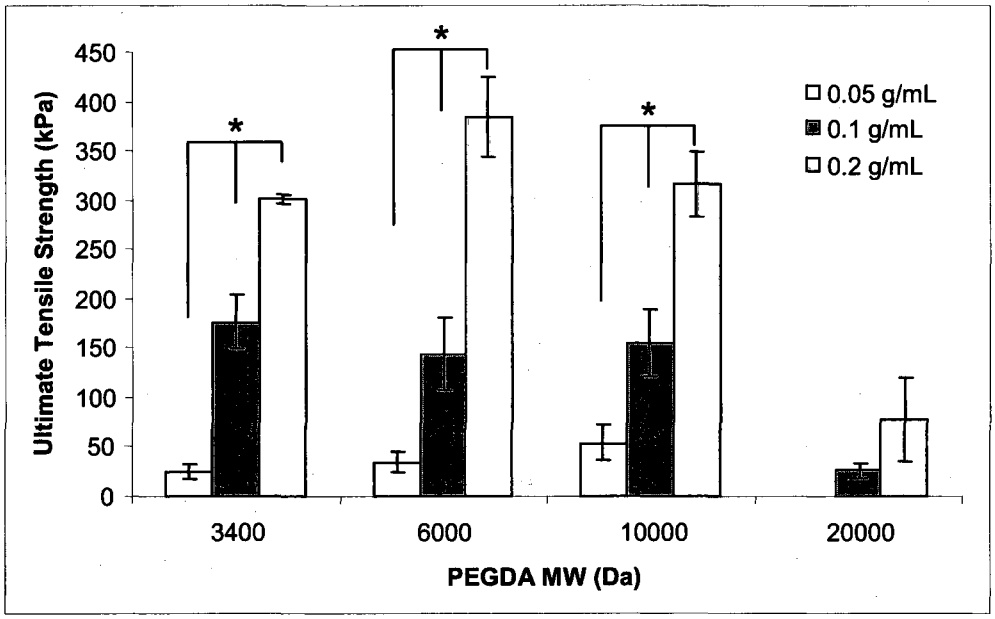

Figure 2-6. Ultimate Tensile Strengths of Various Formulations of PEGDA Hydrogels. Materials with a range of strengths can be generated by modulating the polymer molecular weight and solution concentration. *p< 0.05, other significant differences exist but are not designated here for clarity of the data.

In general, longer polymer chains are known to exhibit greater strengths than those that possess identical chemical composition but are shorter.[105]. This higher rigidity is due to an increase in chain entanglements and Van der Waals interactions as the polymer extends under applied force. To illustrate that the PEGDA hydrogels exhibit this expected relationship, the UTS data for the three different solution concentrations of 3,400 Da, 6,000 Da, and 10,000 Da hydrogels were interpolated/extrapolated to give equimolar formulations. Data for the 20,000 Da samples could not be accurately fit with linear regression since only two data points exist. The results presented in Figure 2-7 clearly show the expected correlation between MW and polymer strength. It should be noted here that although either mass or mole concentrations can be used in describing polymer solutions, this work will continue to utilize the mass notation since it is the convention in the tissue engineering literature and helps relate most clearly the fraction of tissue scaffold occupied by synthetic matrix.

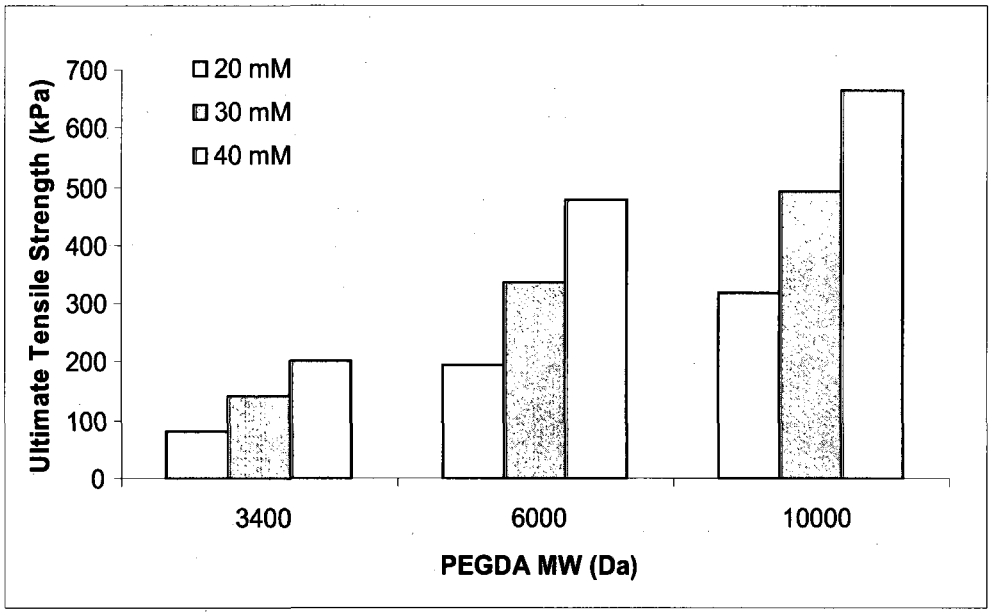

Figure 2-7. Hydrogel UTS in Equimolar PEGDA Concentrations. Hydrogel ultimate tensile strength data was extrapolated to reflect relationships between equimolar concentrations of different molecular weight PEGDA formulations. Data clearly indicate that in addition to greater solution concentration, an increase in PEG chain length also results in higher tensile strength. Values are computed from the mean UTS values of previous experiments and do not represent multiple measurements.

2.3.4 Analysis of Bioactive Peptide Incorporation into PEGDA Hydrogels

The PEG-W conjugation reaction had an efficiency of 85% as determined by ABS_{280} measurements. Results of incorporation of this molecule into PEGDA hydrogels of different MW are included in Table 2-2. All data were corrected for the acrylation of acryloyl-PEG-SCM as reported by the manufacturer (85%). As expected, the percent of initial PEG-W crosslinked into materials that exhibit a large degree of swelling (*e.g.* 20,000 Da, 0.02 g/mL) is much lower than that of those that do not swell significantly. This difference is due to the volume change that takes place in the transition from

fabrication to equilibrium. After correcting for volume change, the percent theoretical values are more consistent among the different samples.

Table 2-2. Incorporation of PEG-W into PEGDA Hydrogels

M_n (Da)	PEGDA Concentration (g/mL)	Initial PEG-W (mM)	PEG-W : Acrylate	PEG-W Incorporation	
				% Initial	% Theoretical
3,400	0.1	1	0.03	45	46
	0.1	2	0.07	39	39
6,000	0.1	1	0.06	35	37
	0.1	2	0.12	35	37
	0.23	1	0.03	27	29
	0.23	2	0.05	29	30
10,000	0.1	1	0.10	29	35
	0.1	2	0.20	28	33
	0.23	1	0.04	19	22
	0.23	2	0.09	21	25
20,000	0.2	1	0.10	25	51
	0.2	2	0.20	15	30

However, the overall low incorporation rates (<50%) reported here were not expected from this hydrogel system. The PEGDA crosslinking scheme with an initiator of free radical polymerization is very efficient, and previous groups have reported 81-97% incorporation of acrylated peptides.[98] This previous study was conducted with hydrogels of 8,000 Da PEGDA at 0.23 g/mL and used acryloyl-PEG-NHS purchased from Nektar, which was reacted with peptide under aqueous conditions. As shown in Table 2-2, higher solution concentrations actually have a negative effect on incorporation rate in the current study. The reason for this effect is not obvious, since increasing the number of acrylate groups increases the available sites for PEG-peptide attachment. Of note is the ratio of PEG-W to acrylates in each formulation (Table 2-2 column 3), which

does not exceed 0.2 indicating that the available acrylates are not being saturated, especially since multiple PEG chains can join at a single crosslinking site. Furthermore, analysis of hydrogel rinse solutions reveals that 60-70% of the initial PEG-W has diffused from the hydrogel. This phenomenon is not unique to PEG-W but has also been identified with PEG-RGDS, PEG-WRGDS, and PEG-YIGSR as well. In addition, the findings of this study were confirmed using a ninhydrin analysis of amino acids within digested hydrogel samples.[106]

The low incorporation of PEG-peptide appears to be a direct result of a loss of acrylate functional groups. Prior to the conjugation reaction, NMR reveals that the percent acrylation of the acryloyl-PEG-SCM is >90%, which is in agreement with the manufacturer's analysis. Acrylation of the PEG-peptide product, however, is less than 50%. This instability was not an issue with the PEG product purchased previously from Nektar, so one possibility is that the new manufacturer is producing a particularly unstable acrylate modification. Because a solution to this problem was not immediately evident, the studies in this work were conducted by correcting for the known incorporation rate in all materials synthesized.

2.4 Conclusions

In summary, this chapter presents a thorough characterization of the properties of PEGDA hydrogels. These analyses provide important foundational knowledge as we continue to explore potential applications for this hydrogel as a cell scaffold. A high water content and advantageous transport properties indicate that the material is capable of supporting encapsulated cells. These material properties, as well as the mechanical properties of PEGDA hydrogels were demonstrated to be highly dependent on the

formulation parameters of the gel precursor solution. Facile modification of polymer solution concentration or PEG chain length results in great variation in the physical properties of these materials. As shown in Figure 2-8 the data can be summarized to illustrate the effects of individual parameters, such as crosslink density, on the physical properties of the hydrogel.

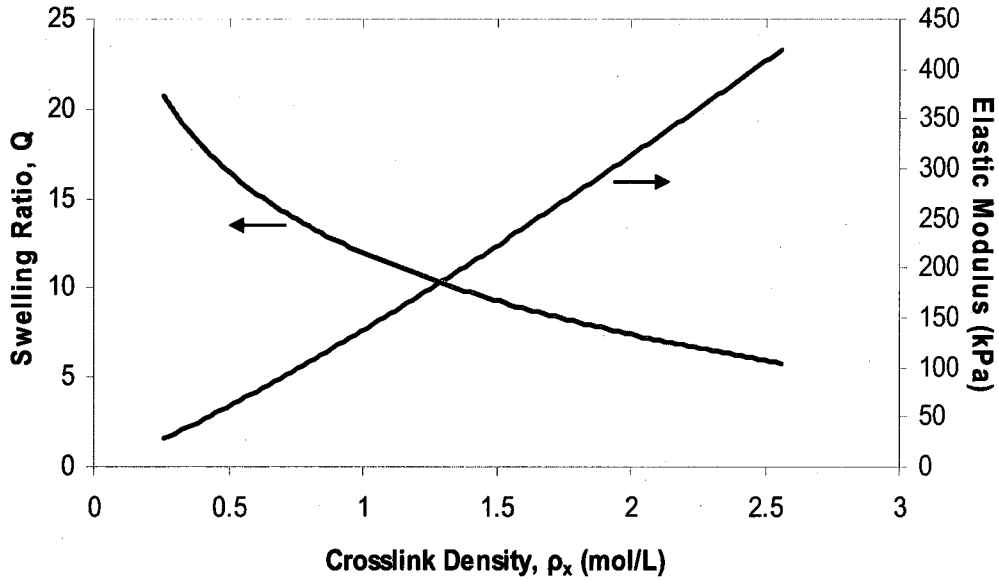

Figure 2-8. Effect of Crosslink Density on Q and E. The physical properties of PEGDA hydrogels can generally be related through the crosslink density. Shown in this plot are the effects on swelling and stiffness.

Tunable mechanical properties, including elastic modulus and tensile strength allow these hydrogel materials to be tailored to various tissue engineering applications. Control of properties such as elasticity is important in vascular graft development, since compliance mismatch is a known contributor to neointimal hyperplasia and graft failure.[107] The hydrogels studied in this work had stiffnesses approaching 400 kPa, which match that of the native aorta.[108] In addition our recent efforts have resulted in

the fabrication of materials with measured elastic moduli in the megapascal range (unpublished data) making them applicable to other tissues such as heart valves, cartilage, and bone.

The final section of this chapter evaluates the modification of PEGDA hydrogels with bioactive peptides. While some of the data obtained were unexpected or seemingly problematic, the beneficial implications of this study are two-fold. First, two different quantitative assays (ABS_{280} and ninhydrin) were successfully employed for characterization of the biochemical modifications of PEGDA hydrogels. Second, the characterization data contained herein provides the information necessary to tailor the mechanical properties of these potential cellular substrates while maintaining constant presentation of biochemical signals such as adhesive ligands. This control is critical in elucidating discrete effects on cellular response and tissue development. As such, the utility of this hydrogel system continues to grow. Finally, the characterization data presented here has served as a basis for the investigation of PEGDA hydrogels as vascular cell scaffolds in the chapters that follow.

3. Influence of Biomimetic Hydrogels on Vascular Smooth Muscle Cells

3.1 Introduction

In the body, cells receive mechanical cues from surrounding tissues which help modulate their phenotype.[59] It is reasonable to expect, then, that cells in contact with a biomaterial substrate are similarly able to sense and respond to their physical environment. This is in fact the case, and after first being demonstrated in epithelial cells and fibroblasts[109, 110] the realization has now been extended to neurons and cells of muscle and vascular tissues, among others.[111-114] While the exact mechanisms by which cell sense and respond to substrate rigidity are not yet fully understood, there is reasonable supposition that they involve a tensegrity feedback loop. Under this hypothesis forces within the actin-cytoskeleton are balanced by the resistive forces of both microtubules and cell-ECM adhesions. [115, 116]

The studies in this chapter were designed to answer fundamental questions regarding the manner in which smooth muscle cells respond to mechanical cues they receive from a biomaterial substrate. Information obtained from cells in contact with materials of different stiffnesses could help predict how the development of a tissue engineered vascular graft could be impacted by varying the magnitude of transluminal strain or longitudinal tension applied during culture. Poly(ethylene glycol) diacrylate (PEGDA) hydrogels with elastic moduli in the range of those used for many tissue engineered scaffolds (~10-100 kPa) were investigated. PEGDA substrates provide the unique opportunity to isolate the effects of substrate rigidity from those of integrin presentation by varying the concentration and/or molecular weight of base polymer while maintaining constant levels of the cell interaction conjugate PEG-RGDS and vice versa (Chapter 2).

3.2 Materials and Methods

All materials are from Sigma (St. Louis, MO) unless otherwise specified.

3.2.1 Hydrogel Synthesis

PEGDA hydrogels were formed by dissolving polymer in HEPES buffered saline (HBS, pH 7.4) at a concentration of 0.1 g/mL. The adhesive ligand PEG-RGDS was added to the final concentrations specified in the individual experiments below, with these concentrations corrected for hydrogel swelling as discussed in Chapter 2. The solution was sterilized by passing through a 0.22 μm syringe filter and all successive steps carried out under sterile conditions. 2,2-dimethoxy-2-phenyl-acetophenone was introduced as the photoiniator at ratio of 10 μL per 1 mL of polymer solution and the mixture added to a rectangular glass mold. The solution was finally exposed to UV light for 2 min with periodic rotation. Resulting hydrogels were removed from the molds and allowed to swell in HBS for 48 h at room temperature. After swelling, hydrogels were punched (1.5 cm) and placed in the wells of a 24-well low-attachment plate.

3.2.2 Influence of Substrate Rigidity on Coronary Artery Smooth Muscle Cells

To assess the influence of hydrogel mechanical properties on the behavior of human coronary artery smooth muscle cells (HCASMC, Cascade Biologics, Portland, OR), hydrogels of stiffnesses ranging from 8 -108 kPa were formed using PEGDA of 3400 – 20,000 Da (characterization details in Chapter 2). HCASMC of passage 3-8 were seeded onto the top of the hydrogels using stainless steel seeding rings (1 cm diameter) at concentrations of 1,000 to 5,000 per cm^2 depending on the assay. All experiments were conducted using smooth muscle cell growth media (SMGS) which consisted of Medium 231 (Cascade) with the following supplements: 4.9% v/v fetal bovine serum (Invitrogen,

Carlsbad, CA), 2 ng/mL human basic fibroblast growth factor (Invitrogen), 0.5 ng/mL human epidermal growth factor (Invitrogen), 5 ng/mL heparin, 5 μg/mL insulin, 0.2 μg/mL bovine serum albumin, 100 U/mL penicillin, and 100 μg/mL of streptomycin. Incubations were carried out in a 37°C humidified environment with 5% CO_2.

3.2.2.1 HCASMC Adhesion to PEGDA Hydrogels

Adhesion of HCASMC to hydrogels of 8, 50, 80, and 108 kPa elastic modulus containing 1 mM PEG-RGDS was determined 3 h after seeding at 5000 cells/cm^2. After the initial incubation, samples were washed 3 times with PBS to remove any non- or loosely adherent cells. Trypsin-EDTA solution at 5 times the normal concentration (2.5 g/L trypsin, 1 g/L EDTA) was applied to hydrogels for 25 min followed by gently scraping to dislodge cells from the surface. Cell number was determined using a coulter counter. To expand this assessment to include softer gels, digital image analysis was employed. In this assay, the hydrogel surface was photographed under low magnification and adjacent view fields tiled in Adobe Photoshop to create a single image of the entire seeding area. All adherent cells were marked in a separate image layer, which was then counted using the particle analysis function in Image J (Figure 3-1).

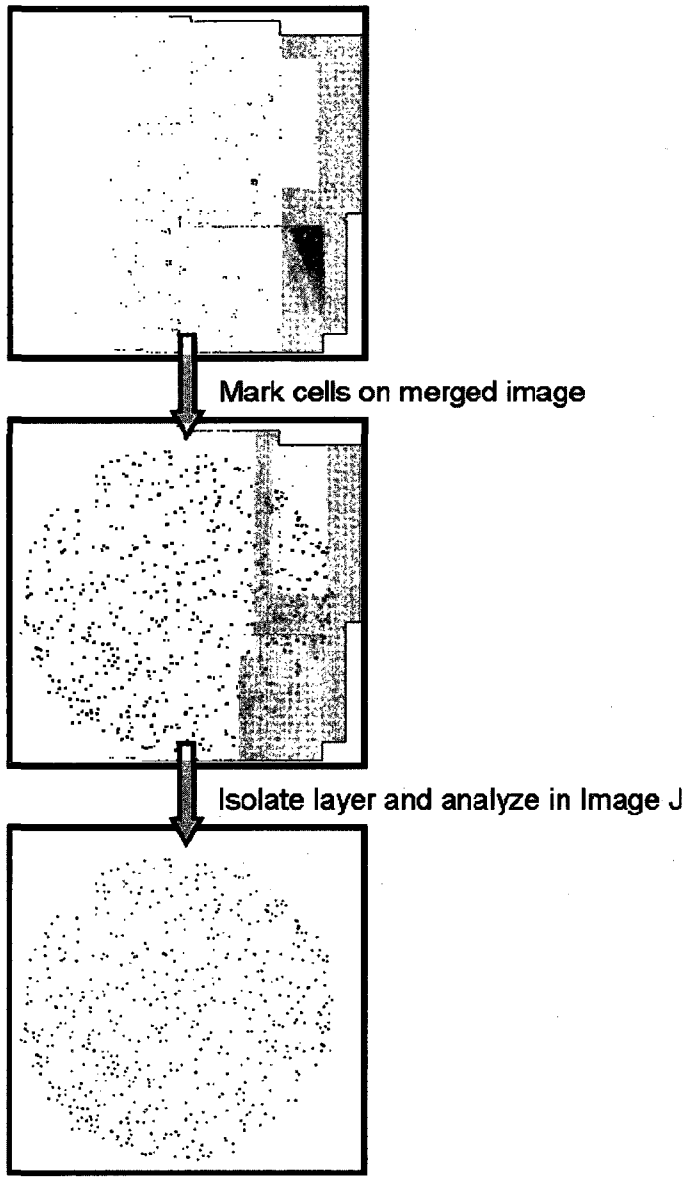

Figure 3-1. Digital Image Analysis for Cells Adherent to a Hydrogel Surface. Overlapping images of the hydrogel surface were merged to create a single field of view. An image overlay containing dots in the location of adherent cells was counted using the particle analyzer function in Image J.

3.2.2.2 Effect of Stiffness on HCASMC Proliferation

HCASMC proliferation was assessed over a period of 48 h on hydrogels of 50, 80, and 108 kPa elastic modulus and containing 1 mM PEG-RGDS. Cells were seeded at a concentration of 5000/cm^2 and then removed at 3 h and 48 h by trypsin-EDTA and scraping as described previously. Cell number was obtained using a coulter counter and cell doubling time, dt, was calculated as

Equation 3-1. Cell Doubling Time

$$dt = x * \frac{\ln(2)}{\ln\left(\frac{c}{b}\right)}$$

where x is the time interval in hours, b is the initial cell count, and c is the cell count at the final time point.

3.2.2.3 Analysis of Cell Spreading on PEGDA Hydrogels

Images of cells on hydrogels of 50 and 108 kPa elastic moduli from the proliferation experiment above were analyzed to determine the number of cells exhibiting a spread morphology after 48 h. All hydrogels contained a final concentration of 1 mM PEG-RGDS. Results are expressed as a percentage of the total adherent cells.

To visualize cytoskeletal components of adherent cells, representative cells on hydrogels of 108 and 8 kPa elastic moduli were incubated with an antibody to the focal adhesion protein vinculin and with phalloidin (Molecular Probes, Carlsbad, CA) which reacts with filamentous actin. A FITC conjugated secondary antibody (Molecular Probes) allowed visualization of the vinculin, while the phalloidin was conjugated to a rhodamine fluorophore. Fluorescent cytoskeletal components were visualized using a confocal microscope.

3.2.2.4 Influence of Adhesive Ligands on Vascular Cells

Studies were also conducted to observe the influence of different combinations of adhesive peptide and hydrogel stiffness on cell behavior. In the first study, HCASMC were seeded at a concentration of 1000 cells per sample onto hydrogels of 108 and 8 kPa elastic moduli containing either 1 or 3 mM PEG-RGDS. In order to assess effects on the immediate attachment and spreading, samples were rinsed 2 h after seeding and then photographed. Cells areas were calculated by creating field of view masks in Adobe Photoshop followed by analysis of total cell area on the mask layer using NIH Image J (Figure 3-2). A low seeding density was used to prevent cell-cell interaction. Only those cells located completely within the view field and not in contact with other cells were measured. HCASMC were also seeded onto hydrogels of 108 and 8 kPa stiffness with either 2 or 4 mM PEG-RGDS at a higher concentration (5,000/sample) in order to quantify cell number using the coulter counter. After 48 h, hydrogels were rinsed and the cells removed using trypsin/EDTA and scraping as described previously.

Figure 3-2. Cell Spreading Analysis. To determine the total area of hydrogel surface occupied by smooth muscle cells, a mask of cell spreading was created in Adobe Photoshop and then analyzed by NIH Image J. Representative image is from a 108 kPa hydrogel with 3 mM PEG-RGDS. Scale bar is 100 μm.

3.3 Results

3.3.1 HCASMC Adhesion to PEGDA Hydrogels

HCASMC adhesion is influenced by the elastic modulus of PEGDA hydrogels with stiffer substrates supporting greater adhesion than softer materials containing the same concentration of adhesive ligand (Figure 3-3). In the range of materials tested (8 – 108 kPa), however, only the softest material showed statistically different adhesion with an average of 14% of cells attaching to the 8 kPa surface compared with 40-50% for the other three formulations (Figure 3-4).

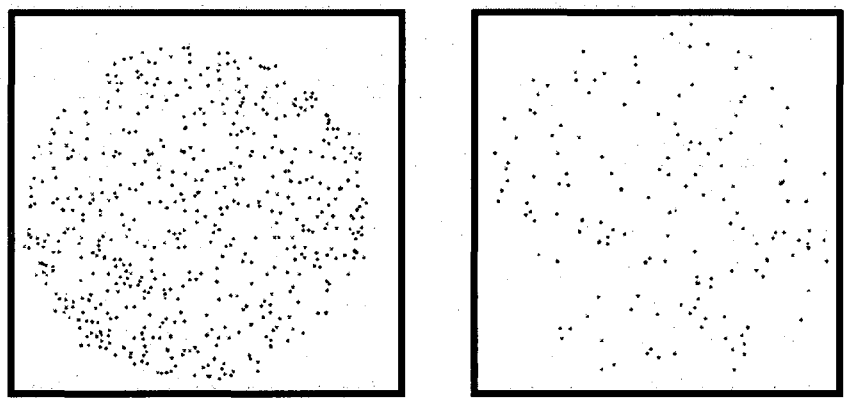

Figure 3-3. Cell Density on PEGDA Hydrogels. Representative cell area masks demonstrate the difference in HCASMC adhesion on stiff (left) and soft (right) hydrogels. Each material contains 1 mM PEG-RGDS.

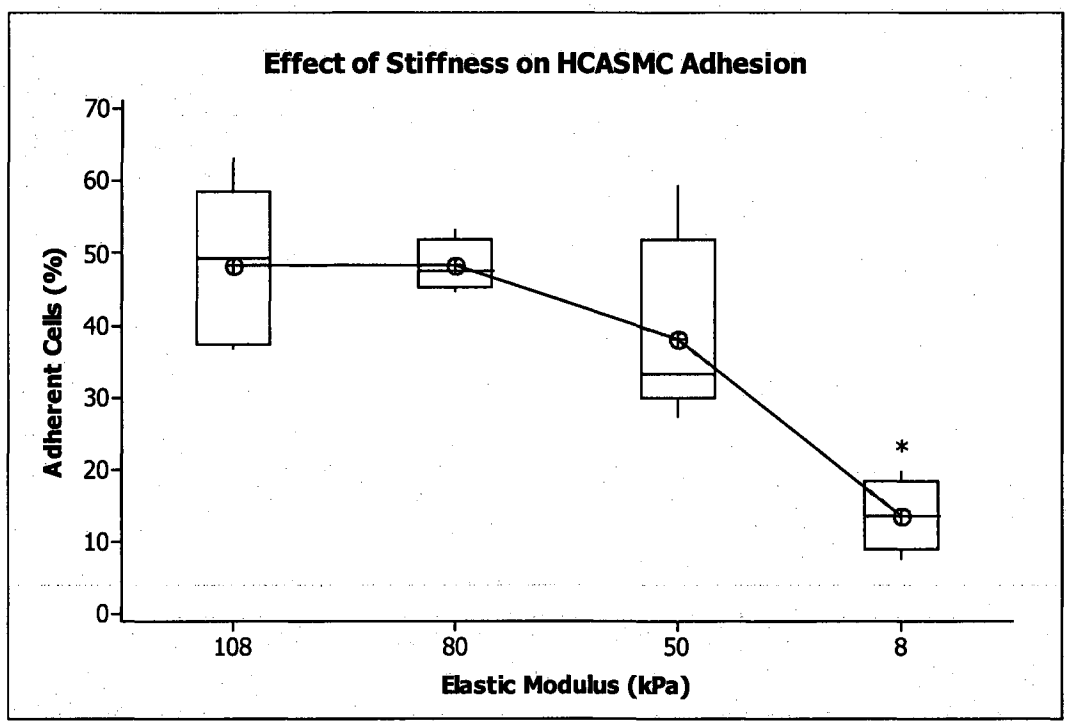

Figure 3-4. Boxplot of Data from Cell Adhesion Experiments. There is no statistical difference in the fraction of adherent cells on hydrogels ranging in stiffness from 108 to 50 kPa. However, on the softest substrate, there is a considerable decrease in the percentage of cells attaching to the surface (*$p<0.05$, ANOVA with Tukey post-hoc). All materials were modified with 1 mM PEG-RGDS.

3.3.2 Proliferation

Results of the proliferation assay are shown in Figure 3-5. Over a period of 48 h, there was a significant increase in the number of cells on all hydrogels (student t-test, $p<0.05$). Using Equation 3-1 HCASMC doubling times were calculated as 40, 54, and 58 h on the 108, 80, and 50 kPa substrates respectively. The data indicate that vascular cells may have an increased rate of proliferation on more rigid materials which is similar to trends reported previously.[117]

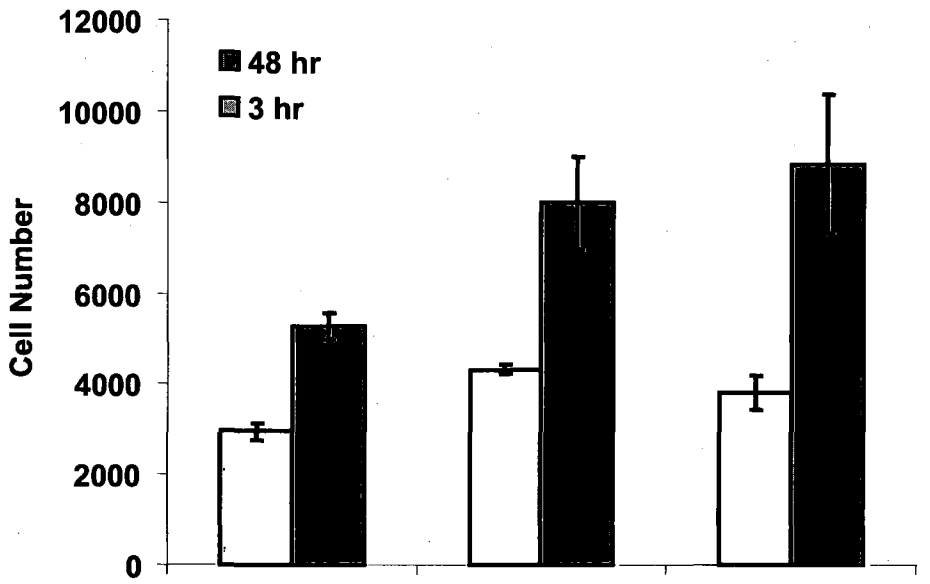

PEGDA MW (Da)	10,000	6,000	3,400
Elastic Modulus (kPa)	50	80	108
Doubling Time (h)	58	54	40

Figure 3-5. Proliferation of HCASMC on PEGDA Hydrogels. While cells proliferated on all surfaces over a 2-day period, based on calculated doubling times it appears that more rigid hydrogels promote a greater rate of proliferation in these smooth muscle cells. All materials were modified with 1 mM PEG-RGDS.

3.3.3 Cell spreading

Forty-eight hours after seeding, HCASMC on both 50 and 108 kPa substrates exhibit normal spreading morphology. As shown in Figure 3-6, there is a significant difference in the proportion of spread and rounded cells on the two materials. A z-test on the difference between the two proportions reveals that stiff hydrogels support a greater fraction of spread cells ($p<0.01$) compared to softer materials.

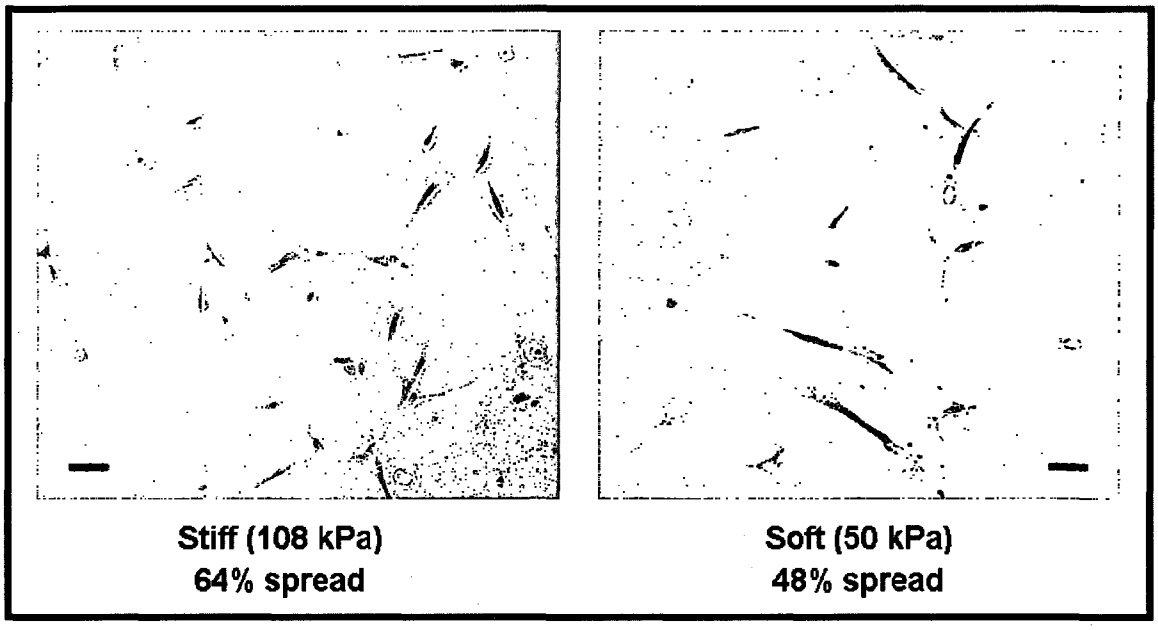

Figure 3-6. Influence of Substrate Rigidity on Fraction of Spread HCASMC. Attached but un-spread cells are indicated by the red circles. Stiff hydrogels support a greater fraction of spread cells at 48 h (z-test, $p<0.01$). Scale bar is 50 μm.

Fluorescent staining of cytoskeletal components of vascular smooth muscle cells on stiff and soft hydrogels further demonstrates a rigidity-influenced difference in morphology (Figure 3-7). Rhodamine phalloidin allows visualization of F-actin while the FITC-conjugated antibody highlights regions concentrated vinculin. On the stiffer 108 kPa hydrogels, actin stress fibers are larger, more highly aligned, and anchored at regions of concentrated vinculin. While cytoplasmic vinculin is evident in the HCASMC on the 8 kPa substrate, the cell does not possess the punctuate focal adhesions present in cells on the stiffer material. Upon closer inspection, it is also evident that many of these focal contacts are highly elongated indicating adhesion maturity.[118] These results are in agreement with similar studies involving the growth of smooth muscle cells on PEGDA[117] and polyacrylamide substrates.[114]

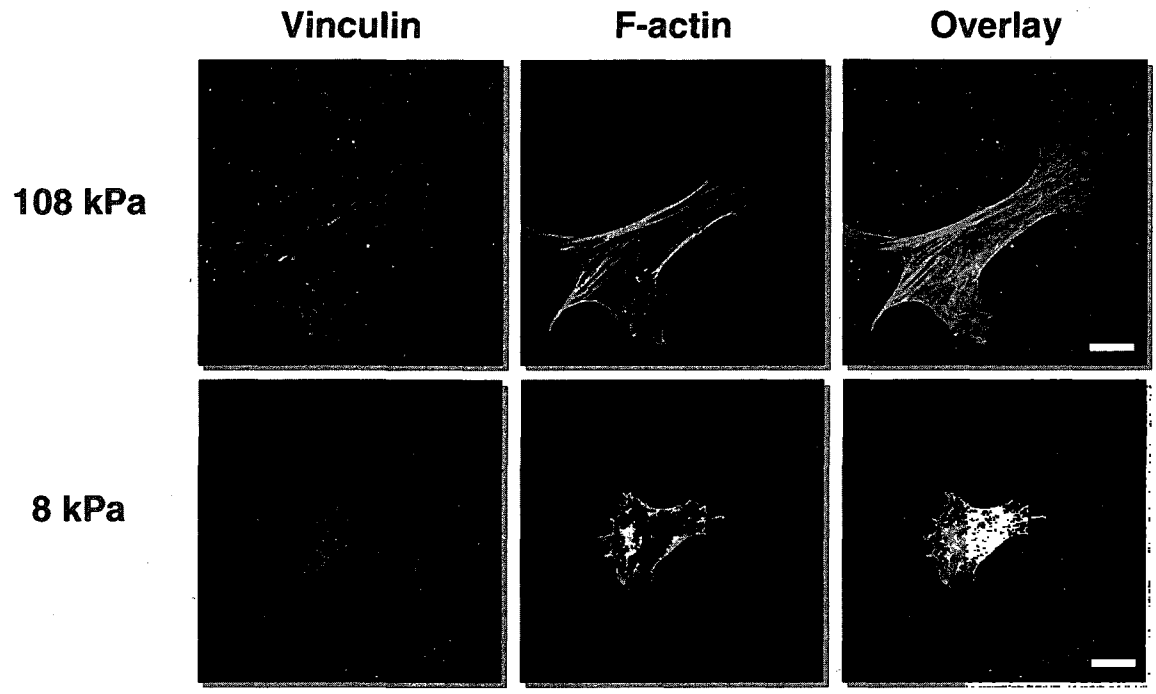

Figure 3-7. Cytoskeletal Differences in HCASMC Cultured on Hydrogels of Different Elastic Moduli. Cells on stiffer substrates are marked by punctuate focal adhesions and larger, more highly aligned actin filaments. Scale bars are 20 μm.

3.3.3.1 Role of Adhesive Ligands in Substrate Influence on Vascular Cells

Results in Figure 3-8 illustrate the effects of increasing adhesive ligand density on the total area of HCASMC on biomimetic PEGDA hydrogels. Trends of increasing total cell area with both increasing ligand density and increasing hydrogel stiffness are evident. For example, hydrogels of 108 kPa elastic modulus containing 3mM PEG-RGDS have a greater cell coverage than both substrates of equal stiffness but lower adhesive ligand density and substrates with equal bioadhesiveness but lower elastic moduli (ANOVA, $p<0.05$). In further analysis, it was shown that on a per cell basis neither hydrogel modulus nor ligand density effect cell spreading (Figure 3-9), at least not for the range of materials tested here. The data do reveal the great heterogeneity in

cell spread area in all formulations of hydrogels investigated (as evidenced by outliers in all groups), which can also be visualized in Figure 3-11. In terms of total number of cells on hydrogels of varying stiffness and adhesiveness, there is again a linear correlation (Figure 3-10), with both increasing stiffness and ligand density supporting the adhesion of a greater number of cells over the 48 h evaluation period. It should be noted that, although no quantitative visual inspection was made, the differences among the individual hydrogel groups appeared qualitatively to be more exaggerated than is shown here. Leading to possible explanation, it was noted that cells on soft materials detach from their substrate very easily, while cells on rigid hydrogels are hardly affected by trypsin/EDTA and require significant mechanical agitation to release. In this manner, it is possible that the cell numbers reported for stiff materials are slightly deflated.

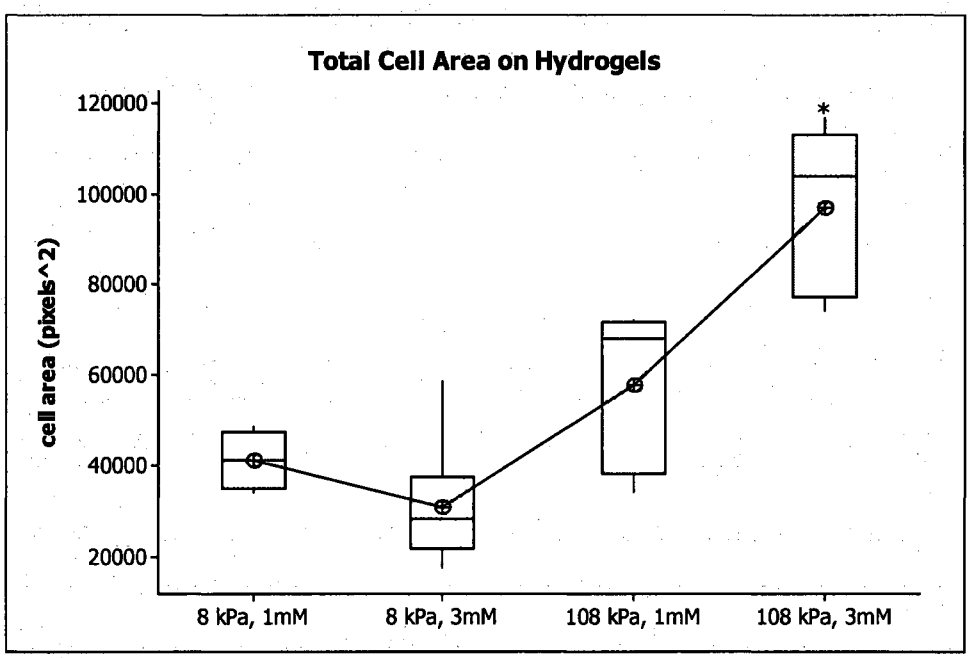

Figure 3-8. Comparison of the Influence of Adhesive Ligand Density and Hydrogel Stiffness on HCASMC. Increasing PEG-RGDS concentration does not appreciably affect the total cell area on soft hydrogels but 108 kPa gels with the higher level of adhesive ligand show a marked difference. * Indicates that this group is statistically different from all other formulations (ANOVA with Tukey post-hoc, $p<0.05$).

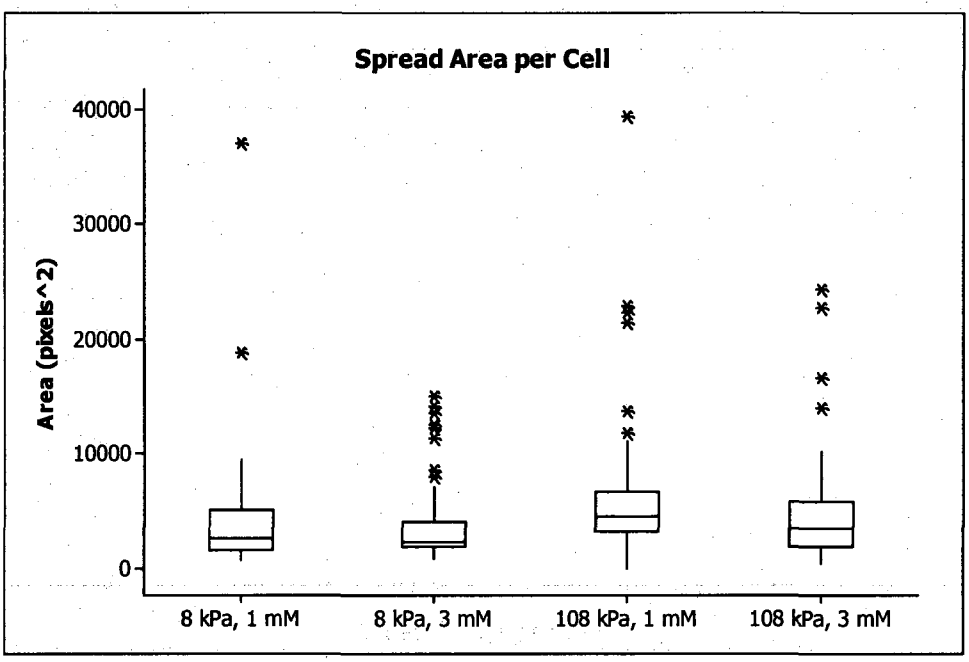

Figure 3-9. Spreading Area per Cell. There is no difference in the average per cell area spread among the four substrates evaluated (ANOVA, $p>0.05$). * Indicate outliers from these large groups of data.

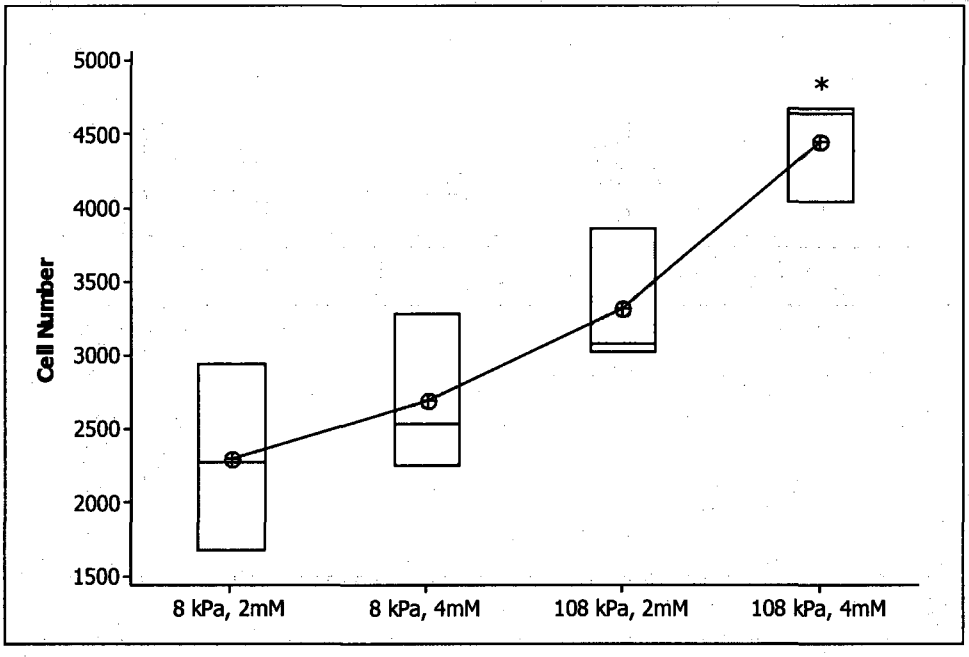

Figure 3-10. Effects of Hydrogel Stiffness and Adhesive Ligand Concentration on Cell Number. A clear trend of increasing cell number with increasing concentration of adhesive ligand and hydrogel elastic modulus is evident. * Indicates significantly different from all other groups (ANOVA, $p<0.05$).

3.4 Discussion and Conclusions

As reported previously, PEGDA hydrogels are easily modified to permit cell attachment and viability.[39, 98, 99, 119]. In the current work, human coronary artery smooth muscle cells were shown to attach, spread, and proliferate on hydrogel substrates of varying stiffness. Furthermore, these cellular responses were shown to be independently modulated by substrate rigidity and adhesive ligand density with increases in each parameter inducing greater cell attachment and a higher rate of proliferation.

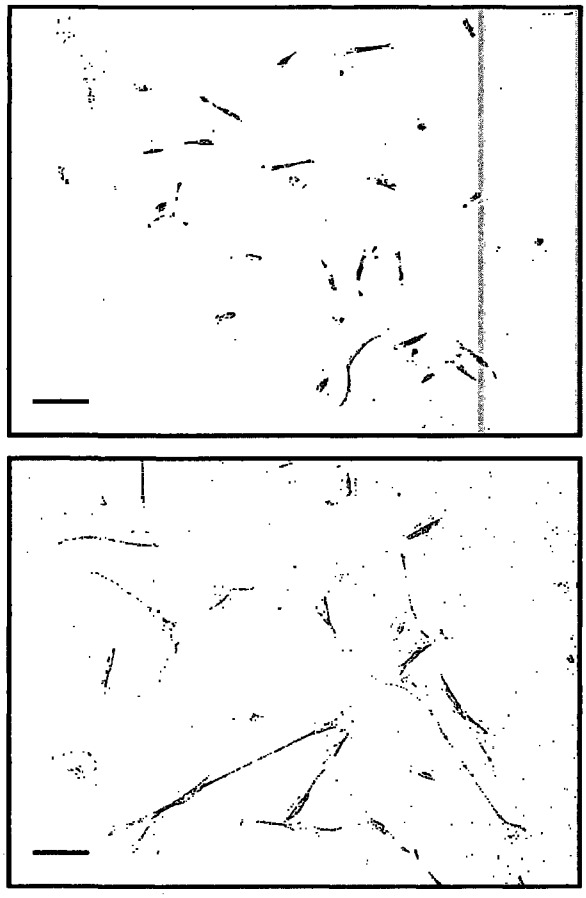

Figure 3-11. PEGDA Hydrogels as a Substrate for HCASMC. Vascular smooth muscle cells readily adhere to PEGDA hydrogels modified with adhesive ligand. Cells present normal morphology 2 h post-seeding (top) and 24 h later extend numerous filopodia indicative of interaction with the substrate and apparent migratory behavior (bottom). Representative images are of cells on a 80 kPa hydrogel with 1 mM PEG-RGDS. Scale bars are 100 μm.

After noting similar results in HCASMC on polyacylamide gels coated with fibronectin, Peyton and Putnam[114] put forth the following mechanism as possible explanation of the findings (Figure 3-12). By their explanation, cells on stiffer substrates must exert a larger pulling force on the material to maintain a basal "pre-stressed" state. In order to achieve this high level of force, the cells organize more robust focal adhesions and assemble large, highly organized actin stress fibers. These cytoskeletal modulations have implications on other cellular activities, such as migration. In subsequent experiments on PEGDA hydrogels, the authors noted that the rate of cell migration is actually decreased significantly on very rigid materials due to the presumed inability for cells to rapidly turn over large focal contacts.[117] This mechanism is supported by the cytoskeletal changes demonstrated in the current study (Figure 3-7) and by anecdotal observations of the removal forces required to detach cells from different stiffness materials here (3.3.3.1) and elsewhere.[120]

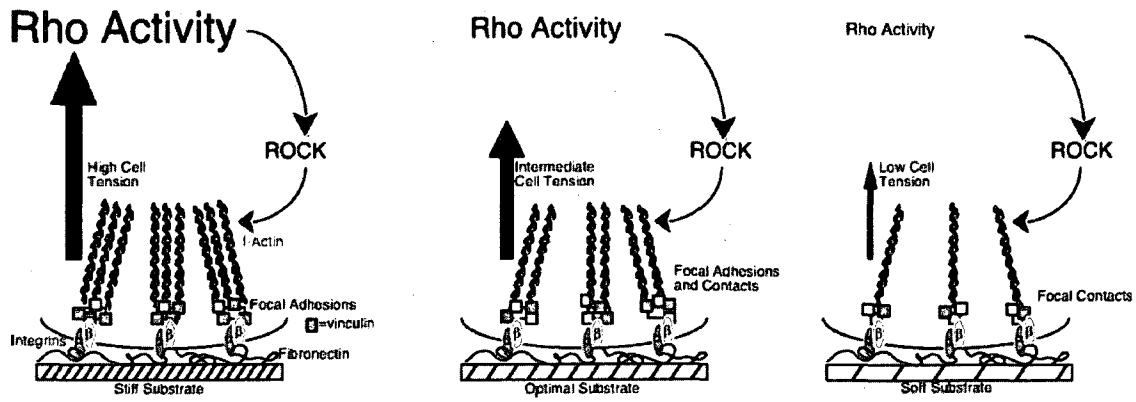

Figure 3-12. Proposed Mechanism of the Influence of Substrate Rigidity on Vascular Cells.[114] Feedback from mechanical cues in the cell substrate induce changes in focal adhesion size and composition which then further influence intra-cellular processes such as migration.

In conclusion, PEGDA hydrogels of varying elastic moduli and biochemical composition were shown to have distinct effects on HCASMC response. This model hydrogel system is easily tunable and lends itself to further investigation of isolated mechanical and biochemical influences on critical cellular processes including migration and extracellular matrix production, which will ultimately affect the choice for materials for tissue engineered vascular grafts, among other applications.

4. Pulsatile Flow Bioreactor Development and Analysis

4.1 Application of Bioreactors to TEVG Culture

As tissue engineering endeavors became more complex, moving from thin, approximately two dimensional structures to 3D constructs with multiple cell and matrix components, new challenges of *in vitro* culture had to be addressed. Significant improvements in tissue viability were accomplished by employing dynamic culture vessels, such as spinner flasks and rotating wall vessels, which help to increase the transport of oxygen and nutrients. However, with the advent of functional tissue engineering strategies, there is a desire to direct cell or tissue development with a specific, functional target as the goal.[121] Tissue engineering bioreactors, therefore, are specialized culture devices that provide a "controllable, reproducible, and mechanically active environment to study and potentially improve tissue structure, properties, and integration".[122] Tissue bioreactors primarily function to maintain tissue viability and accelerate *in vitro* maturation prior to implantation. In some cases, these devices are also used for cell seeding and to evaluate and monitor the progress of tissue maturation.[123]

In vascular graft applications, bioreactors can be designed to study the effects of hydrostatic pressure, pressure wave forms, longitudinal and radial strain, flow, and shear stress on TEVG synthesis and culture. The culture and conditioning methods may be tuned to direct stem cell differentiation down vascular lineages or to regulate the phenotype of smooth muscle cells. Mechanical stimulation also has the potential to influence cell orientation and the production and organization of a tissue matrix, which will improve the mechanical properties of the engineered tissue. As such, bioreactors can

provide the stimulus necessary to develop a functional graft substitute while allowing evaluation of its physiological response to *in vivo* environmental conditions.

4.2 System Design

The primary goal in developing our bioreactor system was to provide a means of conducting large scale studies at physiologically relevant flow conditions over an extended culture time. The ideal system would facilitate batch synthesis of hydrogel constructs in a controlled manner and allow for culture of three to four experimental flow groups and the appropriate number of static controls. In addition to experimental time course and scale, other important considerations were ease handling, especially with regard to setup and culture media changes; minimization of contaminant events; and real-time monitoring of flow parameters.

The system as designed is shown schematically in Figure 4-1 and in a photograph in Figure 4-2. In this flow loop, culture media is pumped from a reservoir to a compliance chamber via a Masterflex L/S variable speed peristaltic pump. The media from the compliance chamber is then directed through a CellMax pulsatile pump, which compresses the tubing in the pump head to produce the desired pulsation and pressure profile. The liquid is next passed through the experimental constructs mounted on the interior ports of a custom glass chamber. From the sample chamber, media flows back to the reservoir vessel for recirculation.

Flow rate is digitally controlled by the peristaltic pump while adjustments to the pressure waveform are made by altering the number of pulsatile pumps connected in series and/or the degree of tubing occlusion in these pumps. Alterations to mean system pressure are made by adjusting the occlusion in a valve located near the inlet of the media

reservoir. In this manner, pressure waveforms and flow rate can be varied independently.

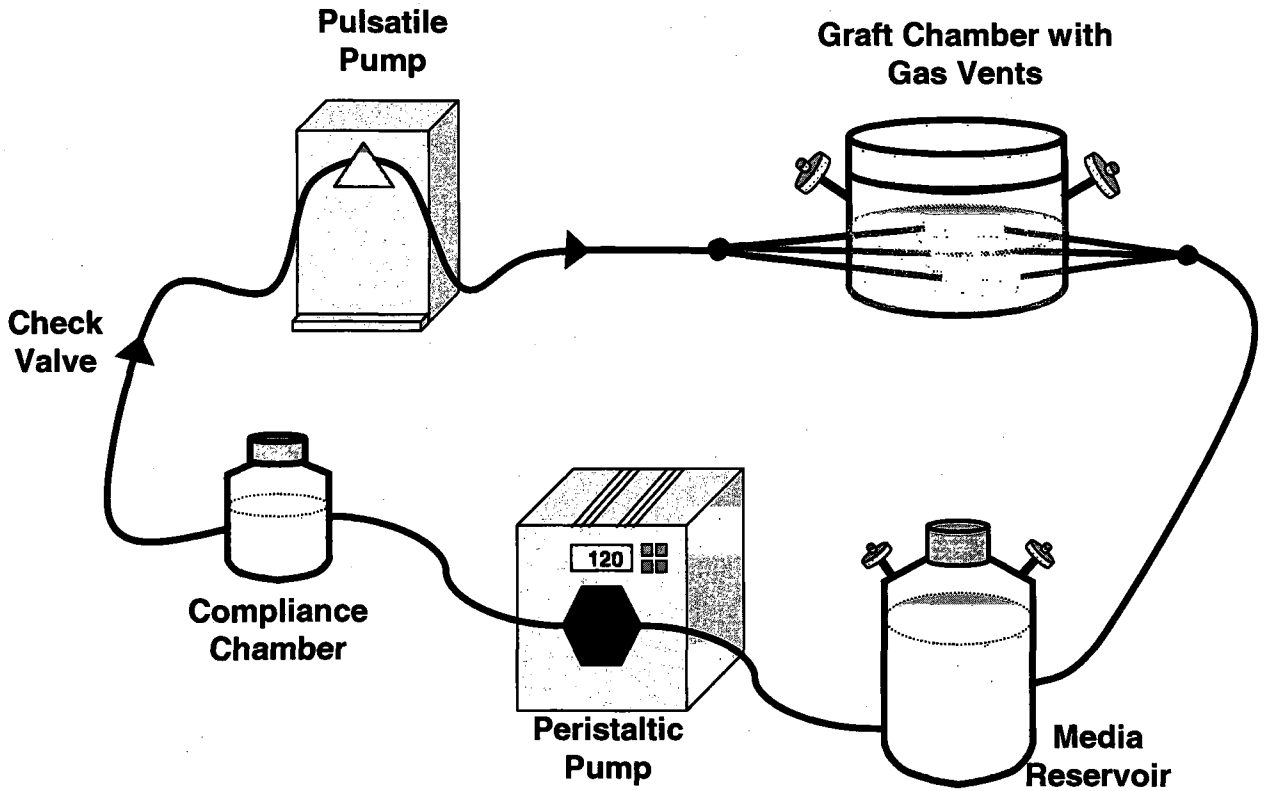

Figure 4-1. Pulsatile Flow Bioreactor Schematic. In the pulsatile flow loop culture media is pumped in clockwise direction from the reservoir container to the compliance vessel via the digital peristaltic pump. A pulsatile pump creates the desired pressure wave form to be delivered to the vascular graft constructs in the graft chamber.

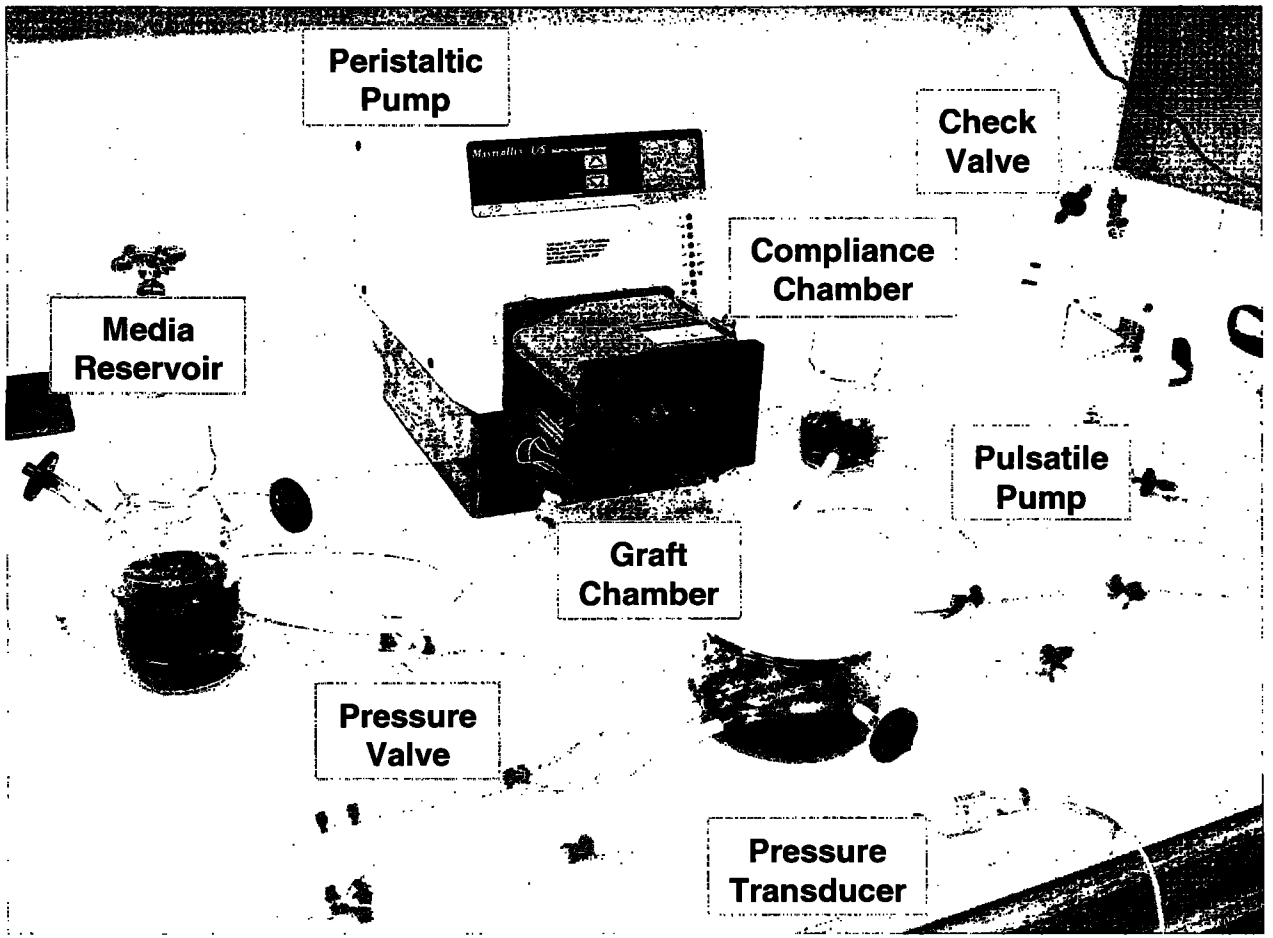

Figure 4-2. Photograph of the Actual Bioreactor Setup. Note that in this image the pressure transducer and pressure control valve are in

4.2.1 Media Vessels and Graft Chamber

The media reservoir and compliance chamber are standard glass storage bottles with screw top caps in 250- and 100-mL volumes, respectively. Bottles were modified by the Rice University glass shop to have inlet and outlet ports near the bottom of the vessels for connection to tubing. The media reservoir also possesses two upper ports for the attachment of 0.2 μm vent filters allowing gas exchange with the incubator environment. The utility of the media reservoir is self evident. In this system, the compliance chamber, which is essentially a volume of media with a column of air above it, serves to damp oscillations in the flow stream created by the motion of the peristaltic pump, which are also pulsatile in nature. In doing so, this noise is minimized and the control of the pulsing nature of fluid is limited to the CellMax pump.

Graft samples are mounted on the interior ports of a custom glass chamber (Figure 4-3). Similar to the media reservoir, the graft chambers also have ports for attachment of vent filters to allow gas exchange. The chambers are constructed from large screw cap bottles which were modified by an external glass company to have three pairs of ports for internal sample mounting and external tubing attachment. As shown in Figure 4-3, one end of each graft is attached to the internal glass port while the other is fixed on a nylon connector and a short length of flexible tubing. This adaptor allows for slight variation in the final length of each graft. The elasticity of the constructs acts to maintain their adherence to the chamber fittings during culture. The chamber reservoir is filled with culture media and, unlike many culture systems,[19, 124] this system places experimental constructs directly in the path of flow allowing transmission of shear stress to luminal wall cells. Static controls are cultured in identical vessels with the exception of the connection of external ports to a flow loop.

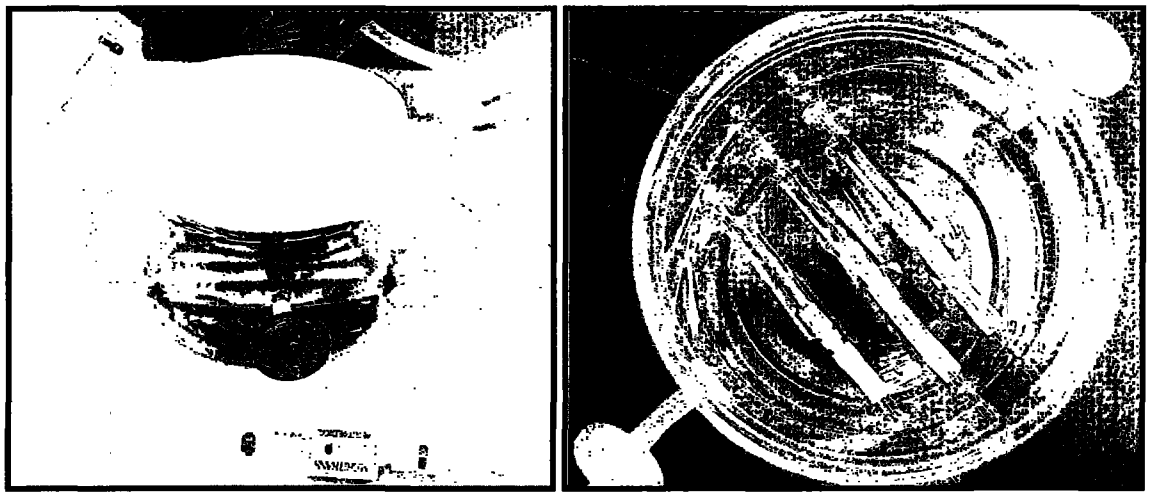

Figure 4-3. Graft Chamber. The image on the left shows the hydrogel graft chamber connected to the flow loop. On the right is a close-up of the interior of the chamber illustrating the connection of the grafts (pink) to the glass ports on one end and tubing extenders on the other.

4.2.2 Mechanical Components

An important decision in the design of this system was to employ equipment that acts externally on tubing rather than directly on the culture media. This provides protection against the contamination that is frequently associated with prolonged culture times (> 72 hr) in systems where the media contacts components of the pump apparatus.

4.2.2.1 Pumps and Tubing

To create the desired volumetric flow rate for culture media in the bioreactor, a Masterflex L/S variable speed digital peristaltic pump fitted with an L/S multi-channel pump head (Cole Palmer, Vernon Hills, IL) was employed. This multi-channel head allows for insertion of up to four flow loops in a single pump. It is also possible to stack two heads on the pump for the simultaneous operation of up to eight flow loops. The heads can be disassembled to allow insertion of the tubing as a loop rather than breaking

the sterile seal and feeding it through in the traditional sense. As mentioned previously, the peristaltic motion of this pump creates a variable pressure signal which is reduced to a suitable level by the compliance chamber.

A CellMax pulsatile pump (Spectrum Labs, Rancho Dominguez, CA) compresses tubing to produce the desired pulsation and pressure profiles. The amount of tubing in the head determines the magnitude of pressure difference (ΔP), with a larger contact area resulting in a higher ΔP. Fluid check valves mounted on either side of the pump prevent back flow. These pulsatile pumps were modified to create pulses of either 60 or 120 beats per minute (bpm), representative of adult and fetal heart rates, respectively. By applying multiple pulsatile pumps in series a physiological profile can be obtained as evident by the traces in Figure 4-4.

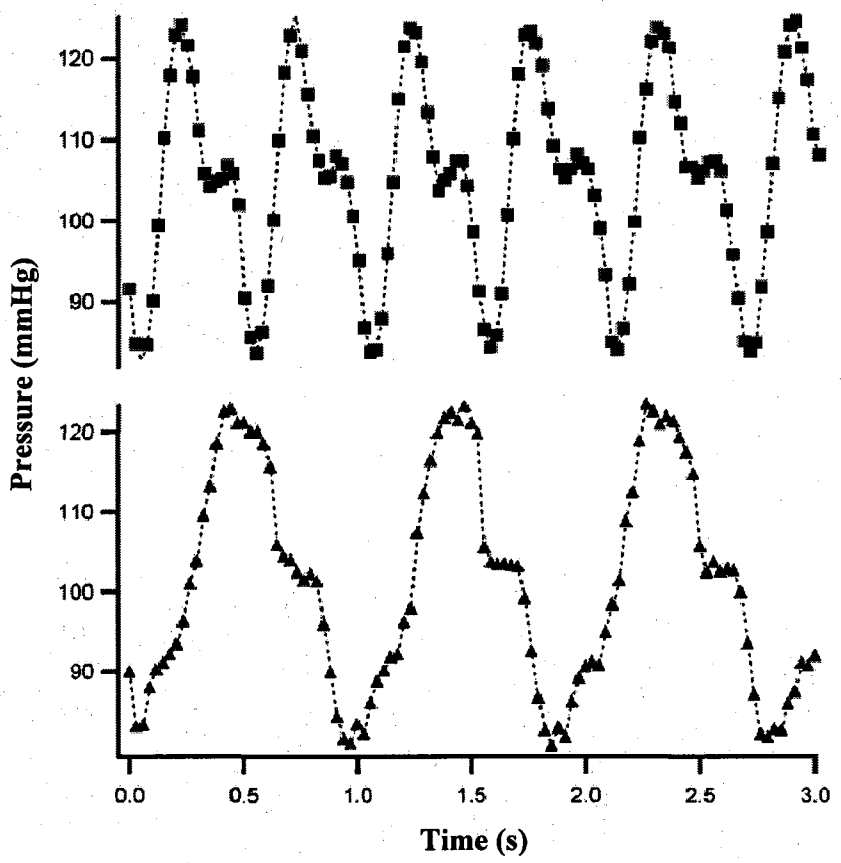

Figure 4-4. Bioreactor Pressure Profile. These representative pressure waveforms generated using the bioreactor with the pulsatile pump set to fetal (top) or adult (bottom) conditions.

All tubing and tubing connectors were purchased from Cole Parmer. Various tubing materials were investigated before deciding on Masterflex® platinum-cured silicon L/S as the primary tubing material. This material is autoclavable and has a high durability. Unlike some tubing tested (*e.g.* L/S PharMed), the silicone tubing does not leach oils or other particles that are incompatible with sterile applications. L/S 24 tubing (ID 6.4 mm) provided appropriate compliance for use in the CellMax pulsatile pump. Other segments of the flow loop were outfitted with L/S 16 (ID 3.1 mm) or L/S 25 (ID 4.8 mm). The

Masterflex® platinum-cured silicon tubing did not have appropriate durability for use in the peristaltic pump during multi-week bioreactor studies, however. Initial investigation determined that this tubing was only able to withstand approximately 8 hr of continuous use. As an alternative, Thermo Fisher Scientific Gore High Resilience tubing style 100C (ID 6.4 mm, wall 2.4 mm) was purchased for long-term studies. This specialized material has excellent durability, lasting a minimum of 4 wk before failure. The primary disadvantage to this product is cost ($175/ft) and as such it was only used for the peristaltic pump head segment. In addition, because this is not the standard tubing recommended for the Masterflex pump, it does not have the appropriate adaptors for connection to the pump head. Metal binder clips where affixed to the tubing on either side of the head as substitute. In addition to providing sterile transport of culture media, all tubing selected for this system is also gas permeable and as such allows for exchange of essential CO_2 from the incubator environment.

All tubing connectors are nylon or, where available, are nylon impregnated with ionic silver to promote anti-microbial action. The only exception is the pressure control valve (stopcock) which was only available in polycarbonate.

4.2.3 Pressure Monitoring and Data Acquisition

A pressure transducer (Merit Medical, South Jordan, UT) placed parallel to the constructs in the graft chamber is used to monitor the applied pressure profile. The transducer is connected to a Macintosh computer via a custom-made analog-to-digital converter box. The single use transducers are supplied sterile and can be ethylene oxide sterilized if re-use is desired. An in house manometer was used to calibrate the transducers with the acquisition software over the range of pressures used in the bioreactor studies.

4.2.4 Sterilization, Assembly, and Housing

System components are sterilized by autoclave with the exception of the polycarbonate stopcock, which requires ethylene oxide. Loop segments are assembled in a laminar-flow hood, and after assembly all tube/connector junctions are reinforced with nylon cable ties for added stability during application of high system pressures. All components except the peristaltic pump are housed in a 37 °C tissue culture incubator with 5% CO_2.

4.2.5 Forming Hydrogels as TEVG Scaffolds

Hydrogels for bioreactor experiments are formed in UV transparent molds consisting of an outer plastic cylinder of OD 6.4 mm and an inner glass mandrel of diameter 3 mm (Figure 4-5). To facilitate fabrication of large batches of cell-seeded hydrogels, a rotating platform was designed and then custom built by Richard Chronister of the Rice Chemical Engineering Machine Shop (Figure 4-6). The device operates at 1 rpm and holds up to 32 cylindrical samples at a time. Once the hydrogel precursor solution is loaded into the molds, the device is placed between two UV lamps to provide constant and equal UV exposure and ensure uniform polymerization.

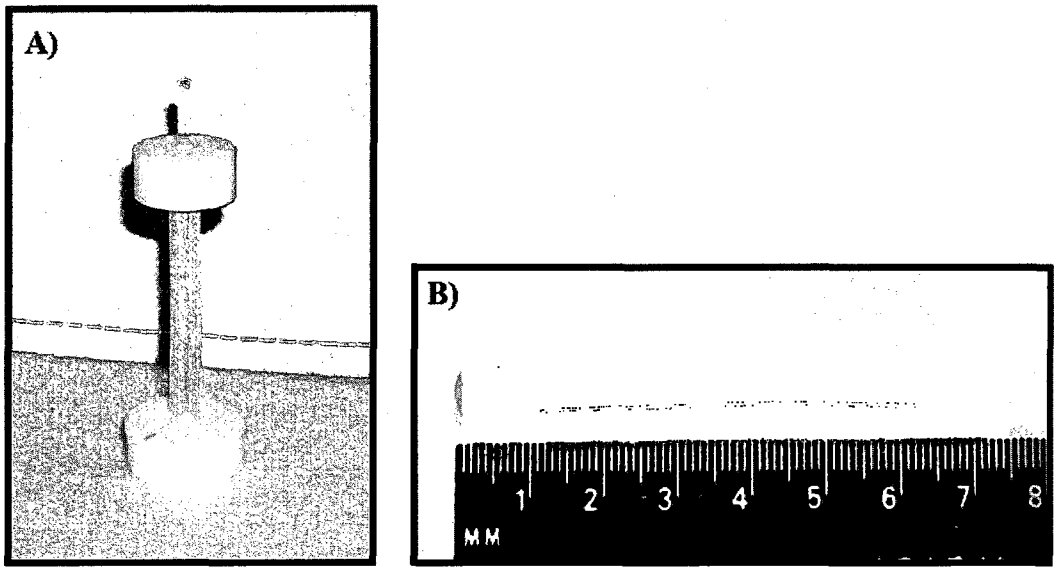

Figure 4-5. Tubular Hydrogels. The tubular PEGDA hydrogels are formed in polymerization molds (A) with an inner mandrel of 3 mm diameter and a hollow plastic outer cylinder of 6.4 mm diameter. The resulting construct has a geometry that mimics that of a blood vessel (B).

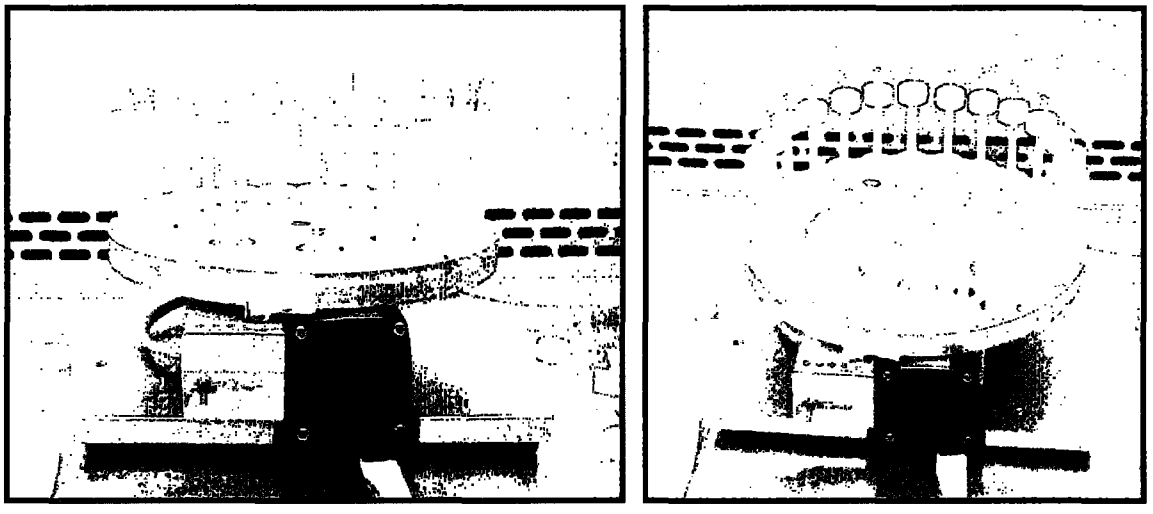

Figure 4-6. Rotating TEVG Device. This rotating platform designed for batch fabrication of bioreactor constructs can accommodate up to 32 samples at a time.

4.3 Analysis of the Bioreactor System

4.3.1 Flow Characterization

Analysis of the bioreactor system began with evaluation flow parameters in sample chambers of two different flow loops. It was important to confirm consistency within and among loops in order to permit comparison system-wide. Although great lengths were taken to assemble reproducible flow systems, this uniformity was not obvious *a priori* because each chamber was individually modified and all tubing cut by hand. Volumetric flow rate was measured at each sample port and in the transducer line for each loop and was found to be similar at every location both within and among loops (ANOVA, $p>0.05$). In addition, the average difference in measured pressure between two ports in a chamber was $1.2\% \pm 0.5\%$, or the equivalent of an average of 0.5 mmHg $\pm$ 0.2 mmHg. Based on this evaluation, the flow profiles imparted to individual samples within the bioreactor system were deemed consistent and reproducible.

Flow in this system was further characterized by calculating the Reynolds number, Re, according to the equation

Equation 4-1. Reynolds Number, Re

$$\mathrm{Re} = \frac{\rho Q D}{\mu A}$$

where ρ is the density, Q is the volumetric flow rate, D is the internal diameter of the graft, μ is the viscosity and A is the internal area of the tube. In addition, using the Poiseuille assumption for steady flow in a pipe, the wall shear stress, τ_w, in cylindrical bioreactor constructs is defined as

Equation 4-2. Wall Shear Stress, τ_w

$$\tau_w = 4\left(\frac{\mu}{\pi}\frac{Q}{R^3}\right)$$

where, R is the radius. The measured viscosity of cell culture media for these experiments was indistinguishable from that of water ($\mu \approx 1$ cps). Density was similarly approximated as that of water (0.993 g/cm^3). Cylindrical hydrogels had a radius of 1.5 mm as restricted by the size of the glass mandrel used for synthesis. Using these parameters, the Reynolds number and wall shear stress for various flow rates were calculated for Table 4-1 below. Of note, modulating the graft flow rate between 30 and 160 mL/min results in physiologically relevant shear stresses[60] and Reynolds numbers indicative of laminar flow which is important for diffusion of nutrients and oxygen to three dimensional constructs.[125]

Table 4-1. Reynolds Numbers and Shear Stresses for Various Volumetric Flow Rates

Q_{total} (mL/min)	*Q_{graft} (mL/min)	Re	τ_w (dynes/cm^2)
120	30	211	1.9
240	60	421	3.8
360	90	632	5.7
480	120	843	7.5
640	160	1124	10.1

**Although each flow loop has three grafts, flow from the pump is split four ways because one line goes to the pressure transducer.*

4.3.2 Batch Synthesis of Bioreactor Samples

Batch fabrication of graft constructs using the rotating platform saves large amounts of time in experiment setup since up to 32 gels can be exposed to UV in 6 min as opposed to 64 min. Shorter times mean that the cells are returned to culture media more quickly and undergo less stress. In addition the method helps to ensure consistent mechanical properties among specimen. Hydrogels exposed to UV on the rotating platform were not statistically different in elastic modulus or ultimate tensile strength. Furthermore, the gelation is uniform along the length of a single gel specimen based on evaluation of tensile properties at three different locations on the sample. These results are in agreement with previous studies reporting reproducibility and uniformity in hydrogel fabrication[57, 96, 126-129] and provide support for the use of this batch synthesis method.

4.3.3 Measurement of Transluminal Strain in Bioreactor Specimens

The transluminal strain imparted on different formulations of PEGDA hydrogels by the pulsatile flow bioreactor was assessed under physiological flow conditions of 120/80 mmHg and 120 mL/min[101] at fetal heart rates of 120 bpm. To measure radial distension, a Nikon Coolpix 5000 digital camera was used to image vessels undergoing mechanical pulsation at a capture rate of 30 frames/s. Two independent observers evaluated the maximum and minimum vessel distensions from the recorded images using the Adobe Photoshop measurement tool. Three measurements per gel were made for three different hydrogel samples for each formulation. The percentage strain was then calculated as

Equation 4-3. Percent Luminal Strain

$$\%=\frac{D_{max}-D_{min}}{D_{min}}*100$$

where D represented the inner diameter of the vessel wall.[130]

To relate measured strain to biomechanical properties, each construct was sectioned into thin rings and the mechanical properties assessed on the Instron, using a modification of the circumferential property testing techniques validated in Johnson *et al.*[131] and Hiles *et al.*[132] Sample dimensions were obtained from digital images (inner and outer diameter) or using calipers (width). Custom mounting brackets provided uniaxial strain application at a rate of 6 mm/min for the ring-shaped hydrogels (Figure 4-7). The area of force application was approximated as two rectangles each with sides equal to the width and wall thickness of the ring. The gauge length was taken to be the outer radius of the ring less the wall thickness (Figure 4-7). For each gel, the measured strain was validated by comparison with the strain, ε, estimated from application of Bernoulli's law to vessel dynamics, namely,

Equation 4-4. Bernoulli Strain

$$\varepsilon=\frac{\Delta P r_v}{h_v E}$$

where ΔP is the peak to trough pressure rise, E is elastic modulus, r_v is vessel inner radius, and h_v is vessel wall thickness.[132]

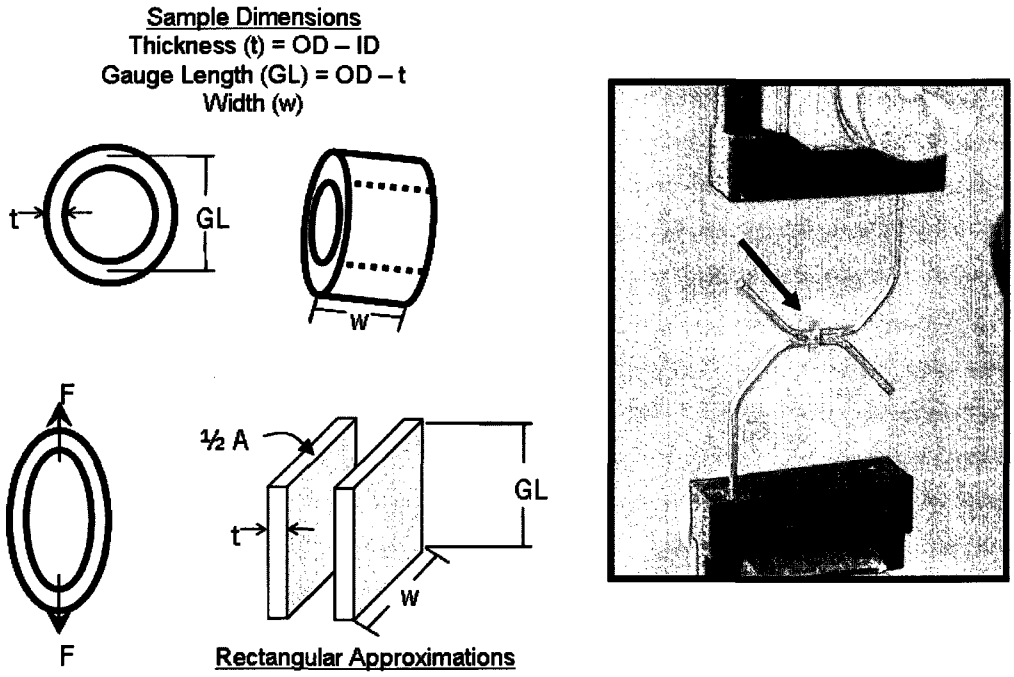

Figure 4-7. Tensile Testing Setup. The dimensions of ring-shaped hydrogel sections were measured as shown and the area of force application estimated as two rectangles. Custom mounting brackets support the test specimen, indicated by the arrow, in the Instron grips during mechanical testing.

As shown in Table 4-2, a range of mechanical properties can be obtained by varying the formulation parameters in the PEG-based hydrogels (*e.g.* polymer molecular weight or solution concentration). Transluminal strains for the materials tested varied from 2.9% for the concentrated 6000 Da gel to 10.7% for the formulation containing 30% degradable PEGDA. This range includes the values of 5-10%, which represent *in vivo* arterial strains [61, 62, 133] and have been found to induce SMC proliferation and ECM production *in vitro*.[134] For each gel formulation, the measured strains correlate closely with the strains predicted by application of Bernoulli's law based on measured pressure profiles and experimentally obtained elastic moduli. Furthermore, because cell behavior has been shown to be significantly altered with changes in network crosslinking density

and modulus, the combined bioreactor-PEG construct system can be used to explore the impact of controlled changes in construct properties on TEVG outcome.

Table 4-2. Transluminal Strain in PEGDA Hydrogels

Formulation	Strain (%)		Modulus (kPa)	UTS (kPa)
	Measured	Bernoulli		
100 mg/mL 3400 Da	6.2 ± 0.4	7.2	92.1 ± 2.7	67.0 ± 6.7
100 mg/mL 6000 Da	6.4 ± 0.5	9.5	81.2 ± 1.2	69.8 ± 8.2
200 mg/mL 6000 Da	2.9 ± 0.4	4.2	140.4 ± 5.3	101.7 ± 12
100 mg/mL 10000 Da	10.9 ± 1.3	10.9	48.4 ± 1.7	66.2 ± 11
200 mg/mL 10000 Da	3.6 ± 0.4	5.5	76.3 ± 2.0	69.8 ± 4.3
70 mg/mL 6000 Da + 30 mg/mL P-LGPA-P	10.4 ± 0.2	11.3	59.3 ± 2.5	43.3 ± 8.4

4.4 Conclusions and Future Directions

All of the primary goals for the pulsatile flow bioreactor system were successfully accomplished. The system is conducive to large scale bioreactor experiments in terms of both graft fabrication (using the rotating gelation platform) and long term culture. Careful selection of culture vessels, pumps, tubing, and connectors has made the flow loop relatively easy to use and, importantly, protects sterile culture media and cell-seeded constructs from bacterial and fungal contamination (as demonstrated by results in Chapter 5 of this thesis). Evaluation of the current system has shown that it is capable of

reproducing consistent, physiologically relevant, flow conditions and that several of these conditions can be independently modulated to access their affects on vascular cell behavior and tissue engineered vascular graft development.

An important benefit of this bioreactor is the direct contact of engineered tissue with flowing culture media, which allows juxtaposed cells to sense fluid shear. This condition becomes very important as endothelial cells are added to the graft luminal surface since EC have been shown to modulate their orientation and morphology in response to shear stresses.[135] In addition, preconditioning with shear has been shown to increase EC adherence to graft surfaces[136, 137] and reduce neointimal thickening open implantation.[136] It is significant to note, however, that these beneficial effects on EC orientation, morphology, and function are observed only in laminar and not turbulent flow conditions.[138]

There is one primary environmental constraint missing from the current bioreactor setup – longitudinal strain. In the current system, cell-seeded hydrogels are secured to the inner ports of the culture chamber in a relaxed state, while i*n vivo* blood vessels exist with inherent longitudinal strain.[72] As a TEVG matures, this strain may become important in influencing the orientation of emerging collagen bundles and elastic fibers. The current graft chamber can be modulated to accommodate a static longitudinal strain by securing the ends of the PEGDA hydrogels to the sample ports. Although the hydrogels do not respond well to suturing, fibrous materials (e.g. sterile gauze) have been successfully polymerized into the ends of the polymer to allow for suturing or other modes fixation. The material remains integrated with the hydrogel even when the polymer is stretched to 120% of its original length.

A final consideration would be to adapt the pulsatile flow bioreactor to serve as a device for real-time monitoring of TEVG mechanical properties. One such system was designed to evaluate the mechanical properties of *ex vivo* arteries during short-term flow experiments.[123, 139] Another device, the ElectroForce® BioDynamic™ test instrument manufactured by Bose Corporation is designed for pulsatile flow culture of vascular constructs and uses catheter pressure transducers to provide real-time measurements of luminal and abluminal pressures, as well as, optical or laser micrometers to assess changes in outer diameter due to strain, creep, or tension. Similar functionality could be built into the current bioreactor system to expand its utility in vascular graft development.

5. TEVG Culture in a Pulsatile Flow Bioreactor

5.1 Introduction

Blood vessel replacements are frequently necessary in the treatment of advanced atherosclerosis, aneurysmal and peripheral vascular disease, and trauma. Autologous saphenous veins and mammary arteries are currently the preferred graft materials. However, the availability of tissues of appropriate dimensions is limited[140], and donor site morbidity is a significant complication in these procedures. When autologous tissue is unavailable, synthetic materials (mainly Dacron and polytetrafluoroethylene) are frequently used for the treatment of peripheral vascular disease, but their use is limited to high-flow/low resistance conditions[9, 10], *i.e.*, to greater than 6 mm internal diamter vessels, because of their thrombogenicity, relatively poor elasticity, and low compliance[11]. Tissue engineering represents a potential means to construct functional grafts that could be used in vascular replacement procedures where autologous tissue is unavailable and synthetic materials fail[141].

Blood vessels consist of three layers: a thin monolayer of endothelial cells, a medial layer composed of smooth muscle cells (SMC) embedded within a dense network of collagen and elastic fibers, and a loosely organized adventitial layer comprised of fibroblasts. Since the medial layer is the primary load bearing layer of the arterial wall, much of the previous research in tissue engineered vascular grafts (TEVG) has focused on developing a bioartificial medial layer[142, 143]. While initial results with many of the TEVG constructed to date are very encouraging, a number of technical hurdles remain before they can be considered a viable vascular replacement option[49]. The potential for aneurysmal failure is a significant concern, since the mechanical integrity of

TEVG is generally less than that of the arteries they replace and since the mechanical integrity of the engineered grafts may not be maintained with time. In addition, many TEVG studies have been plagued in the *in vivo* setting by thrombosis and intimal hyperplasia[49].

One approach that several investigators have taken to improve TEVG mechanical and biochemical outcome involves exploiting the ability of cells to sense and respond to mechanical stimuli. Mechanical stretching of SMC has been shown to have profound effects on the cell phenotype[144, 145], orientation[145], ECM deposition[146, 147], growth factor release[148], and mechanical properties[134, 149]. Important work by Kim *et al.* showed a 15% increase in SMC proliferation and a 49% increase in elastin content for polymeric scaffolds cultured for 10 weeks with cyclic strain at an amplitude of 7% compared to unloaded controls[134]. Additionally, the elastic moduli and ultimate tensile strengths (UTS) of these constructs were significantly higher in the mechanically stimulated group. In total, these findings provide support for the inclusion of physiologically relevant mechanical stimulation in the development of tissue engineered constructs containing SMCs.

While the aforementioned mechanical conditioning studies have shown promising results in terms of increasing construct stiffness and strength, ECM deposition, and SMC phenotype, none has applied a fully physiological pulsatile wave to the constructs. In the current work, a pulsatile flow bioreactor has been designed to allow for both physiological shear and pulsatile conditioning to examine the effects of these combined stresses on TEVG outcome using poly(ethylene glycol) (PEG) hydrogels as a model scaffold material.

Diacrylate-derivatized PEG (PEGDA) macromers readily dissolve in aqueous solution, forming an optically transparent, low viscosity mixture that is photopolymerizable in the presence of cells[150, 151]. Thus, seamless, mechanically isotropic[152] cylindrical constructs with homogenously seeded cells[96, 126-129, 153] can be readily formed by pouring a solution of photoactive PEG macromers, cells, and photoinitiator into an appropriately shaped mold and applying light. In addition, PEG hydrogels are highly elastic, which is important in the vasculature where tissues must maintain their form in response to prolonged mechanical stress. PEG hydrogels also have tunable mechanical properties, meaning that the strain experienced by the scaffold can be varied independently of an applied pulsatile waveform and shear stress by changing the scaffold composition. Thus, the custom-built reactor combined with PEG-based hydrogels creates a versatile system in which strain amplitude, pulse shape, pulse frequency, and shear can be varied independently and their roles in vascular development examined.

Reported in this chapter are the results of three studies using the pulsatile flow bioreactor. The studies explore the effects of dynamic culture at physiological and sub-physiolgoical conditioning regimes and two different cell types – mouse 10T1/2 smooth muscle progenitor cells (10T1/2) and human coronary artery smooth muscle cells (HCASMC). In addition the effects on the hydrogel matrix degradation potential are investigated by varying the content of two covalently incorporated peptides (**GGLGPAGGK** and GGGPQGIWGQGK) that are sensitive to cleavage by matrix metalloproteinases (MMP). [154-156]

Table 5-1 summarizes the parameters for each of the bioreactor studies. Included are the cell type and initial seeding density, the hydrogel formulation giving ratios of PEGDA to degradable polymer and the cell adhesive moiety PEG-RGDS. Listed next are the specific flow parameters achieved in each study including flow rate (mL/min), pressure differential (mmHg), pulse rate (bpm), and shear stress (dynes/cm^2).

Table 5-1. Experimental Parameters for Bioreactor Studies

Study	Cell Type & Density	Hydrogel Formulation	Flow Parameters	Time Course
10T1/2 LGPA	mouse embryonic progenitor $1.3x10^6$/mL	70% 6 kDa PEGDA 30% PEG-LGPA-PEG 2.8 mM PEG-RGDS	120 mL/min 110/70 mmHg 120 bpm 7.5 dynes/cm^2	8 wk (0, 4, 8)
SMC Low PQ	HCASMC $10x10^6$/mL	70% 6 kDa PEGDA 30% PEG-PQ-PEG 2.8 mM PEG-RGDS	40 mL/min 45/5 mmHg 120 bpm 2 dynes/cm^2	5 wk (0, 5)
SMC High PQ	HCASMC $8x10^6$/mL	30% 6 kDa PEGDA 70% PEG-PQ-PEG 2.8 mM PEG-RGDS	60 mL/min 55/15 mmHg 120 bpm 4 dynes/cm^2	8 wk (0, 4, 8)

5.2 Methods and Materials

All materials were obtained from Sigma (St. Louis, MO) unless otherwise noted.

5.2.1 Synthesis of PEGDA and PEG Derivatives

Poly(ethylene) diacrylate (PEGDA) and bioactive PEG derivates were synthesized as described previously in detail (2.2.1). Briefly, PEGDA of molecular weight 6000 Da was synthesized by reaction PEG with acryloyl chloride and triethylamine in anhydrous conditions. The solution was washed with K_2CO_3 and the organic phase dried with $MgSO_4$ before precipitation in diethyl ether. The MMP sensitive peptide sequences GG**LGPA**GGK[154] and GGG**PQ**GIWGQGK[155, 156] were formed using solid phase peptide synthesis with standard Fmoc-chemistry, and were conjugated, along with the commercially available RGDS, to monoacrylated PEG. In the 10T1/2 LGPA study this reaction was carried out under aqueous conditions with acryloyl-PEG-NHS and for HCASMC PQ studies the peptides were reacted with acryloyl-PEG-SCM in organic buffer.

5.2.2 Cell Culture

All cell expansion procedures and bioreactor experiments were carried out in a 37°C humidified environment with 5%CO_2. Cell culture media was replaced every two to three days.

5.2.2.1 10T1/2 Smooth Muscle Progenitor Cells

In the first study, mouse embryonic 10T1/2 smooth muscle (SM) progenitor cells (ATCC, Manassa, VA) were expanded in monolayer culture between passages 4-6. Prior to encapsulation within hydrogels, cells were maintained in Eagle's Minimum Essential

Medium (MEM, ATCC) supplemented with 10% heat-inactivated fetal bovine serum (FBS) and without the use of antibiotics/antimycotics. This media maintains the undifferentiated state in these progenitor cells.[157] Once in bioreactor experiments, 10T1/2 cells were cultured in MEM supplemented with 10% FBS, 10 ng/mL TGF-β1 (R&D systems, Minneapolis, MN), 10 μg/mL insulin, 50 mM L-ascorbic acid, 10 μg/mL ciprofloxacin, 100 mU/mL penicillin, 100 mg/L streptomycin, and 0.25 μg/mL fungizone (Gibco, Carlsbad, CA). The cocktail of growth factors and L-ascorbic acid added to the media was selected for two reasons. First, 10T1/2 SM progenitor cells have been shown to display a smooth muscle cell phenotype when cultured in the presence of TGF-β1. In addition, smooth muscle cells have been shown to increase both collagen and elastin production relative to basal levels when in the combined presence of L-ascorbic acid, TGF-β1, and insulin.[158]

5.2.2.2 Human Coronary Artery Smooth Muscle Cells

Human coronary artery smooth muscle cells (HCASMC, Cascade Biologics, Portland, OR) were used between passages 3-8 and expanded prior to experiments in smooth muscle cell growth media (SMGM) which consisted of Medium 231 (Cascade) with the following supplements: 4.9% v/v fetal bovine serum (Invitrogen, Carlsbad, CA), 2 ng/mL human basic fibroblast growth factor (Invitrogen), 0.5 ng/mL human epidermal growth factor (Invitrogen), 5 ng/mL heparin, 5 μg/mL insulin, 0.2 μg/mL bovine serum albumin, 100 U/mL penicillin, and 100 μg/mL of streptomycin. This medium served to maintain the HCASMC in the growth or proliferative phase. After 4 wk in culture during the SMC High PQ study, the culture medium in one flow loop was changed to smooth muscle cell differentiation media (SMDM) which consisted of Medium 231 with 1% v/v fetal bovine

serum and 30 μg/mL heparin. The lower serum concentration and heparin supplementation are known to induce differentiation to the contractile phenotype in these cells[159-161]. Examples of the different effects of the two media types are shown by immunocytochemical analysis of HCASMC cultured on tissue culture polystyrene (Figure 5-1). Of note are significant increases in the expression of the contractile protein smooth muscle α-actin (SM α-actin) and the SM α-actin associated protein calponin. In addition while a majority of cells in SMGM stain positive for proliferating cell nuclear antigen (PCNA), indicating cells in G-phase of mitosis, few if any proliferating cells are found in SMDM.

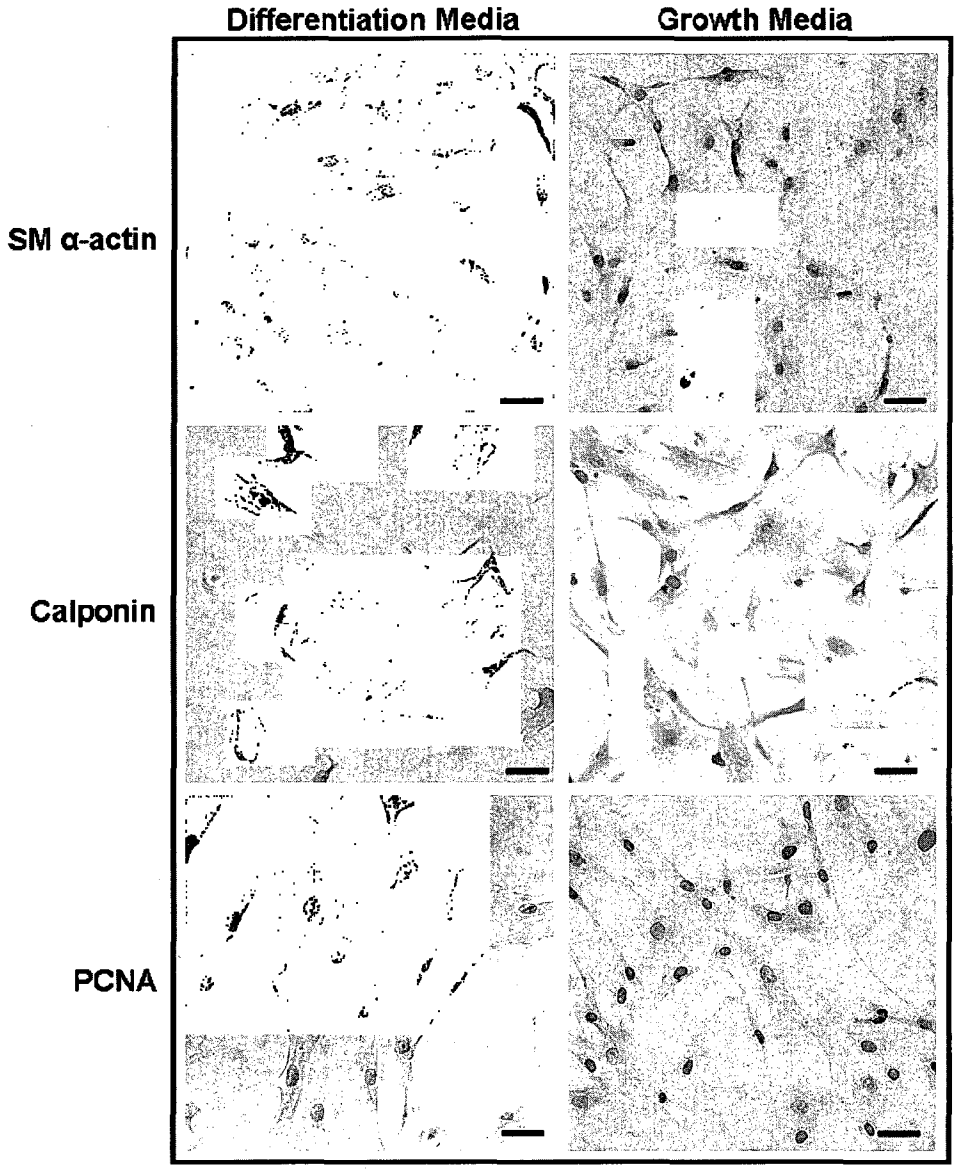

Figure 5-1. Expression Differences between HCASMC in SMDM and SMGM. Differentiation media promotes expression of the contractile proteins SM α-actin and calponin and inhibits proliferation as demonstrated by a lack of positive reaction with an antibody to PCNA. The diffuse staining for calponin in cells cultured in growth media is the result of reaction of the antibody with cytoplasmic calponin which is a different isoform, not associate with SM α-actin fibers. Scale bars are 50 μm.

5.2.3 Cell Encapsulation

A precursor solution containing a total of 0.1 g/mL PEGDA and PEG-peptide-PEG along with 2.8 mM PEG-RGDS was prepared in HEPES buffered saline (HBS; 10 mM HEPES, 100 mM NaCl, pH 7.4) and sterilized via filtration. Cells were trypsinized and immediately resuspended in the precursor solution at a concentration of 1.3 x 10^6 cells/mL (10T1/2 LGPA), 10 x 10^6 cell/mL (SMC Low PQ), or 8 x 10^6 cell/mL (SMC High PQ). 10 μl of a 300 mg/mL solution of UV photoinitiator 2,2-dimethoxy-2-phenyl-acetophenone dissolved in N-vinylpyrrolidone (NVP) was added per mL of the cell-precursor solution mixture. The low viscosity mixture was gently agitated with a vortex, and the cell suspension rapidly pipetted into transparent cylindrical molds consisting of a 6.4 mm diameter hollow plastic cylinder fitted with inner glass mandrels 3 mm in diameter. Long wavelength UV light (10 mW/cm^2, 365nm) was applied to the hydrogels under constant rotation of the constructs for an average of 3 min/gel to produce uniform polymerization within and between gels. Long wavelength UV light has been extensively used at similar intensities and exposure times to induce rapid polymerization of PEGDA macromers with minimal concomitant cell damage in numerous tissue engineering applications[96, 126-129, 153, 162, 163].

5.2.4 Cyclic Mechanical Conditioning

The polymerized constructs were removed from the molds and allowed to swell in media for 1 hr at 5% CO_2 / 37°C. Ring samples were cut from each hydrogel construct and analyzed biomechanically as described below. The constructs were then transferred to the bioreactor chambers, and maintained under static conditions for one week in culture media. After one week of static culture, constructs were randomly assigned to static and

dynamic groups. The constructs in the static groups continued to be grown under static conditions during the remaining culture time. Over the course of three to seven days, the flow in each of the dynamic constructs was increased to the final conditioning parameters, which were at or near physiological levels depending on the experiment (Table 5-1). A single pulsing pump was used to generate a pulsatile waveform with a pressure difference of 20 mmHg and pulse rate of 120 bpm. Wall shear stress was calculated from Equation **4-2** to be 7.5 dynes/cm^2 (10T1/2 LGPA), 2 dynes/cm^2 (SMC Low PQ), 4 dynes/cm^2 (SMC High PQ) which are similar to, although slightly lower than, physiological baseline wall shear of ~10 dynes/cm^2.[164]

At each designated time point, samples from both the static and dynamic groups were harvested and cut into a series of rings for biochemical, biomechanical, and histological analyses. Wet weights of the constructs used for biochemical analyses were recorded and the samples were immediately frozen at -80°C.

5.2.5 Biomechanical Testing

Biomechanical testing was performed using a modification of the circumferential property testing techniques validated in Johnson *et al.*[131] and Hiles *et al.*[132] and described previously (4.3.3) Sections for biomechanical analysis were obtained by placing TEVG constructs on a glass mandrel and subsequently cutting the gels into thin rings using nylon monofilament sutures. Sample dimensions were obtained from digital images (inner and outer diameter) or using calipers (width). Material properties were then measured using an Instron Model 3340 materials testing device equipped with a 10 N load cell (Instron). System control and data analysis were accomplished using Instron Series IX/s software. Custom mounting brackets provided uniaxial strain application at a

rate of 6 mm/min for the ring-shaped hydrogels. Each sample was run in triplicate and the stress-strain data was used to obtain the ultimate tensile stress (UTS) and average elastic modulus. The reported UTS for each sample was the maximum of the three measured failure stresses. Modulus was defined as the slope of the linear region of the stress-strain curve at a reference stress of 30 kPa.

5.2.6 Biochemical Analyses

Segments of each vessel, 100-200 mg wet weight, were analyzed for DNA, collagen content, and elastin content. The constructs were hydrolyzed in 700 μL of 0.1 N NaOH per 200 mg hydrogel wet weight for 36 hr at 37 °C. The samples were then centrifuged (10,000 x g for 10 min), and a 10 μL aliquot was taken from each sample for DNA quantification. Any material pelleted during centrifugation was resuspended by vortexing, and additional hydrolysis was carried out by transferring the samples to a 100 °C oven for 90 min. This hydrolysis step served to solubilize collagen but not elastin fibers. Hydrolyzed samples were then cooled to room temperature and centrifuged to pellet elastin (10,000 x g for 10 minutes). The elastin pellet was washed three times with distilled water and stored at -80 °C. The supernatant was retrieved for collagen quantification.

5.2.6.1 DNA Analysis

Aliquots of the hydrolyzed samples retrieved for DNA analyses were neutralized. Sample DNA levels were then assessed using the Molecular Probes PicoGreen assay reagents (Invitrogen, Carlsbad, CA) and calf thymus DNA standards that had experienced the same base hydrolysis conditions as the constructs. DNA was translated to cell number using the conversion factor for murine cells of 6.6 pg DNA per cell[165] and 6

pg DNA per smooth muscle cell.[166] The conversion from DNA to cell number is commonly used to assess the cellularity of tissue engineered constructs.[126, 143, 167-169]

5.2.6.2 Collagen Analysis

The supernatants retrieved for collagen quantification were subjected to acid hydrolysis in 6 N HCl at 110 °C for 15-18 hr. For the 10T1/2 LGPA experiment, equal mass aliquots from each hydrolyzed static sample were pooled and the hydroxyproline (OHPr) content of this pooled sample was measured in duplicate by amino acid analysis (AAA Service Laboratory, Damascus, OR). Similarly, equal mass aliquots of hydrolyzed dynamic samples were pooled and the OHPr content of this pooled sample was measured in duplicate by amino acid analysis. Sample collagen content was calculated from measured OHPr levels using a conversion factor of 8 mg collagen per mg OHPr[170] and was normalized to cell number.

In HCASMC PQ experiments the collagen content of hydrolyzed samples was determined using a colorimetric assay for OHPr.[171] In this assay, hydrolysis in 6N HCl proceeded for 16 h at 110°C followed by evaporation of HCl to dryness. All samples and OHPr standards were reconstituted in acetate-citrate buffer (pH 6.0) and then mixed with a chloramine-T reagent and incubated at room temperature for 20 min. After this time an aldehyde/perchloric acid solution was added to all samples followed by heating to 60°C for 15 min. Finally, the absorbance at 558 nm was read to determine the concentration of OHPr and conversion to collagen mass.

5.2.6.3 Elastin Content

Elastin levels were determined according to the procedure detailed in Long *et al.* [158] Briefly, elastin pellets were digested in 6 N HCl at 100 °C for 24 hr. Samples were then dried on a rotary evaporator, and the resulting free amino acids were dissolved in 100 µl of 0.1 M sodium citrate buffer (pH 5.0). Following addition of an equal volume of ninhydrin reagent, samples were boiled for 15 min, cooled, and their absorbance read at 570 nm. Hydrolyzed α-elastin (Elastin Products Company, Owensville, MO) was used as the standard, and measured elastin levels were normalized to cell number.

5.2.7 Histological Analysis

Segments from each TEVG were harvested at designated time points in each study and immediately submerged in freezing media (Triangle Biomedical Sciences, Durham, NC). For the study involving 10T1/2 cells, 30 µm frozen sections were immuno-stained to detect the presence of the SMC markers calponin and SM α-actin[172] to confirm that the 10T-1/2 precursor cells were displaying a SMC-like phenotype. Briefly, fixation in 10% neutral buffered formalin (VWR Scientific, West Chester, PA) for 10 min was followed by a two-step blocking procedure (BEAT Block, Zymed, Carlsbad, CA) to prevent non-specific interactions. Sections were next incubated with primary antibodies to either calponin (C2687, Sigma), or SM α-actin (A2547, Sigma) for 18 hr at 4 °C followed by the application of Peroxo-Block for 45 s to quench any endogenous peroxidase activity (Peroxo-Block, Zymed). Positive staining was visualized after successive incubations with a biotinylated secondary antibody for 30 min, an enzyme conjugate for 20 min, and an AEC substrate chromagen mixture for 10 min (Histomouse-SP, Zymed). Nuclei were

counterstained with hematoxylin and coverslips mounted using GVA mount (Zymed). Sections not exposed to primary antibodies served as negative controls.

In studies with HCASMC, sections were analyzed using antibodies for ECM components including elastin (Elastin Products, PR385), collagen (Abcam, Cambridge, MA, ab24117), and fibronectin (Sigma, F3648). Frozen sections were cut and fixed as described above followed by blocking with a 3% BSA solution overnight. Incubation with primary antibodies for 8 h was followed by overnight application of a fluorescent secondary antibody (Invitrogen, A11008). All incubations were at 4°C.

5.2.8 Detection of Matrix Metalloproteinase Activity

Frozen sections of bioreactor specimen from the HCASMC High PQ study were analyzed for evidence of matrix metalloproteinase (MMP) activity using a method of *in situ* zymography.[173, 174] Samples of static and flow conditioned hydrogels cultured for 8 weeks were analyzed. For the flow conditioned set, both differentiation and growth media sections were assayed. In this assay, glass slides were coated with an agarose solution mixed 1:1 with two different fluorescently labeled MMP substrates. Briefly, casein-fluorscien and gelatin-Oregan Green™ 488 (Molecular Probes, 1 mg/mL) were each mixed in equal parts with 1% agarose in Tris-HCl buffer (50 mM, pH 7.4) containing 10 mM Ca chloride and 0.05% Brij 35. The solution was coated onto slides in a manner similar to that used to make blood smears and the films allowed to solidify at room temperature protected from light. Frozen sections cut to 30 μm were placed on the solidified films and covered with a drop of Tris-HCl buffer. For negative controls, sections were covered with Tris-buffer containing 10 mM 1, 10 phenanthroline. Coverslips were carefully placed on top of the samples and all slides incubated for 48 h at

37°C in a humidified chamber in the dark. After 48 h sections were inspected using a fluorescent microscope with black zones of substrate lysis indicating substrate breakdown via MMP activity.[173]

5.3 Results and Discussion

5.3.1 Biochemical Analyses

5.3.1.1 Summary Cell and Matrix Data

After culture, the degradable constructs exposed to physiological pulsatile flow conditioning were analyzed biochemically and compared to constructs cultured under static conditions. Mean results for all three study groups are summarized in Table 5-2 with plots from individual data sets following subsequently for observation of trends and variances within each study. For clarity, only data collected for the final time points in each study are reported in the summary table below.

Table 5-2. Cell Number and ECM Content in TEVG

		Cell Number (Cell/g wet weight)	**Elastin Content** (ug/cell) (ug/g wet weight)	**Collagen Content** (ug/cell) (ug/g wet weight)
10T1/2 LGPA	Static	8.5×10^5 *	3.5×10^{-5} 29	1.5×10^{-4} * 179 *
	Dynamic	10×10^5 *	3.5×10^{-5} 35	1.8×10^{-4} * 133 *
SMC Low PQ	Static	3.3×10^6 *	3.7×10^{-6} 12 *	5.5×10^{-6} 13
	Dynamic	1.8×10^6 *	2.7×10^{-6} 5 *	6.3×10^{-6} 11
SMC High PQ	Static	1.5×10^6	7.6×10^{-6} 11	1.5×10^{-6} 21
	Dynamic SMDM	1.4×10^6	10×10^{-6} 14	4.8×10^{-6} 11
	Dynamic SMGM	1.1×10^6	9.5×10^{-6} 10	0.8×10^{-6} * 31 *

* indicates a statistically significant difference from other groups in the same study, $p<0.05$

The cell number in the dynamic constructs at final time point was significantly higher than that in the static constructs for the 10T1/2 LPGA and statistically lower in the SMC Low PQ studies (student t-test, $p<0.05$). For the 10T1/2 LPGA group this likely indicates that dynamic conditioning is enhancing cell survival/proliferation. This result is consistent with previous studies regarding the effects of pulsation on TEVG cell density at moderate strains[175]. However because the condition regimes for the SMC groups are similar and the primary differences in the two studies are degradable content and final culture time (5 wk for SMC Low PQ and 8 wk for SMC High PQ), analysis of the full data sets are necessary to draw further conclusions.

Comparable amounts of elastin were measured in the static and dynamic constructs of all groups ($p>0.05$), indicating that mechanical conditioning did not effectively enhance elastin production/retention over the time of culture. Significant variability in terms of the effects of mechanical stimuli on elastin production has been reported in literature[124, 176], variability which may be due in part to differences in cell source, media additives[158], scaffold[158], and experimental time scale.[176] This being said, in the 10T1/2 LGPA study, the elastin levels in both the static and dynamic constructs compare well on a per cell basis with elastin levels characteristic of native arteries (roughly 8×10^{-5} μg/cell to 6.7×10^{-5} μg/cell, depending on the type of artery).[177, 178] Elastin levels in the SMC High PQ study was slightly lower than this value while that in the SMC Low PQ studies was an order of magnitude lower. Again, this could be primarily due to the time course (5 wk instead of 8 wk) of SMC Low PQ experiment.

In contrast to the elastin results, the dynamic constructs in the 10T1/2 LGPA study showed a 18.3% increase in the amount collagen per cell compared to static samples (students t-test, $p < 0.05$). These results are consistent with other studies that have demonstrated enhanced collagen production by vascular cells in response to mechanical stretch. Importantly, the collagen produced on a per cell basis in the dynamic constructs by week 8 (~$1.8x10^{-4}$ μg/cell) compares favorably with per cell collagen content of native arteries, which ranges from roughly 3.1×10^{-4} μg/cell to 9.7×10^{-4} μg/cell[124, 177]. Since collagen is a primary structural protein responsible for the mechanical integrity of blood vessels under the high blood pressure and flows experienced *in vivo*, collagen levels approaching native tissue are critical for the success of TEVG. In the SMC groups there was again, no difference in the static versus dynamic culturing methods and notably, the magnitude of collagen production was much less than in the 10T1/2 LGPA study.

5.3.1.2 Individual Study Data - Biochemical Analyses

The data plots for the biochemical analyses of the 10T1/2 LGPA, SMC Low PQ, and SMC High PQ studies follow. All data are mean ± SEM.

Figure 5-2 displays the cell and ECM content information for the 10T1/2 LGPA study, which shows a significant increase in both 10T1/2 number and collagen content in dynamically culture TEVG over the 8 week study. In the SMC Low PQ study there are significantly fewer cells in dynamically cultured grafts, but no difference in ECM content after 5 weeks (Figure 5-3).

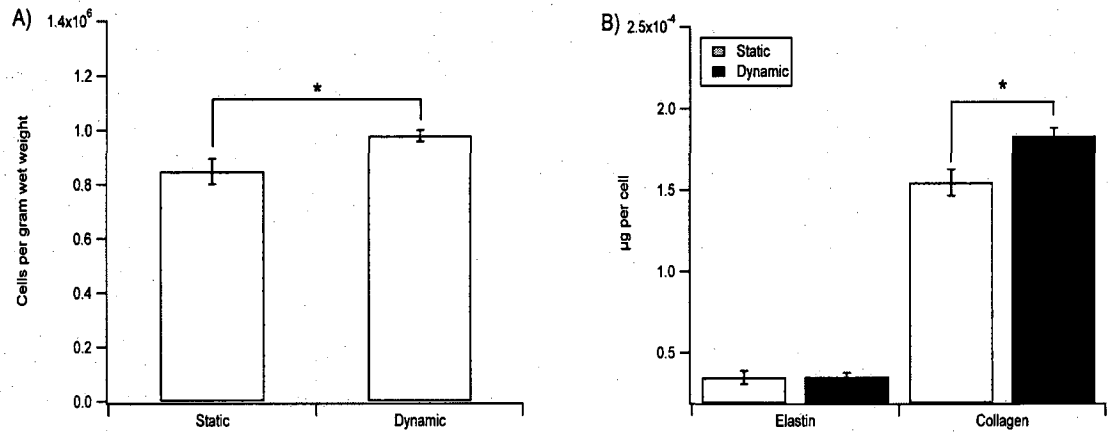

Figure 5-2. Cell Number and ECM Content for TEVG from the 10T1/2 LGPA Study. Biochemical analyses show an increase in cell number (A) and collagen content (B) in constructs cultured under pulsatile flow conditions at 120 bpm. Similar amounts of elastin were measured in each group. * Indicates a statistical difference, cell number: $p < 0.05$, collagen content: $p < 0.05$.

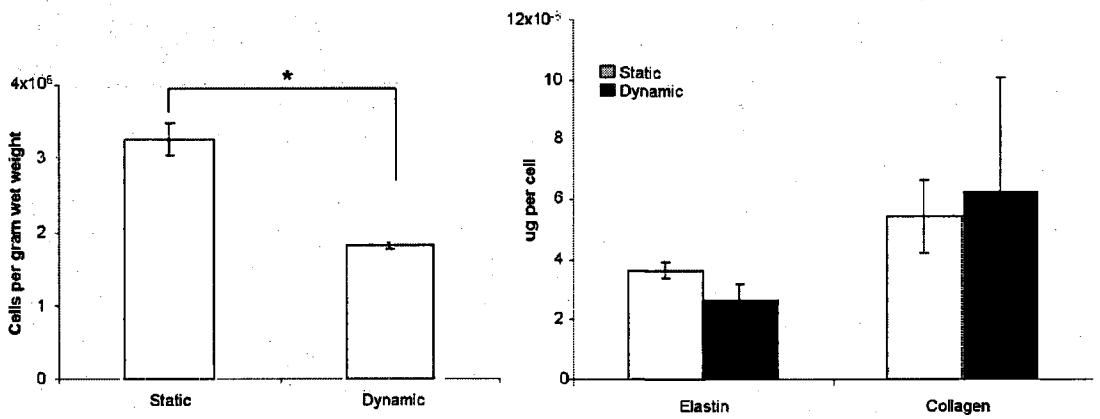

Figure 5-3. HCASMC Cell Number and ECM Content in the Low PQ Study. There are statistically more cells in the statically cultured constructs at this 5 week time point (ANOVA, $p<0.05$). No significant differences exist between the culture conditions for either of these ECM components when normalized to cell number (ANOVA, $p>0.05$).

Results for the SMC high PQ study are slightly more complex since there were two time points and two media types for the latter part of the culture period. From this data, it is evident that there is a statistical increase in the number of HCASMC at the 4 week time point in dynamically culture TEVG compared to static controls (Figure 5-4). At the end of the experiment, however, this relationship is reversed with fewer cells in the dynamic constructs for the SMGM group and no difference when compared with the SMDM samples. There is a general downward trend in cell number for the two HCASMC studies with final cells number in the range of 10-20% of the seeded values.

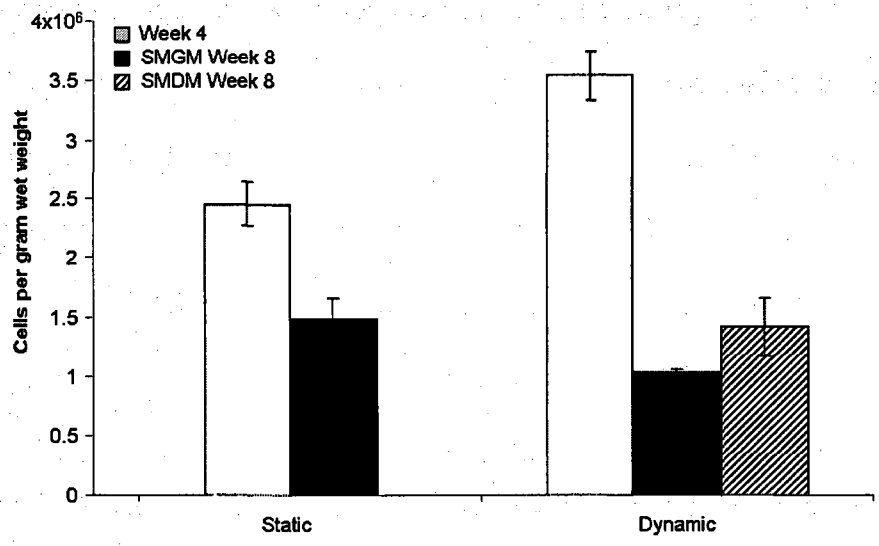

Figure 5-4. Number of HCASMC in the High PQ Study. All groups are statistically different from each other except Dynamic Week 8 SMDM which is similar to both Static Week 4 and Dynamic Week 8 SMGM (ANOVA, $p<0.05$).

Elastin content on a per cell basis is significantly improved over the course of this 8 week study (Figure 5-5). Collagen synthesis and retention, however, remains relatively unaffected with the exception of the Dynamic SMDM group which seems to significantly increase collagen content compared to other groups.

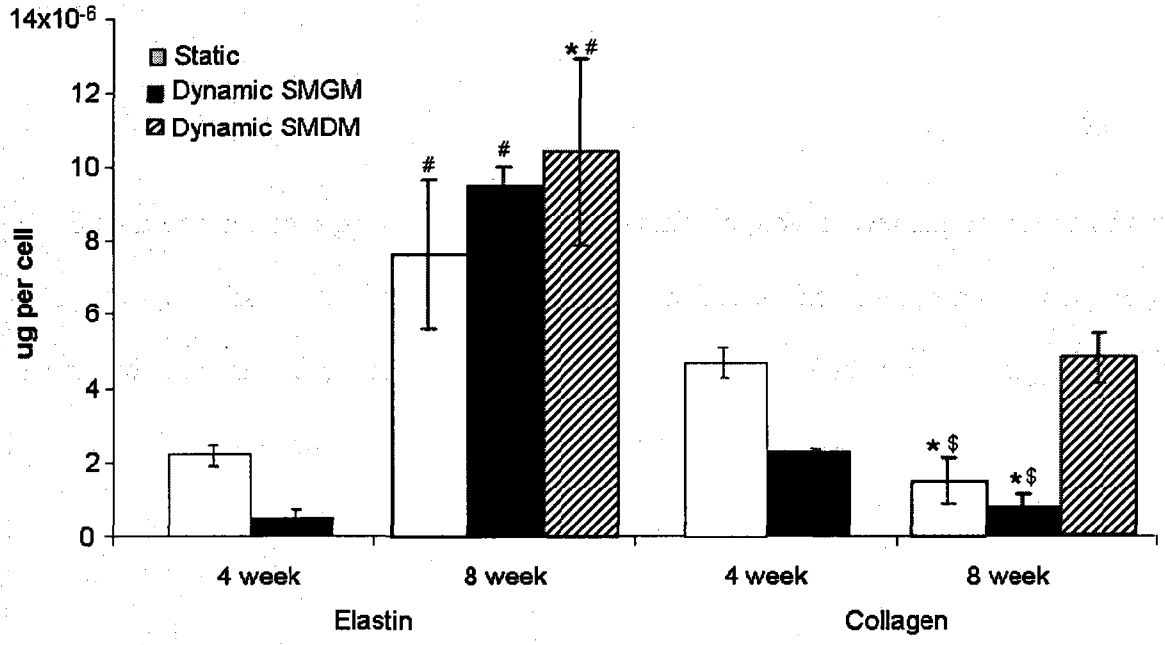

Figure 5-5. Elastin and Collagen Content for SMC High PQ Study. *Indicates statistically different from Static Week 4 group, # is statistically different from Flow Week 4, and $ is different from Dynamic Week 8 SMDM (ANOVA, $p<0.05$).

5.3.2 Biomechanical Analyses

To monitor the changes in construct mechanical properties with time, biomechanical analyses were conducted. As shown in Figure 5-6, there is a significant decrease in TEVG stiffness during the first 4 weeks of culture for the 10T1/2 LPGA samples (A) and the dynamic group from the SMC High PQ study (C, ANOVA, $p<0.05$). For the final 4 weeks, the dynamic constructs in each case recover to values that are no longer different

from the initial time point ($p>0.05$), while the static group containing 10T1/2 cells continues to decline ($p<0.05$). Static TEVG in the SMC High PQ study remain unchanged throughout the 8 week culture period. The constructs in the SMC Low PQ study (B) do not match this trend and instead demonstrate a significant increase in stiffness over the 5 week study. The construct UTS (Figure 5-7) increases in the SMC Low PQ study, but remains unchanged in other groups. This is not unexpected as the UTS measurements in this analysis typically have large within group variations.

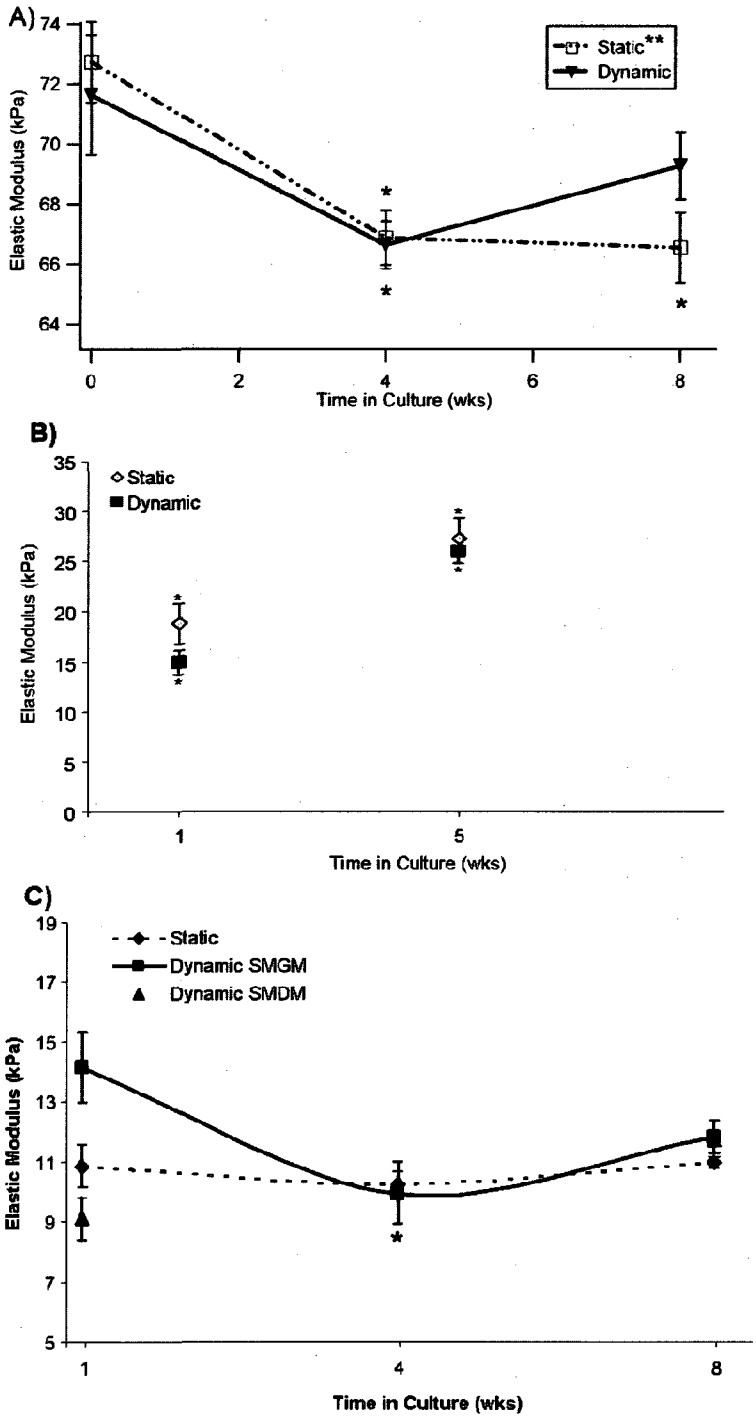

Figure 5-6. Elastic Moduli of Bioreactor TEVG. For 10T1/2 LGPA (A) and HCASMC High PQ (C) groups there is a general trend of decreasing stiffness over the first 4 wk of culture followed by an increase to the end of the experiment. This is not the case in the Low PQ SMC study where the second time point is statistically higher for both static and dynamic groups. *Indicates statistically different from the initial time point (ANOVA, $p<0.05$).

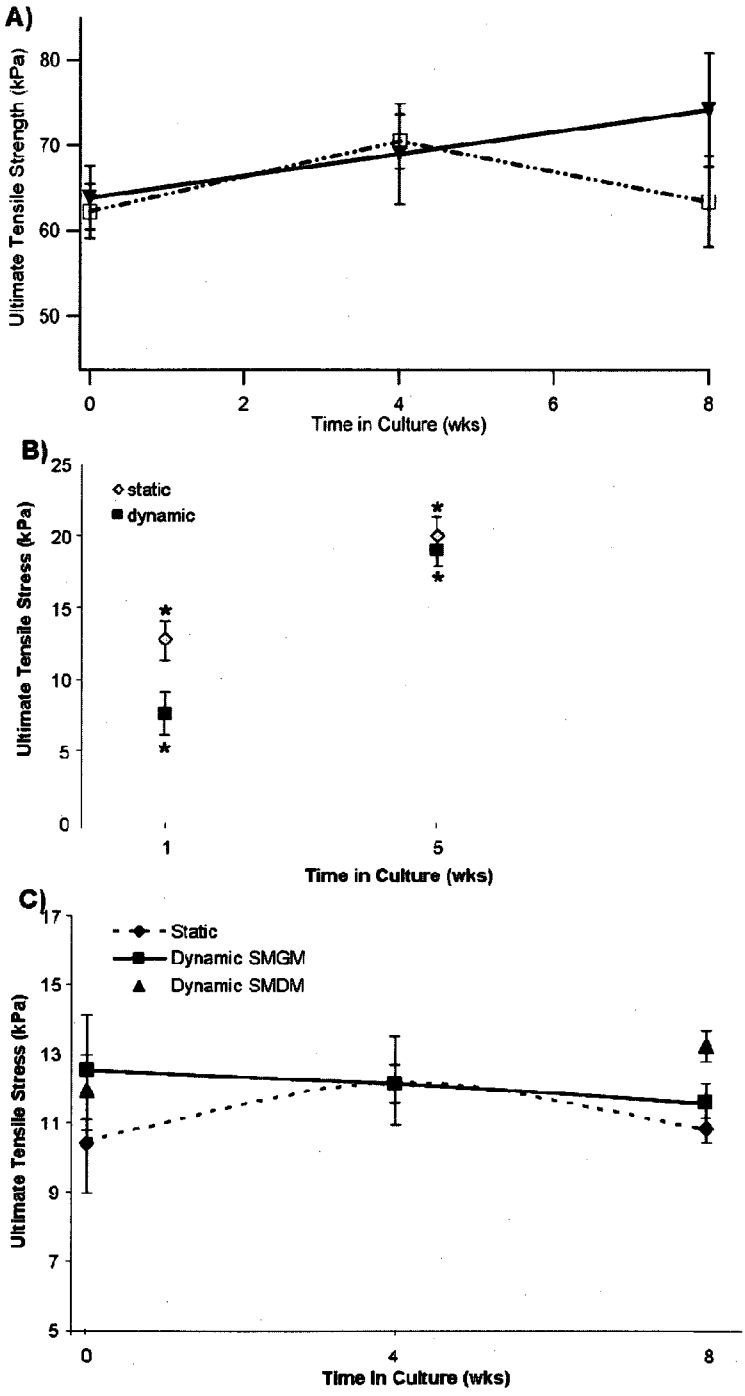

Figure 5-7. Ultimate Tensile Stresses for Bioreactor TEVG. There is a statistical increase in the UTS for constructs in the SMC Low PQ study (B, ANOVA, $p<0.05$), while all other groups remain unchanged during culture.

Another primary observation from these mechanical analyses is the overall decrease in modulus and UTS values from the 10T1/2 study to the HCASMC studies. For example, the modulus in 10T1/2 LGPA samples ranges from ~66-73 kPa while in the HCASMC studies the range is ~9-27 kPa. This is a dramatic difference, but was expected since the nearly 10-fold increase in cell number adds significant non-fluid mass to the hydrogel formulation prior to initiation of the crosslinking event. Cells effectively function to disrupt the final network structure and thereby decrease the resultant hydrogel stiffness. This lower stiffness can be a drawback since more compliant gels do not adhere as tightly to graft chamber ports and consequently leak at high pressures and large pressure differentials. For that reason, the HCASMC studies were conducted at sub-physiological flow conditions.

Analysis of these results suggests that the initial decrease in modulus observed for the 10T1/2 LGPA and SMC High PQ studies may be due to a reduction in hydrogel crosslinking density as the result of degradation of the collagenase sensitive peptide linking the PEG chains present in the constructs. With increasing time in culture, the moduli of the static hydrogels continued to deteriorate, perhaps due to a continued degradation of the network that was not matched by new protein production. It could also be proposed, then, that if the HCASMC in the SMC Low PQ study degrade the low percentage PEG-PQ-PEG hydrogel at a very slow rate, this would account for the lack of an initial decrease in mechanical properties for hydrogels in the SMC Low PQ study.

5.3.3 Histological Analysis

Although TGF-β1 was added to the cell culture media to induce SMC-like phenotype in the encapsulated 10T-1/2 SM progenitor cells[179], it was still important to verify that

the encapsulated progenitor cells were indeed displaying SMC-like phenotype. Calponin and SM α-actin are two standard markers used to identify cells expressing a SMC phenotype[172, 180]. Immunohistochemical analyses of both static and dynamic constructs revealed comparable expression of calponin and SM α-actin (Figure 5-8) in each. These results indicate the expression of a SMC-like phenotype under the current culture conditions and validate the use of these progenitor cells for applications in vascular graft regeneration.

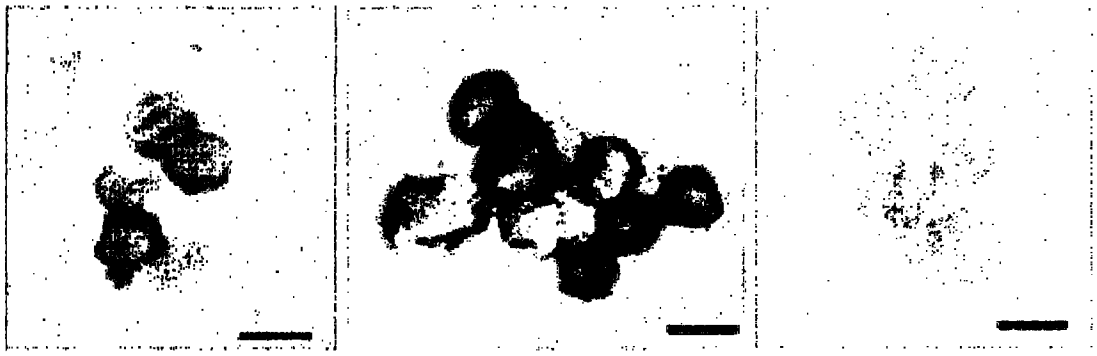

Figure 5-8. Immunohistochemical Staining for SMC Markers in 10T1/2 Cells. Immunohistochemical analysis confirms the presence of the smooth muscle cell markers calponin (left) and smooth muscle α-actin (middle) in sections from TEVGs cultured in this study. These representative samples demonstrate the level of staining that was seen in both the mechanically stimulated and static groups. The red color indicates reaction with the primary antibodies, which were not applied in the negative control (right). Scale bars are 10 μm.

Immunofluorescent staining of hydrogel constructs after 8 wk of culture in the SMC High PQ study reveal homogenous cell distribution in all culture groups (Figure 5-9). This is an important observation that indicates that there are no diffusion limitations within the hydrogels which would selectively jeopardize cell viability. ECM proteins were localized to the immediate pericellular region in all groups consistent with the low

magnitude of protein detected by biochemical assays (5.3.1). The low accumulation of EMC molecules could be the result of the permissive hydrogel network structure, which is protein non-fouling by design and has a relatively large mesh size (Table 2-1). Nascent proteins may actually be escaping from the hydrogel during culture, though media samples would need to be analyzed in order to confirm this assumption. Finally, a differentail interference contrast (DIC) image reveals the topography of a hydrogel section (Figure 5-9, D) and shows that encapsulated HCASMC exhibit a mostly round morphology, which may have implications in the decreased cell viability with time in culture.[181]

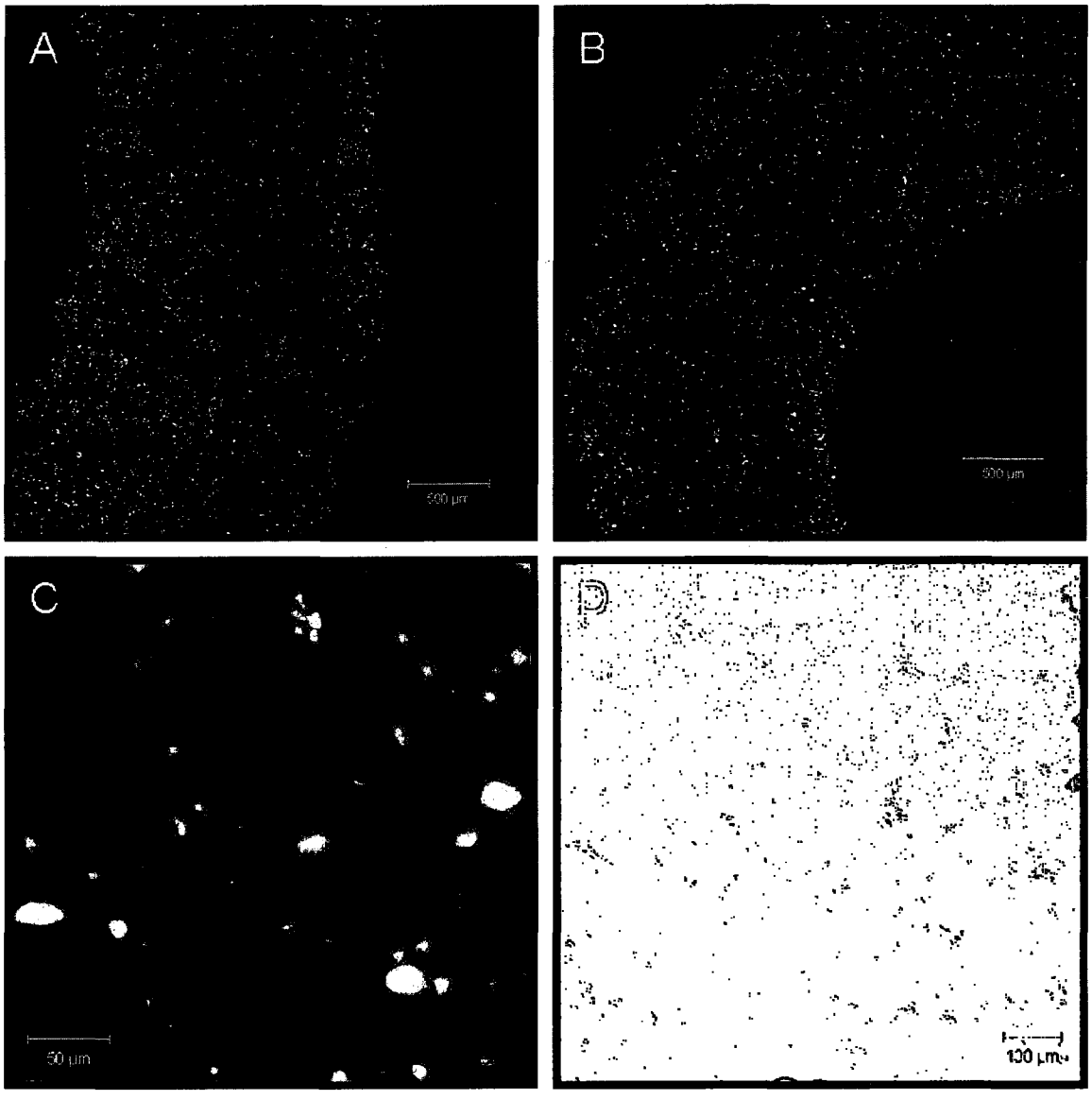

Figure 5-9. IHC Sections of Demonstrating HCASMC Distribution and Morphology in Bioreactor Samples. There was no obvious difference in staining or cell distribution in dynamic (A) or static (B) nor in SMDM versus SMGM (not shown). Staining for ECM components (Fibronectin is shown) indicate only pericellular localization (C). The DIC image (D) reveals cell morphology within the hydrogel section.

5.3.4 Detection of Matrix Metalloproteinase Activity

In a final assessment, *in situ* zymography was used to detect the presence of MMP within the TEVG constructs. Preliminary results indicate that HCASMC have indeed synthesized enzymes capable of degrading a gelatin substrate, but not casein (Figure 5-10). This would imply the presence of gelatinases such as MMP 2 and MMP 9 and is consistent with the targeted recognition for the GGG**PQ**GIWGQGK peptide.[156] The presence of the degrading enzymes is a good indicator of the potential of HCASMC to remodel their surrounding hydrogel matrix in route to organization of a mature tissue construct.

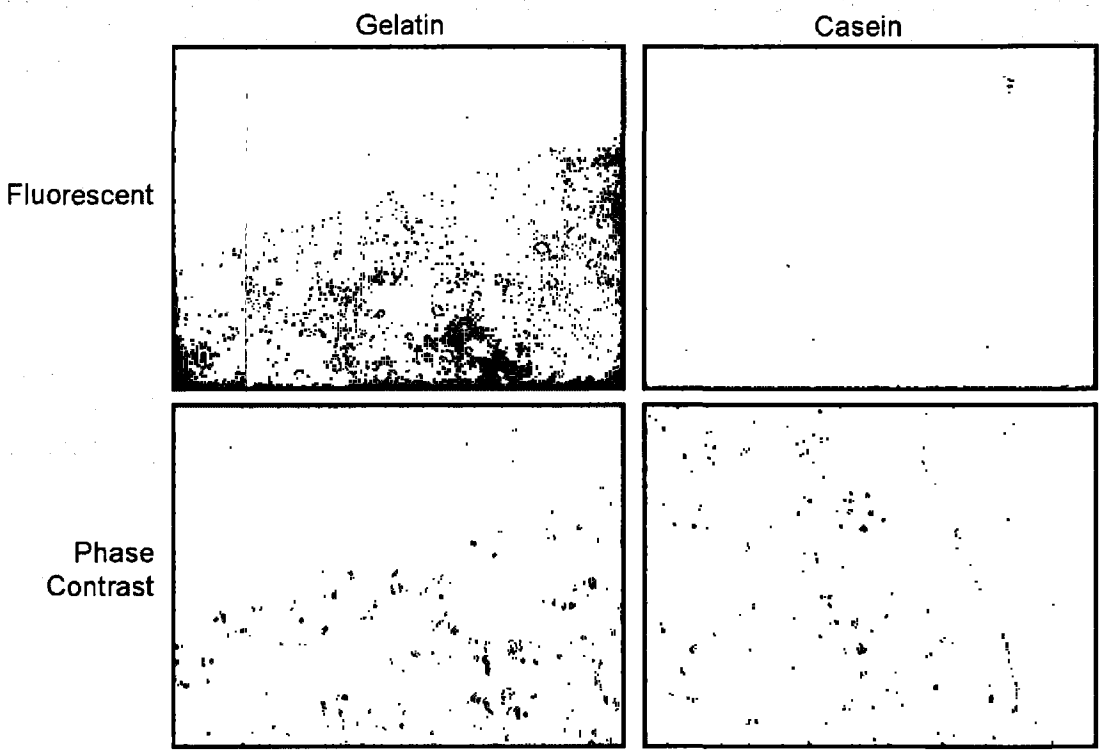

Figure 5-10. MMP Activity in Bioreactor Samples. Black areas in the location of the hydrogel sample in the upper left image demonstrate MMP activity and cleavage of the gelatin substrate. A lack of cleavage of the casein substrate indicates that MMP produced are not active against this protein. Phase contrast images are included for reference and "h" indicates location of the hydrogel, while "s" indicates location of fluorescent substrate. Scale bar is 100 μm.

5.4 Conclusions

In conclusion, this chapter summarizes a series of initial bioreactor investigations. Studies demonstrate the utility and flexibility of the designed flow system to accommodate a range of conditioning parameters. When combined with the tunable, biomimetic PEGDA hydrogel, the system offers great potential for evaluating the individual effects of biochemical and mechanical factors on TEVG development. Results herein indicate that mechanical conditioning can positively influence the cell and ECM content of hydrogel scaffolds and also modulate mechanical properties. These impacts are especially evident with flow conditions close to physiological levels. In addition to flow parameters, initial cell density and degradable matrix content also influence outcomes of bioreactor constructs. In summary, this system will serve as an important tool for the analysis of tissue engineered vascular graft development and maturation.

6. Conclusions and Future Directions

6.1 Thesis Summary

The prevalence of coronary artery disease combined with a paucity of suitable vessel substitutes act as driving forces for cardiovascular tissue engineering research, and as such, have served as motivation for this thesis. The global objectives for this work were two-fold. First, a thorough characterization of poly(ethylene glycol) diacrylate (PEGDA) hydrogels was warranted. This evaluation focused primarily on the network structure of the hydrogel material and on its mechanical properties (Chapter 2). Subsequent studies in Chapter 3 explored the effect of these hydrogel properties the material's ability to serve as a tunable substrate for vascular smooth muscle cells. A special focus is placed on the ability to independently tune the hydrogel's biochemical properties (*e.g.* cell adhesivity) and biomechanical properties (*e.g.* stiffness) in an effort to identify parameters most important to cell-substrate interaction.

The second primary objective was to design, develop, and evaluate a pulsatile flow culture system for tissue engineered vascular graft constructs that was capable of achieving physiologically relevant fluid flow parameters. It was necessary that the system be amenable to long term culture of moderate to large sample size experiments in order to maximize the impact on data acquisition. Details of the design and characterization of the pulsatile flow bioreactor system are included in Chapter 4. In Chapter 5, a series of experiments with cell-seeded tissue engineered vascular grafts (TEVG) demonstrated the utility and versatility of this system.

6.2 Conclusions

6.2.1 PEGDA Hydrogels as Scaffolds for Vascular Smooth Muscle Cells

Bulk properties of PEGDA hydrogels formed from a range of polymer molecular weights and solution concentrations were characterized. Resultant materials demonstrate tunable stiffness and strength, and transport properties (*e.g.* mesh size and crosslink density) that are appropriate for supporting viability of encapsulated cells. Hydrogel stiffnesses ranging from ~10-400 kPa are of the appropriate compliance to be tailored to match the mechanical properties of a variety of tissues from muscle to cartilage. Even more recent work has revealed hydrogel formulations with moduli in the MPa range, making them suitable substitutes for hard tissues such as bone.

Human coronary artery smooth muscle cells (HCASMC) seeded on top of these PEGDA hydrogels exhibit changes in attachment, proliferation, and morphology that can be directly correlated to the rigidity of the substrate material. In general, stiffer materials encourage greater attachment, a higher rate of proliferation, and the development of a mature, spread morphology. Finally, these responses were shown to be independently modulated by changing either the hydrogel material properties or the peptide directed bio-adhesiveness of the substrate.

6.2.2 A Pulsatile Flow Tissue Bioreactor

The tissue bioreactor presented in this work is capable of imparting physiological fluid flow (120 mL/min), shear (5-10 dynes/cm^2), pressure waveforms (120/80 mmHg), and pulse rates (60 or 120 bpm). Evaluation of the bioreactor system shows good reproducibility in flow parameters, and importantly that the system has good "ease of use", which is critical for long term experiments requiring frequent maintenance. Cell-

laden hydrogel constructs cultured for up to 8 wk in this system responded to mechanical stimulation with increases in cell and extracellular matrix (ECM) content and positive modulations to material properties. Though the magnitude of ECM accumulation is quite low, changes in hydrogel stiffness and the presence of degrading enzymes indicate that the encapsulated vascular cells are working towards a more biologically appropriate surrounding. While all the appropriate parameters for TEVG culture are not yet understood, this device will serve as an important tool in the development of a small diameter vessel substitute.

6.3 Further Investigation of Biomimetic Hydrogels

There are numerous potential applications of biomimetic PEGDA hydrogels to studies of fundamental cell-substrate interactions. For instance, it would be extremely interesting to delve more into the underlying mechanism of cellular response to substrate rigidity by probing cells with monoclonal antibodies to specific adhesive moieties (integrin and otherwise) to determine which are most prominent on soft and stiff hydrogels, respectively.

In light of our interest in TEVG development, however, it may be most appropriate to expand these investigations to 3D cell environments. As shown in the current work (**Figure 6-1**) and elsewhere,[117] vascular cells, which are highly spread *in vivo* and on 2D substrates are rounded in the current hydrogel formulations and have an apparent decreased viability with time in culture. This suggests that it may be necessary to enhance the biochemical signals incorporated in the hydrogel to promote greater cell interaction. Of particular benefit would be functionalities which could also stimulate the synthesis and retention of ECM molecules.

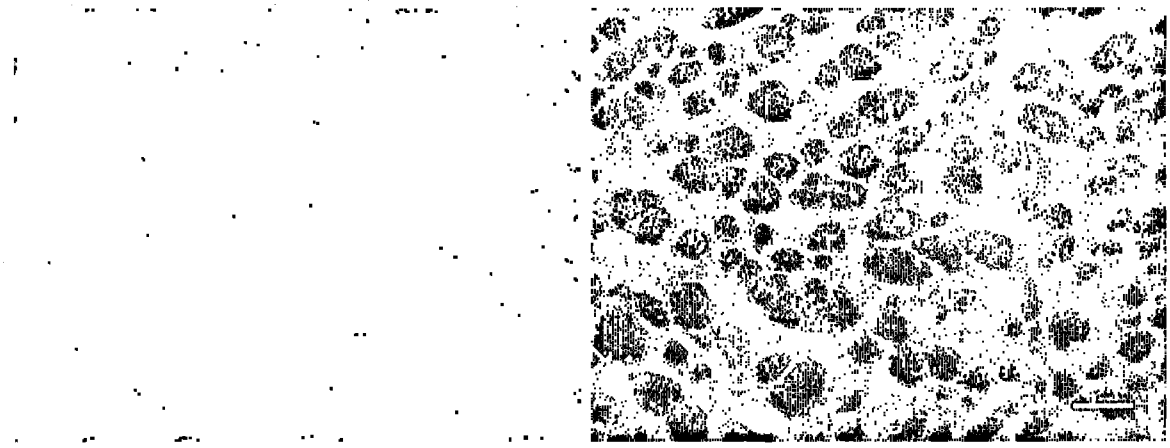

Figure 6-1. Photomicrograph of HCASMC in a Degradable PEGDA Hydrogel. Cells are evenly dispersed throughout the hydrogel matrix (left) after 8 wk in culture and display a rounded morphology. An unseeded hydrogel is included as a reference (right). Scale bar is 100 μm.

6.4 Towards an Implantable Tissue Engineered Vascular Graft

Though most efforts in TEVG development thus far have focused on reproduction of the medial layer of the blood vessel, it is widely accepted that successful vascular graft substitutes must also contain an intact endothelium. In native blood vessels, the intima consists of a monolayer of endothelial cells (EC) which helps prevent platelet adhesion and aggregation, and regulates vessel permeability, vascular smooth muscle cell behavior, and homeostasis.[49, 72, 89] As such the endothelium serves as important mediator in the vessel – blood interaction in vivo. To further our work towards an implantable TEVG and to increase the blood compatibility of poly(ethylene glycol)-based tissue engineered grafts, efforts should be made to seed EC on the luminal surface of tubular hydrogels. This attachment can be accomplished by functionalizing the luminal surface with a second layer of hydrogel material that contains EC-specific peptide sequences. Potential sequences include the laminin-derived peptides YIGSR and

IKVAV, which have been shown to promote EC attachment in non-integrin mediated processes [182], and REDV, which is an EC adhesive sequence derived from the protein fibronectin and acts via the α4β1 integrin receptor.[38, 40, 46-48] Importantly, literature referenced here and elsewhere shows that these ligands are not adhesive for platelets.

Once the hydrogels have been functionalized to permit EC attachment, the tissue culture bioreactor developed in the current work can be modified to seed cells. As shown in Figure 6-2, use of the peristaltic pump and custom graft chamber allow a cell suspension to be re-circulated through the TEVG constructs, effectively depositing cells on the luminal surface of the hydrogels. In recent work in our lab, we used this modified system to seed human coronary artery endothelial cells onto metal stents that had been deployed within tubular PEGDA hydrogels.[183] Cells were seeded under low flow conditions for 1 week and then allowed to proliferate to confluence.

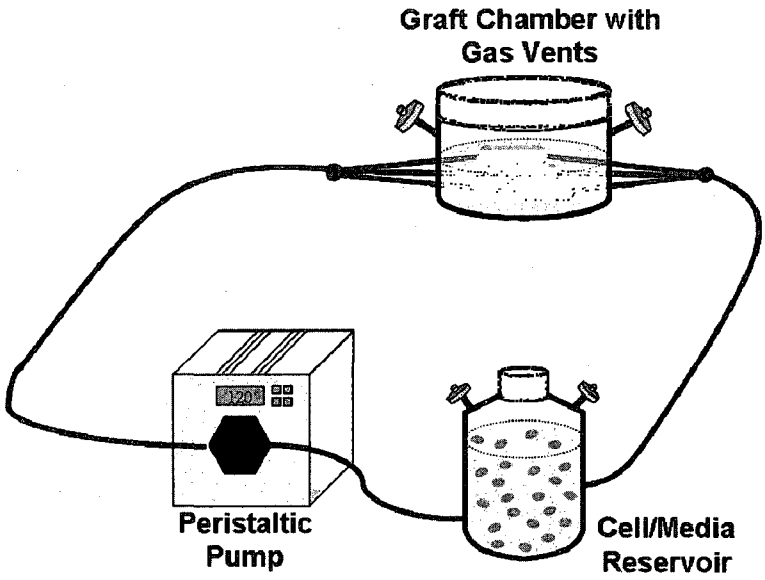

Figure 6-2. Bioreactor Flow Loop Modified for Endothelial Cell Seeding. The peristaltic pump and graft chamber can be used to seed suspensions of endothelial cells onto the luminal surface of PEGDA hydrogels.

Establishment of a functional endothelial layer will not only increase the blood compatibility of the TEVG, but also has potential for regulating and directing the encapsulated smooth muscle cells. Working in conjugation, the cells will be able to reorganize the available PEGDA hydrogel material and newly synthesized tissue matrix in order to form a biologically functional blood vessel substitute.

7. REFERENCES

1. Rosamond, W., et al., *Heart Disease and Stroke Statistics--2008 Update: A Report From the American Heart Association Statistics Committee and Stroke Statistics Subcommittee.* Circulation, 2008. **117**(4): p. e25-146.

2. Barron, V., et al., *Bioreactors for cardiovascular cell and tissue growth: A review.* Annals of Biomedical Engineering, 2003. **31**(9): p. 1017-1030.

3. Kangasniemi, K. and H. Opas, *Suomalainen lääkärikeskus (in Finnish).* Toinen painos, 1997.

4. Ratcliffe, A., *Tissue engineering of vascular grafts.* Matrix Biol, 2000. **19**(4): p. 353-7.

5. Wu, K.K. and P. Thiagarajan, *Role of endothelium in thrombosis and hemostasis.* Annu Rev Med, 1996. **47**: p. 315-31.

6. Association, A.H. *Atherosclerosis.* American Heart Association 2005 [cited 2006 Feb 15]; Available from: http://www.americanheart.org/presenter.jhtml?identifier=4440.

7. Giudiceandrea, A., et al., *Effect of prolonged pulsatile shear stress in vitro on endothelial cell seeded PTFE and compliant polyurethane vascular grafts.* Eur J Vasc Endovasc Surg, 1998. **15**(2): p. 147-54.

8. Coury, A.J., et al., *Degradation of Materials in the Biological Environment*, in *Biomaterials Science*, B.D. Ratner, et al., Editors. 2004, Elsevier: New York.

9. Faries, P., et al., *A comparative study of alternative conduits for lower extremity revascularization: all-autogenous conduit versus prosthetic grafts.* Journal of Vascular Surgery, 2000. **32**: p. 1080-1090.

10. Whittemore, A., et al., *What is the proper role of polytetrafluoroethylene grafts in infrainguinal reconstruction?* Journal of Vascular Surgery, 1989. **10**: p. 299-305.

11. Greisler, H., *Interactions at the blood/material interface.* Annals of Vascular Surgery, 1990. **4**: p. 98-103.

12. Sayers, R.D., et al., *Long-term results of femorotibial bypass with vein or polytetrafluoroethylene.* Br J Surg, 1998. **85**(7): p. 934-8.

13. Strandness, D.E. and D.S. Summer *Hemodynamics for Surgeons*. 1975, New York: Grune & Stratton, Inc.

14. Schoen, F.J., *Interventional and Surgical Cardiovascular Pathology: Clinical Correlations and Basic Principles*. 1989, Philadelphia: W.B. Saunders.

15. Niklason, L.E., et al., *Functional arteries grown in vitro.* Science, 1999. **284**(5413): p. 489-93.

16. Long, J.L. and R.T. Tranquillo, *Elastic fiber production in cardiovascular tissue-equivalents.* Matrix Biol, 2003. **22**(4): p. 339-50.

17. Isenberg, B.C. and R.T. Tranquillo, *Long-term cyclic distention enhances the mechanical properties of collagen-based media-equivalents.* Ann Biomed Eng, 2003. **31**(8): p. 937-49.

18. Kim, B.S., et al., *Cyclic mechanical strain regulates the development of engineered smooth muscle tissue.* Nat Biotechnol, 1999. **17**(10): p. 979-83.

19. Seliktar, D., et al., *Dynamic mechanical conditioning of collagen-gel blood vessel constructs induces remodeling in vitro.* Annals of Biomedical Engineering, 2000. **28**(4): p. 351-362.

20. Roeder, R., et al., *Compliance, elastic modulus, and burst pressure of small-intestine submucosa (SIS), small-diameter vascular grafts.* J Biomed Mater Res, 1999. **47**(1): p. 65-70.

21. L'Heureux, N., et al., *A completely biological tissue-engineered human blood vessel.* Faseb J, 1998. **12**(1): p. 47-56.

22. Campbell, J.H., J.L. Efendy, and G.R. Campbell, *Novel vascular graft grown within recipient's own peritoneal cavity.* Circ Res, 1999. **85**(12): p. 1173-8.

23. Jarrell, B.E., et al., *Use of freshly isolated capillary endothelial cells for the immediate establishment of a monolayer on a vascular graft at surgery.* Surgery, 1986. **100**(2): p. 392-9.

24. Schmidt, S.P., et al., *Endothelial cell--seeded four-millimeter Dacron vascular grafts: effects of blood flow manipulation through the grafts.* J Vasc Surg, 1984. **1**(3): p. 434-41.

25. Deutsch, M., et al., *Clinical autologous in vitro endothelialization of infrainguinal ePTFE grafts in 100 patients: a 9-year experience.* Surgery, 1999. **126**(5): p. 847-55.

26. Jeong, S.I., et al., *Manufacture of elastic biodegradable PLCL scaffolds for mechano-active vascular tissue engineering.* J Biomater Sci Polym Ed, 2004. **15**(5): p. 645-60.

27. Uurto, I., et al., *Biodegradable self-expanding poly-L/D-lactic acid vascular stent: a pilot study in canine and porcine iliac arteries.* J Endovasc Ther, 2004. **11**(6): p. 712-8.

28. Furukawa, K.S., et al., *Hybrid of gel-cultured smooth muscle cells with PLLA sponge as a scaffold towards blood vessel regeneration.* Cell Transplant, 2002. **11**(5): p. 475-80.

29. Iwai, S., et al., *Biodegradable polymer with collagen microsponge serves as a new bioengineered cardiovascular prosthesis.* J Thorac Cardiovasc Surg, 2004. **128**(3): p. 472-9.

30. Lommen, E., et al., *Development of a neo-artery induced by a biodegradable polymeric vascular prosthesis.* Trans Am Soc Artif Intern Organs, 1983. **29**: p. 255-9.

31. van der Lei, B., et al., *Regeneration of the arterial wall in microporous, compliant, biodegradable vascular grafts after implantation into the rat abdominal aorta. Ultrastructural observations.* Cell Tissue Res, 1985. **242**(3): p. 569-78.

32. Mann, B.K., et al., *Smooth muscle cell growth in photopolymerized hydrogels with cell adhesive and proteolytically degradable domains: synthetic ECM analogs for tissue engineering.* Biomaterials, 2001. **22**(22): p. 3045-51.

33. Scott, S.M., et al., *A collagen coated vascular prosthesis.* J Cardiovasc Surg (Torino), 1987. **28**(5): p. 498-504.

34. Hirt, S.W., et al., *Collagen-presealed or uncoated aortic bifurcation Dacron prostheses: a 5-year clinical follow-up study.* Thorac Cardiovasc Surg, 1991. **39**(6): p. 365-70.

35. Seeger, J.M. and N. Klingman, *Improved endothelial cell seeding with cultured cells and fibronectin-coated grafts.* J Surg Res, 1985. **38**(6): p. 641-7.

36. Schrenk, P., et al., *Fibrin glue coating of e-PTFE prostheses enhances seeding of human endothelial cells.* Thorac Cardiovasc Surg, 1987. **35**(1): p. 6-10.

37. Mazzucotelli, J.P., et al., *Endothelial cell seeding: coating Dacron and expanded polytetrafluoroethylene vascular grafts with a biological glue allows adhesion and growth of human saphenous vein endothelial cells.* Int J Artif Organs, 1991. **14**(8): p. 482-90.

38. Fittkau, M.H., et al., *The selective modulation of endothelial cell mobility on RGD peptide containing surfaces by YIGSR peptides.* Biomaterials, 2005. **26**(2): p. 167-74.

39. Gobin, A.S. and J.L. West, *Val-ala-pro-gly, an elastin-derived non-integrin ligand: smooth muscle cell adhesion and specificity.* J Biomed Mater Res A, 2003. **67**(1): p. 255-9.

40. Massia, S.P. and J.A. Hubbell, *Human endothelial cell interactions with surface-coupled adhesion peptides on a nonadhesive glass substrate and two polymeric biomaterials.* J Biomed Mater Res, 1991. **25**(2): p. 223-42.

41. Massia, S.P. and J.A. Hubbell, *Vascular endothelial cell adhesion and spreading promoted by the peptide REDV of the IIICS region of plasma fibronectin is mediated by integrin alpha 4 beta 1.* J Biol Chem, 1992. **267**(20): p. 14019-26.

42. Drumheller, P.D. and J.A. Hubbell, *Polymer networks with grafted cell adhesion peptides for highly biospecific cell adhesive substrates.* Anal Biochem, 1994. **222**(2): p. 380-8.

43. Massia, S.P. and J. Stark, *Immobilized RGD peptides on surface-grafted dextran promote biospecific cell attachment.* J Biomed Mater Res, 2001. **56**(3): p. 390-9.

44. Jun, H.W. and J. West, *Development of a YIGSR-peptide-modified polyurethaneurea to enhance endothelialization.* J Biomater Sci Polym Ed, 2004. **15**(1): p. 73-94.

45. Jun, H.W. and J.L. West, *Modification of polyurethaneurea with PEG and YIGSR peptide to enhance endothelialization without platelet adhesion.* J Biomed Mater Res, 2004.

46. Kuzuya, M., et al., *Inhibition of endothelial cell differentiation on a glycosylated reconstituted basement membrane complex.* Exp Cell Res, 1996. **226**(2): p. 336-45.

47. Ponce, M.L., et al., *Identification of endothelial cell binding sites on the laminin gamma 1 chain.* Circ Res, 1999. **84**(6): p. 688-94.

48. Schnaper, H.W., H.K. Kleinman, and D.S. Grant, *Role of laminin in endothelial cell recognition and differentiation.* Kidney Int, 1993. **43**(1): p. 20-5.

49. Schmedlen, R.H., et al., *Tissue engineered small-diameter vascular grafts.* Clinics in Plastic Surgery, 2003. **30**(4): p. 507-+.

50. Girton, T.S., et al., *Mechanisms of stiffening and strengthening in media-equivalents fabricated using glycation.* J Biomech Eng, 2000. **122**(3): p. 216-23.

51. Elbjeirami, W.M., et al., *Enhancing mechanical properties of tissue-engineered constructs via lysyl oxidase crosslinking activity.* Journal Of Biomedical Materials Research Part A, 2003. **66A**(3): p. 513-521.

52. Vorp, D.A., T. Maul, and A. Nieponice, *Molecular aspects of vascular tissue engineering.* Front Biosci, 2005. **10**: p. 768-89.

53. Gombotz, W.R., et al., *Protein adsorption to poly(ethylene oxide) surfaces.* J Biomed Mater Res, 1991. **25**(12): p. 1547-62.

54. Gobin, A.S. and J.L. West, *Effects of epidermal growth factor on fibroblast migration through biomimetic hydrogels.* Biotechnol Prog, 2003. **19**(6): p. 1781-5.

55. Bryant, S.J., C.R. Nuttelman, and K.S. Anseth, *Cytocompatibility of UV and visible light photoinitiating systems on cultured NIH/3T3 fibroblasts in vitro.* J Biomater Sci Polym Ed, 2000. **11**(5): p. 439-57.

56. Cruise, G.M., D.S. Scharp, and J.A. Hubbell, *Characterization of permeability and network structure of interfacially photopolymerized poly(ethylene glycol) diacrylate hydrogels.* Biomaterials, 1998. **19**(14): p. 1287-94.

57. Bryant, S.J. and K.S. Anseth, *Hydrogel properties influence ECM production by chondrocytes photoencapsulated in poly(ethylene glycol) hydrogels.* J Biomed Mater Res, 2002. **59**(1): p. 63-72.

58. Schmedlen, R.H., *Development of Hydrogel Scaffolds and a Bioreactor for Vascular Tissue Engineering*, in *Bioengineering*. 2004, TX: Houston.

59. Discher, D.E., P. Janmey, and Y.L. Wang, *Tissue cells feel and respond to the stiffness of their substrate.* Science, 2005. **310**(5751): p. 1139-43.

60. Diamond, S.L., S.G. Eskin, and L.V. McIntire, *Fluid flow stimulates tissue plasminogen activator secretion by cultured human endothelial cells.* Science, 1989. **243**(4897): p. 1483-5.

61. Taylor, L.M., Jr., J.M. Edwards, and J.M. Porter, *Present status of reversed vein bypass grafting: five-year results of a modern series.* J Vasc Surg, 1990. **11**(2): p. 193-205; discussion 205-6.

62. Oates, C., *Cardiovascular Haemodynamics and Doppler Waveforms Explained.* 2001, San Francisco: Cambridge Universtiy Press. 192.

63. Lehoux, S. and A. Tedgui, *Signal transduction of mechanical stresses in the vascular wall.* Hypertension, 1998. **32**(2): p. 338-45.

64. Sumpio, B.E., et al., *Enhanced collagen production by smooth muscle cells during repetitive mechanical stretching.* Arch Surg, 1988. **123**(10): p. 1233-6.

65. O'Callaghan, C.J. and B. Williams, *Mechanical strain-induced extracellular matrix production by human vascular smooth muscle cells: role of TGF-beta(1).* Hypertension, 2000. **36**(3): p. 319-24.

66. Gorfien, S.F., et al., *Cyclic biaxial strain of pulmonary artery endothelial cells causes an increase in cell layer-associated fibronectin.* Am J Respir Cell Mol Biol, 1990. **3**(5): p. 421-9.

67. Von Offenberg Sweeney, N., et al., *Cyclic strain-mediated regulation of vascular endothelial cell migration and tube formation.* Biochem Biophys Res Commun, 2005. **329**(2): p. 573-82.

68. Liu, S.Q. and J. Goldman, *Role of blood shear stress in the regulation of vascular smooth muscle cell migration.* IEEE Trans Biomed Eng, 2001. **48**(4): p. 474-83.

69. Papadaki, M., et al., *Nitric oxide production by cultured human aortic smooth muscle cells: stimulation by fluid flow.* Am J Physiol, 1998. **274**(2 Pt 2): p. H616-26.

70. Stamatas, G.N., C.W. Patrick, Jr., and L.V. McIntire, *Intracellular pH changes in human aortic smooth muscle cells in response to fluid shear stress.* Tissue Eng, 1997. **3**(4): p. 391-403.

71. Asada, H., et al., *Sustained orbital shear stress stimulates smooth muscle cell proliferation via the extracellular signal-regulated protein kinase 1/2 pathway.* J Vasc Surg, 2005. **42**(4): p. 772-80.

72. Clerin, V., et al., *Mechanical environment, donor age, and presence of endothelium interact to modulate porcine artery viability ex vivo.* Ann Biomed Eng, 2002. **30**(9): p. 1117-27.

73. Eskin, S.G., N.A. Turner, and L.V. McIntire, *Endothelial cell cytochrome P450 1A1 and 1B1: up-regulation by shear stress.* Endothelium, 2004. **11**(1): p. 1-10.

74. Eskin, S.G., et al., *Response of cultured endothelial cells to steady flow.* Microvasc Res, 1984. **28**(1): p. 87-94.

75. Ives, C.L., S.G. Eskin, and L.V. McIntire, *Mechanical effects on endothelial cell morphology: in vitro assessment.* In Vitro Cell Dev Biol, 1986. **22**(9): p. 500-7.

76. Nollert, M.U., S.G. Eskin, and L.V. McIntire, *Shear stress increases inositol trisphosphate levels in human endothelial cells.* Biochem Biophys Res Commun, 1990. **170**(1): p. 281-7.

77. Nollert, M.U., N.J. Panaro, and L.V. McIntire, *Regulation of genetic expression in shear stress-stimulated endothelial cells.* Ann N Y Acad Sci, 1992. **665**: p. 94-104.

78. Sampath, R., et al., *Shear stress-mediated changes in the expression of leukocyte adhesion receptors on human umbilical vein endothelial cells in vitro.* Ann Biomed Eng, 1995. **23**(3): p. 247-56.

79. Frangos, J.A., et al., *Flow effects on prostacyclin production by cultured human endothelial cells.* Science, 1985. **227**(4693): p. 1477-9.

80. Nollert, M.U., et al., *The effect of shear stress on the uptake and metabolism of arachidonic acid by human endothelial cells.* Biochim Biophys Acta, 1989. **1005**(1): p. 72-8.

81. Sharefkin, J.B., et al., *Fluid flow decreases preproendothelin mRNA levels and suppresses endothelin-1 peptide release in cultured human endothelial cells.* J Vasc Surg, 1991. **14**(1): p. 1-9.

82. McCormick, S.M., et al., *DNA microarray reveals changes in gene expression of shear stressed human umbilical vein endothelial cells.* Proc Natl Acad Sci U S A, 2001. **98**(16): p. 8955-60.

83. McCormick, S.M., et al., *Microarray analysis of shear stressed endothelial cells.* Biorheology, 2003. **40**(1-3): p. 5-11.

84. Seliktar, D., R.M. Nerem, and Z.S. Galis, *The role of matrix metalloproteinase-2 in the remodeling of cell-seeded vascular constructs subjected to cyclic strain.* Ann Biomed Eng, 2001. **29**(11): p. 923-34.

85. Baguneid, M., et al., *Shear-stress preconditioning and tissue-engineering-based paradigms for generating arterial substitutes.* Biotechnol Appl Biochem, 2004. **39**(Pt 2): p. 151-7.

86. Chan, B.P., et al., *In vivo performance of dual ligand augmented endothelialized expanded polytetrafluoroethylene vascular grafts.* J Biomed Mater Res B Appl Biomater, 2005. **72**(1): p. 52-63.

87. Williams, C. and T.M. Wick, *Perfusion bioreactor for small diameter tissue-engineered arteries.* Tissue Eng, 2004. **10**(5-6): p. 930-41.

88. Williams, S.K., et al., *Formation of a functional endothelium on vascular grafts.* J Electron Microsc Tech, 1991. **19**(4): p. 439-51.

89. Clerin, V., et al., *Tissue engineering of arteries by directed remodeling of intact arterial segments.* Tissue Engineering, 2003. **9**(3): p. 461-472.

90. Peppas, N.A., et al., *Hydrogels in biology and medicine: From molecular principles to bionanotechnology.* Advanced Materials, 2006. **18**(11): p. 1345-1360.

91. Jen, A.C., M.C. Wake, and A.G. Mikos, *Review: Hydrogels for cell immobilization.* Biotechnology and Bioengineering, 1996. **50**(4): p. 357-364.

92. Ma, P.X. and J.H. Elisseeff, *Scaffolding in tissue engineering*. 2005, Boca Raton: Taylor&Francis. xvi, 638 p.

93. Ratner, B.D., et al., *Biomaterials science: An introduction to materials in medicine*. 2nd ed. 2004, London: Elsevier Academic Press.

94. Harris, J.M. and S. Zalipsky, *Poly(ethylene glycol): Chemistry and biological applications*. 1997, Washington DC: American Chemical Society.

95. Elisseeff, J., et al., *Photoencapsulation of chondrocytes in poly(ethylene oxide)-based semi-interpenetrating networks.* Journal of Biomedical Materials Research, 2000. **51**(2): p. 164-171.

96. Burdick, J. and K. Anseth, *Photoencapsulation of osteoblasts in injectable RGD-modified PEG hydrogels for bone tissue engineering.* Biomaterials, 2002. **23**: p. 4315-4323

97. Nuttelman, C.R., M.C. Tripodi, and K.S. Anseth, *Synthetic hydrogel niches that promote hMSC viability.* Matrix Biology, 2005. **24**(3): p. 208-218.

98. Hern, D.L. and J.A. Hubbell, *Incorporation of adhesion peptides into nonadhesive hydrogels useful for tissue resurfacing.* J Biomed Mater Res, 1998. **39**(2): p. 266-76.

99. DeLong, S.A., A.S. Gobin, and J.L. West, *Covalent immobilization of RGDS on hydrogel surfaces to direct cell alignment and migration.* J Control Release, 2005. **109**(1-3): p. 139-48.

100. Langer, R. and N.A. Peppas, *Advances in biomaterials, drug delivery, and bionanotechnology.* Aiche Journal, 2003. **49**(12): p. 2990-3006.

101. Merrill, E.W., K.A. Dennison, and C. Sung, *Partitioning and diffusion of solutes in hydrogels of poly(ethylene oxide).* Biomaterials, 1993. **14**(15): p. 1117-26.

102. Schultz, S.G. and A.K. Solomon, *Determination of the effective hydrodynamic radii of small molecules by viscometry.* J Gen Physiol, 1961. **44**: p. 1189-99.

103. Jossang, T., J. Feder, and E. Rosenqvist, *Photon correlation spectroscopy of human IgG.* J Protein Chem, 1988. 7(2): p. 165-71.

104. Bryant, S.J., et al., *Crosslinking density influences the morphology of chondrocytes photoencapsulated in PEG hydrogels during the application of compressive strain.* Journal Of Orthopaedic Research, 2004. **22**(5): p. 1143-1149.

105. Odian, G., *Principles of polymerization.* 3rd ed. 1991, New York: Wiley. xxii, 768 s.

106. Hahn, M.S., et al., *Photolithographic patterning of polyethylene glycol hydrogels.* Biomaterials, 2006. **27**(12): p. 2519-24.

107. Xue, L. and H.P. Greisler, *Biomaterials in the development and future of vascular grafts.* J Vasc Surg, 2003. **37**(2): p. 472-80.

108. Barra, J.G., et al., *Assessment of smooth muscle contribution to descending thoracic aortic elastic mechanics in conscious dogs.* Circ Res, 1993. **73**(6): p. 1040-50.

109. Pelham, R.J., Jr. and Y.L. Wang, *Cell locomotion and focal adhesions are regulated by the mechanical properties of the substrate.* Biol Bull, 1998. **194**(3): p. 348-9; discussion 349-50.

110. Pelham, R.J., Jr. and Y. Wang, *Cell locomotion and focal adhesions are regulated by substrate flexibility.* Proc Natl Acad Sci U S A, 1997. **94**(25): p. 13661-5.

111. Deroanne, C.F., C.M. Lapiere, and B.V. Nusgens, *In vitro tubulogenesis of endothelial cells by relaxation of the coupling extracellular matrix-cytoskeleton.* Cardiovasc Res, 2001. **49**(3): p. 647-58.

112. Wang, H.B., M. Dembo, and Y.L. Wang, *Substrate flexibility regulates growth and apoptosis of normal but not transformed cells.* Am J Physiol Cell Physiol, 2000. **279**(5): p. C1345-50.

113. Engler, A., et al., *Substrate compliance versus ligand density in cell on gel responses.* Biophys J, 2004. **86**(1 Pt 1): p. 617-28.

114. Peyton, S.R. and A.J. Putnam, *Extracellular matrix rigidity governs smooth muscle cell motility in a biphasic fashion.* J Cell Physiol, 2005. **204**(1): p. 198-209.

115. Ingber, D.E., *Tensegrity II. How structural networks influence cellular information processing networks.* J Cell Sci, 2003. **116**(Pt 8): p. 1397-408.

116. Ingber, D.E., *Tensegrity I. Cell structure and hierarchical systems biology.* J Cell Sci, 2003. **116**(Pt 7): p. 1157-73.

117. Peyton, S.R., et al., *The use of poly(ethylene glycol) hydrogels to investigate the impact of ECM chemistry and mechanics on smooth muscle cells.* Biomaterials, 2006. **27**(28): p. 4881-93.

118. Zamir, E., et al., *Molecular diversity of cell-matrix adhesions.* J Cell Sci, 1999. **112 (Pt 11)**: p. 1655-69.

119. Mann, B.K. and J.L. West, *Cell adhesion peptides alter smooth muscle cell adhesion, proliferation, migration, and matrix protein synthesis on modified surfaces and in polymer scaffolds.* J Biomed Mater Res, 2002. **60**(1): p. 86-93.

120. Engler, A.J., et al., *Myotubes differentiate optimally on substrates with tissue-like stiffness: pathological implications for soft or stiff microenvironments.* J Cell Biol, 2004. **166**(6): p. 877-87.

121. Freed, L.E., et al., *Advanced tools for tissue engineering: scaffolds, bioreactors, and signaling.* Tissue Eng, 2006. **12**(12): p. 3285-305.

122. Bordenave, L., P. Menu, and C. Baquey, *Developments towards tissue-engineered, small-diameter arterial substitutes.* Expert Rev Med Devices, 2008. **5**(3): p. 337-47.

123. Mironov, V., et al., *Cardiovascular tissue engineering I. Perfusion bioreactors: a review.* J Long Term Eff Med Implants, 2006. **16**(2): p. 111-30.

124. Niklason, L., et al., *Functional arteries grown in vitro.* Science, 1999. **284**(16): p. 489-493.

125. Carrier, R.L., et al., *Cardiac tissue engineering: cell seeding, cultivation parameters, and tissue construct characterization.* Biotechnol Bioeng, 1999. **64**(5): p. 580-9.

126. Bryant, S., et al., *Crosslinking density influences chondrocyte metabolism in dynamically loaded photocrosslinked poly(ethylene glycol) hydrogels.* Annals of Biomedical Engineering, 2004. **32**(3): p. 407-417.

127. Bryant, S.B., RJ, K. Durand, and K. Anseth, *Encapsulating chondrocytes in degrading PEG hydrogels with high modulus: Engineering gel structural changes to facilitate cartilaginous tissue production.* Biotechnology and Bioengineering, 2004. **86**(7): p. 747-755.

128. Elisseeff, J., et al., *Transdermal photopolymerization for minimally invasive implantation.* Proceedings of the National Academy of Science USA, 1999. **96**: p. 3104-3107.

129. Liu, V.A. and S.N. Bhatia, *Three-dimensional photopatterning of hydrogels containing living cells.* Biomedical Microdevices, 2002. **4**(4): p. 257-266.

130. Benbrahim, A., et al., *Characteristics of vascular wall cells subjected to dynamic cyclic strain and fluid shear conditions in vitro.* Journal of Surgical Research, 1996. **65**: p. 119-127.

131. Johnson, C., et al., *A biomechanical study of the human vertebral artery with implications for fatal arterial injury.* Forensic Science International, 2000. **109**: p. 169-182.

132. Hiles, M., et al., *Mechanical properties of xenogeneic small-intestinal submucosa when used as an aortic graft in the dog.* Journal of Biomedical Materials Research, 1995. **29**: p. 883-891.

133. Ku, D. and C. Zhu, *The mechanical environment of the artery*, in *Hemodynamic forces and vascular cell biology*, B. Sumpio, Editor. 1993, RG Landes Company: Austin. p. 1-23.

134. Kim, B.S., et al., *Cyclic mechanical strain regulates the development of engineered smooth muscle cell tissue.* Nature Biotechnology, 1999. **17**: p. 979-983.

135. Nerem, R.M., *Atherogenesis: hemodynamics, vascular geometry, and the endothelium.* Biorheology, 1984. **21**(4): p. 565-9.

136. Dardik, A., A. Liu, and B.J. Ballermann, *Chronic in vitro shear stress stimulates endothelial cell retention on prosthetic vascular grafts and reduces subsequent in vivo neointimal thickness.* J Vasc Surg, 1999. **29**(1): p. 157-67.

137. Isenberg, B.C., C. Williams, and R.T. Tranquillo, *Endothelialization and Flow Conditioning of Fibrin-Based Media-Equivalents.* Ann Biomed Eng, 2006.

138. Davies, P.F., et al., *Turbulent fluid shear stress induces vascular endothelial cell turnover in vitro.* Proc Natl Acad Sci U S A, 1986. **83**(7): p. 2114-7.

139. Gleason, R.L., et al., *A multiaxial computer-controlled organ culture and biomechanical device for mouse carotid arteries.* J Biomech Eng, 2004. **126**(6): p. 787-95.

140. Kempczinski, R., ed. *Vascular Surgery.* ed. R. Rutherford. 2000, WB Saunders: Denver.

141. Vacanti, J. and R. Langer, *Tissue engineering: the design and fabrication of living replacement devices for surgical reconstruction and transplantation.* Lancet, 1999. **354**: p. SI32-SI34.

142. Tranquillo, R., et al., *Magnetically orientated tissue-equivalent tubes: application to a circumferentially orientated media-equivalent.* Biomaterials, 1996. **17**: p. 349-357.

143. Isenberg, B. and R. Tranquillo, *Long-term cyclic distention enhances the mechanical properties of collagen-based media-equivalents.* Annals of Biomedical Engineering, 2003. **31**: p. 937-939.

144. Birukov, K. and V. Shirinsky, *Stretch affects phenotype and proliferation of vascular smooth muscle cells.* Mol Cell Biochem, 1995. **144**: p. 131-9.

145. Kanda, K. and T. Matsuda, *Mechanical stress induced cellular orientation and phenotypic modulation of 3D cultured smooth muscle cells.* ASAIO, 1993. **39**(M686-690).

146. Chiquet, M. and M. Matthisson, *Regulation of extracellular matrix synthesis by mechanical stress.* Biochem Cell Biol, 1996. **74**: p. 737-44.

147. Kulik, T. and S. Alvarado, *Effect of stretch on growth and collagen synthesis in cultured rat and lamb pulmonary arterial smooth muscle cells.* Journal of Cellular Physiology, 1993. **157**: p. 615-624.

148. Cheng, G. and W. Briggs, *Mechanical strain tightly controls fibroblast growth factor-2 release from cultured human vascular smooth muscle cells.* Circulation Research, 1997. **80**: p. 28-36.

149. Solan, A., et al., *Effect of pulse rate on collagen deposition in the tissue-engineered blood vessel.* Tissue Engineering, 2003. **9**(4): p. 579-586.

150. West, J.L. and J.A. Hubbell, *Photopolymerized hydrogel materials for drug delivery applications.* Reactive Polymers 1995. **25**(2-3): p. 139-47.

151. Hill-West, J.L., et al., *Inhibition of thrombosis and intimal thickening by in situ photopolymerization of thin hydrogel barriers.* Proceedings of the National Academy of Science U.S.A., 1994. **91**(13): p. 5967-71.

152. Anseth, K.S., C.N. Bowman, and L. BrannonPeppas, *Mechanical properties of hydrogels and their experimental determination.* Biomaterials, 1996. **17**(17): p. 1647-1657.

153. Bryant, S.J. and K.S. Anseth, *Hydrogel properties influence ECM production by chondrocytes photoencapsulated in poly(ethylene glycol) hydrogels.* Journal of Biomedical Materials Research, 2002. **59**(1): p. 63-72.

154. Gobin, A.S. and J.L. West, *Cell migration through defined, synthetic extracellular matrix analogues.* FASEB Journal, 2002. **16**(3).

155. Lee, S.H., et al., *Proteolytically degradable hydrogels with a fluorogenic substrate for studies of cellular proteolytic activity and migration.* Biotechnol Prog, 2005. **21**(6): p. 1736-41.

156. Parks, W.C. and R.P. Mecham, *Substrate specificity and mechanisms of substrate recognition of the matrix metalloproteinases.*, in *Matrix Metalloproteinases*, V. Imper and H.E. Van Wart, Editors. 1998, Academic Press: San Diego. p. 219-242.

157. Hirschi, K.K., et al., *Endothelial cells modulate the proliferation of mural cell precursors via platelet-derived growth factor-BB and heterotypic cell contact.* Circ Res, 1999. **84**(3): p. 298-305.

158. Long, J. and R. Tranquillo, *Elastic fiber production in cardiovascular tissue-equivalents.* Matrix Biology, 2003. **22**: p. 339-350.

159. Newcomb, P.M. and I.M. Herman, *Pericyte growth and contractile phenotype: modulation by endothelial-synthesized matrix and comparison with aortic smooth muscle.* J Cell Physiol, 1993. **155**(2): p. 385-93.

160. Reilly, C.F., L.M. Fritze, and R.D. Rosenberg, *Heparin inhibition of smooth muscle cell proliferation: a cellular site of action.* J Cell Physiol, 1986. **129**(1): p. 11-9.

161. Castellot, J.J., Jr., et al., *Inhibition of vascular smooth muscle cell growth by endothelial cell-derived heparin. Possible role of a platelet endoglycosidase.* J Biol Chem, 1982. **257**(19): p. 11256-60.

162. Williams CG, et al., *Variable cytocompatibility of six cell lines with photoinitiators used for polymerizing hydrogels and cell encapsulation.* Biomaterials, 2005. **26**(11): p. 1211-1218.

163. Bryant, S.J., C.R. Nuttelman, and K.S. Anseth, *Cytocompatibility of UV and visible light photoinitiating systems on cultured NIH/3T3 fibroblasts in vitro.* Journal Of Biomaterials Science-Polymer Edition, 2000. **11**(5): p. 439-457.

164. Brossollet, L., *Mechanical issues in vascular grafting: a review.* The International Journal of Artificial Organs, 1992. **15**(10): p. 579-584.

165. Gregory, T.R., *Nucleotypic effects without nuclei: Genome size and erythrocyte size in mammals.* Genome, 2000. **43**(5): p. 895-901.

166. Labarca, C. and K. Paigen, *A simple, rapid, and sensitive DNA assay procedure.* Anal Biochem, 1980. **102**(2): p. 344-52.

167. Jeong, S.I., et al., *Mechano-active tissue engineering of vascular smooth muscle using pulsatile perfusion bioreactors and elastic PLCL scaffolds.* Biomaterials, 2005. **26**: p. 1405-1411.

168. Lu, H.H., et al., *In vitro bone formation using muscle-derived cells: a new paradigm for bone tissue engineering using polymer-bone morphogenetic protein matrices.* Biochem Biophys Res Commun, 2003. **305**: p. 882-889.

169. Gomes, M.E., et al., *Effect of flow perfusion on the osteogenic differentiation of bone marrow stromal cells cultured on starch-based three-dimensional scaffolds.* J Biomed Mater Res A, 2003. **67**: p. 87-95.

170. Miller, E.J. and S. Gay, *Collagen - an Overview.* Methods in Enzymology, 1982. **82**: p. 3-32.

171. Stegemann, H. and K. Stalder, *Determination of hydroxyproline.* Clin Chim Acta, 1967. **18**(2): p. 267-73.

172. Cappadona, C., et al., *Phenotype dictates the growth response of vascular smooth muscle cells to pulse pressure in vitro.* Experimental Cell Research, 1999. **250**: p. 174-186.

173. Galis, Z.S., G.K. Sukhova, and P. Libby, *Microscopic localization of active proteases by in situ zymography: detection of matrix metalloproteinase activity in vascular tissue.* Faseb J, 1995. **9**(10): p. 974-80.

174. Faia, K.L., et al., *Matrix metalloproteinases and tissue inhibitors of metalloproteinases in hamster aortic atherosclerosis: correlation with in-situ zymography.* Atherosclerosis, 2002. **160**(2): p. 325-37.

175. Wilson, E., K. Sudhir, and H. Ives, *Mechanical strain of rat vascular smooth muscle cells is sensed by specific extracellular matrix/integrin interactions.* Journal of Clinical Investigation, 1995. **96**: p. 2364-2372.

176. Ross, J. and R. Tranquillo, *ECM gene expression correlates with in vitro tissue growth and development in fibrin gel remodeled by neonatal smooth muscle cells.* Matrix Biology 2003. **22**: p. 477-490.

177. Clerin, V., et al., *Tissue engineering of arteries by directed remodeling of intact arterial segments.* Tissue Engineering, 2003. **9**(3).

178. Fung, Y.C., *Biomechanics: mechanical properties of living tissues*. 2 ed. 1993, New York: Springer-Verlag.

179. Hirschi, K.K., et al., *Gap junction communication mediates TGF-β activation and endothelial-induced mural cell differentiation.* Circulation Research, 2003. **93**: p. 429-437.

180. Li, C. and Q. Xu, *Mechanical stress-initiated signal transductions in vascular smooth muscle cells.* Cellular Signaling, 2000. **12**: p. 435-445.

181. Chen, C.S., et al., *Geometric control of cell life and death.* Science, 1997. **276**: p. 1425-28.

182. Zaidi, T.N., et al., *Adhesion of platelets to surface-bound fibrinogen under flow.* Blood, 1996. **88**(8): p. 2967-72.

183. Bergmann, N., J. Restrepo, and J.L. West. *Bioactive Polyurethanes as Stent Coatings to Reduce Thrombosis*. in *8th World Biomaterials Congress*. 2008. Amsterdam RAI, The Netherlands.